TAMU-Princeton-Casper-Baylor-CSU-UIUC

Summer School

From Laser fusion
to Quantum physics and Gravity

Quantum Science Camp

Casper College, Casper, Wyoming
July 15-26, 2024

Fest celebrating birthday of Profs. Marlan Scully and Shiyao Zhu

TAMU-Princeton-Casper-Baylor-CSU-UIUC Summer School

"From Laser fusion to Quantum physics and Gravity"

Casper College, Casper, Wyoming, July 15-26, 2024

Sunday, July 14, 2024

3:00 PM: Snack food is being delivered to the Residence Hall kitchen (1st floor, Rooms 144 & 192)

6:00 PM: Dinner is set in the Residence Hall kitchen (1st floor) and stored in fridge for late arrivals

Monday, July 15, 2024

All Talks will be in the Wold Physical Science Center, Room 103 (**PS103**)

7:00 – 8:00 AM	**BREAKFAST**	Tobin Cafeteria on bottom floor of Union/University (UU building)
PS103	Session chair: Bob Brick	
8:10 – 8:50 AM	Marlan Scully, *Quantum Camp & Symposium* Brandon Kosine, *Interim President of Casper College* Steve Degenfelder, *Casper College Board of Trustees* John Junkins, *TAMU*	**Overview and Welcome**
8:50 – 9:00 AM	BREAK	
9:00 – 9:40 AM	Marlan Scully, *TAMU*	Entanglement in Unruh and Hawking radiation from a quantum optical perspective
9:40 – 10:20 AM	Girish Agarwal, *TAMU*	Time Reversed Quantum Metrology
10:20 – 10:50 AM	BREAK	
Session chair: Dmitri Voronine		
10:50 – 11:30 AM	Yanhua Shih, *UMBC*	Can a coherent CW laser beam produce intensity correlation like thermal light?
11:30 – 12:10 PM	Konstantin Dorfman *Hainan University*	Time-domain quantum light spectroscopy and sensing
12:10 PM	**LUNCH**	Tobin Cafeteria (bottom floor UU Bldg.)
Afternoon recreational activities		
6:15 – 7:00 PM	**DINNER**	Outside PS 103
PS103	Session chair: Konstantin Dorfman	
7:00 – 7:30 PM	Gordon Chen, *TAMU*	Animal shapes and their modal analysis (I): Basic model and properties
7:30 – 8:00 PM	Gordon Chen, *TAMU*	Animal shapes and their modal analysis (II): Movie making with AI applications
8:00 – 8:30 PM	POSTER SESSION / BREAK	

Link to Book of Abstracts and Quantum Science Camp Program

Tuesday, July 16, 2024

7:00 – 8:00 AM	**BREAKFAST**	Tobin Cafeteria
PS103	Session chair: Olga Kocharovskaya	
8:10 – 8:50 AM	Wolfgang Schleich *Universität Ulm*	A gravitational wave detector with atoms: an intriguing precursor
8:50 – 9:30 AM	Leon Cohen, *City University of New York*	Generalization of the Edgeworth and Gram-Charlier series and application to quantum mechanics
9:30 – 10:10 AM	Gershon Kurizki *Weizmann Ins. of Science*	Observers, Controllers and The World: What Has Quantum Mechanics Changed?
10:10 – 10:40 AM	POSTER SESSION / BREAK	
Session chair: Wolfgang Schleich		
10:40 – 11:20 AM	Olga Kocharovskaya *TAMU*	Towards Nuclear Clocks and Nuclear Memories
11:20 – 11:40 AM	Xiwen Zhang, *TAMU*	Facile control of hard X-ray quantum memory
11:40 – 12:00 PM	Wenzhuo Zhang, *TAMU*	Quantum evolution of mixed states and efficiency of quantum heat engines
12:00 PM	**LUNCH**	Tobin Cafeteria
Afternoon recreational activities		
6:15 – 7:00 PM	**DINNER**	Outside PS 103
PS103	Session chair: Bob Brick	
7:00 – 8:00 PM	**Poster Presentations**	Posters 1-12
8:00 – 8:30 PM	POSTER SESSION / BREAK	
8:30 – 9:30 PM	**Poster Presentations**	Posters 13-22

Wednesday, July 17, 2024

7:00 – 8:00 AM	**BREAKFAST**	Tobin Cafeteria
PS103	Session chair: Janos Bergou	
8:10 – 8:50 AM	Mikhail Lukin, *Harvard*	Exploring quantum computing frontier with programmable atom arrays
8:50 – 9:30 AM	Susanne Yelin, *Harvard*	Quantum chemistry on a quantum computer
9:30 – 10:10 AM	Vitaly Kocharovsky, *TAMU*	Universal mechanism behind quantum supremacy of many-body systems
10:10 – 10:40 AM	POSTER SESSION / BREAK	
Session chair: Vitaly Kocharovsky		
10:40 – 11:20 AM	Patrice Genevet, *Colorado School of Mines*	Scattering singularities & Metasurfaces
11:20 – 12:00 PM	William Case *Grinnell College*	Physics of the Swing
12:00 PM	**LUNCH**	Tobin Cafeteria
Afternoon recreational activities		

5:00 PM, Dinner in honor of Profs. Marlan Scully and Shiyao Zhu in connection with their 85th and 80th birthdays

Gateway Center (GW) 221/225

Thursday, July 18, 2024

7:00 – 8:00 AM	**BREAKFAST**	Tobin Cafeteria
PS103	Session chair: Gershon Kurizki	
8:10 – 8:50 AM	Shiyao Zhu & Dawei Wang *Zhejiang University*	Quantum simulation in superradiance lattices
8:50 – 9:20 AM	Muhammad Miskeen Khan *JILA*	Generating EPR correlations for teleporting collective spin states
9:20 – 10:00 AM	Philip Stamp, *Univ. of BC*	Quantum avalanches
10:00 – 10:30 AM	POSTER SESSION / BREAK	
	Session chair: Philip Stamp	
10:30 – 11:10 AM	Anzhong Wang, *Baylor*	From Loop Quantum Cosmology to Loop Quantum Black Holes: a Rough Road
11:10 – 12:00 PM	Anatoly Svidzinsky, *TAMU*	The nature of dark energy and electromagnetic origin of electron mass
12:00 PM	**LUNCH**	Tobin Cafeteria
	Afternoon recreational activities	
6:15 – 7:00 PM	**DINNER**	Outside PS 103
PS103		
7:00 – 7:50 PM	Carlo Fiorina, *TAMU*	Post-Ignition Physics and Engineering of Target Chambers in Inertial Fusion Energy Systems, Zoom
7:50 – 8:30 PM	Robert Nevels, *TAMU*	Radio and the Science of Wireless Transmission
8:30 – 8:50 PM	POSTER SESSION / BREAK	
8:50 – 9:30 PM	Aart Verhoef & Alma Fernandez, *TAMU*	Identification of molecules using Raman spectrometer

Friday, July 19, 2024

7:00 – 8:00 AM	**BREAKFAST**	Tobin Cafeteria
PS103	Session chair: Aart Verhoef	
8:10 – 8:50 AM	Zhenhuan Yi, *TAMU*	Cooperative Emissions in Atomic and Molecular systems
8:50 – 9:30 AM	Dmitri Voronine *Univ. of South Florida*	Raman Bronchoalveolar Lavage
9:30 – 10:00 AM	Jizhou Wang, *TAMU*	Wide-Field In Vivo Label-free Imaging with kHz frame rate
10:00 – 10:30 AM	POSTER SESSION / BREAK	
	Session chair: Arash Azizi	
10:30 – 11:10 AM	Janos Bergou, *Hunter College*	Wave-particle duality and beyond
11:10 – 11:50 AM	Yusef Maleki, *TAMU*	Gravitational Quantum Eraser
12:00 PM	**LUNCH**	Tobin Cafeteria
	Afternoon recreational activities	
6:15 – 7:00 PM	**DINNER**	Outside PS 103
PS103		
7:00 – 7:50 PM	Ed Fry, *TAMU*	Recent Nobel Prize and the Bell Inequalities
7:50 – 8:20 PM	POSTER SESSION / BREAK	
8:20 – 9:10 PM	Aart Verhoef, *TAMU*	Attosecond Physics

Saturday & Sunday, July 20-21, 2024, Dorm Kitchen (Rooms 144 & 192**)**

8:00 AM **BREAKFAST**	12:00 PM **LUNCH**	6:00 PM **DINNER**

Monday, July 22, 2024

7:00 – 8:00 AM	**BREAKFAST**	Tobin Cafeteria (bottom floor UU Bldg.)
PS103	Session chair: Weng Chow	
8:10 – 9:00 AM	Shaul Mukamel, *University of California, Irvine*	Multidimensional spectroscopy with quantum light, entangled photons, and X ray pulses
9:00 – 9:15 AM	John Barrasso, *U.S. Senator*	Overview and Welcome
9:15 – 10:00 AM	Zhenrong Zhang, *Baylor*	Phase Transition and Melting of Oxide via Plasmonic Heating
10:00 – 10:30 AM	POSTER SESSION / BREAK	
Session chair: Zhenrong Zhang		
10:30 – 11:00 AM	Jiru Liu, *TAMU*	Detecting multimode entanglement from classical-nonclassical polarity
11:00 – 11:30 AM	Mohit Khurana, *TAMU*	Photonic Integrated Circuits for applications in biosensing
11:30 – 12:00 PM	Yidan Wang, *Harvard*	Exploring universality in scattering theory through general dispersion relations
12:00 PM	**LUNCH**	Tobin Cafeteria (bottom floor UU Bldg.)
Afternoon recreational activities		

5:00 PM, Dinner, Hamburgers & hot Dogs, Gateway Center (GW) 221/225

Tuesday, July 23, 2024

7:00 – 8:00 AM	**BREAKFAST**	Tobin Cafeteria
PS103	Session chair: Gary Eden	
8:10 – 8:50 AM	*Matthew Wolford, U.S. Naval Research Laboratory*	Excimer Driver Technology for Laser Driven Inertial Confinement Fusion Energy, Zoom
8:50 – 9:30 AM	John Kline, *LANL*	Basics of laser fusion energy
9:30 – 10:10 AM	Carmen Menoni *Colorado State University*	The demands on optical materials in high power lasers for inertial fusion energy
10:10 – 10:40 AM	POSTER SESSION / BREAK	
Session chair: Carmen Menoni		
10:40 – 11:20 AM	Jorge Rocca *Colorado State University*	Ultra-intense laser interactions with nanostructures: creating extreme plasma conditions and high energy ions for fusion energy with ultrafast lasers
11:20 – 12:00 PM	Weng Chou, *Sandia*	Model for KrF amplifier and laser scaling
12:00 PM	**LUNCH**	Tobin Cafeteria
Afternoon recreational activities		
6:15 – 7:00 PM	**DINNER**	Outside PS 103
7:00 – 7:50 PM	Lorin Matthews, *Baylor*	Cosmic Dust Bunnies and Laboratory Dust Crystals: Modeling Complex Interactions in a Complex Plasma
7:50 – 8:20 PM	POSTER SESSION / BREAK	
8:20 – 9:10 PM	Kavita Kabelitz, *University of Illinois Urbana-Champaign*	Introduction of High-Power Laser Systems for Inertial Fusion Energy

Wednesday, July 24, 2024

7:00 – 8:00 AM	**BREAKFAST**	Tobin Cafeteria
PS103	Session chair: Aleksei Zheltikov	
8:10 – 8:50 AM	Arianna Gleason-Holbrook, *SLAC/Stanford*	From planetary interiors to harnessing star power: exploring the frontier matter at extreme conditions, Zoom
8:50 – 9:30 AM	Alexei Sokolov, *TAMU*	Novel Nonlinear Optics Enabled by Quantum Coherence
9:30 – 10:00 AM	POSTER SESSION / BREAK	
10:00 – 10:40 AM	Gary Eden, *TAMU/UIUC*	Krypton Fluoride as the Laser Driver for Inertial Fusion Energy
10:40 – 11:20 AM	Siegfried Glenzer SLAC/Stanford	The road to ignition and fusion energy gain
11:20 – 12:00 PM	Jean-Pierre Cayol *International Atomic Energy Agency*	The International Atomic Energy Agency: a Central Role in the Development and Promotion of Nuclear Applications for Sustainable Development
12:00 PM	**LUNCH**	Tobin Cafeteria
Afternoon recreational activities		
6:15 – 7:00 PM	**DINNER**	Outside PS 103
7:00 – 7:50 PM	Aleksei Zheltikov, *TAMU*	Rogue waves, black swans, and laser beam instabilities
7:50 – 8:10 PM	POSTER SESSION / BREAK, Session chair: Kavita Kabelitz	
8:10 – 8:40 PM	Barnabas Kim, *TAMU*	Introduction to the BGK relaxation model for the Boltzmann transport equation
8:40 – 9:10 PM	Arash Azizi, *TAMU*	Statistical mechanics and laser fusion: From BGK to BBGKY
9:10 – 9:40 PM	Reed Nessler, *TAMU*	Boltzmann equation and BGK for stimulated Brillouin scattering

Thursday, July 25, 2024

7:00 – 8:00 AM	**BREAKFAST**	Tobin Cafeteria
PS103	Session chair: Zhenhuan Yi	
8:10 – 8:50 AM	Truell Hyde*, Baylor/CASPER*	Complex Plasma Physics
8:50 – 9:10 AM	Rohil Kayastha*, Baylor*	Nano-Focusing and Characterization of the OAM Beam through an Optical Fiber Using Plasmonic Nanostructure
9:10 – 9:30 AM	Joi Malone, *Howard University*	Exploration of Magnetosensitive Proteins with Optically Pumped Quantum Sensors
9:30 – 9:50 AM	Zhenfei Jiang, *TAMU*	Mitigation of Scattering in a Quantum System Using an Integrating Sphere
9:50 – 10:10 AM	Alma Fernández*, TAMU*	Deep Super-Resolution Imaging with Three-Photon Image Scanning Microscopy
10:10 – 10:40 AM	POSTER SESSION / BREAK	
Session chair: Alma Fernández		
10:40 – 11:20 AM	Cleo Bentley, Jr., *Prairie View A&M University*	The Hydrogen, Lithium, Boron, and Nitrogen atom fine structure energy levels from electron average-path elliptical orbits and spin
11:20 – 11:50 AM	Christopher Marble, *Tarleton State University*	Hyper-Raman Spectroscopy of Biomolecules
11:50 – 12:10 PM	Tuo Jia, *TAMU*	Nambu Mechanics
12:10 PM	**LUNCH**	Tobin Cafeteria
Afternoon recreational activities		
6:15 – 7:00 PM	**DINNER**	Outside PS 103
PS103		
7:00 – 8:00 PM	**Presentations by high-school students**	
8:00 – 8:30 PM	POSTER SESSION / BREAK	
8:30 – 9:30 PM	**Presentations by high-school students**	

Friday, July 26, 2024

7:00 – 8:00 AM	**BREAKFAST**	Tobin Cafeteria
PS103	Session chair: Wenzhuo Zhang	
8:10 – 8:50 AM	Bob Nevels, TAMU	Progress in the Vector Diagram for Maxwell's Equations
8:50 – 9:20 AM	Suyash Bajpai *Howard University*	Optimizing slime mold solutions to NP-hard problems using synchronization indices
9:20 – 9:45 AM	Yiyun Li, *TAMU*	Lidar in entomological studies
9:45 – 10:15 AM	POSTER SESSION / BREAK	
10:15 AM	Brandon Kosine, *Interim President of Casper College* Mark Gordon*, Governor of Wyoming* Steve Degenfelder, *Casper College Board of Trustees* Marlan Scully, *Quantum Camp & Symposium*	**Concluding remarks, Group Photo, Certificates awarding ceremony**
12:00 PM	**LUNCH**	Tobin Cafeteria
Afternoon recreational activities		

Friday evening, July 26, 2024

6:00 – 7:00 PM: Dinner, Tobin Cafeteria (bottom floor UU Bldg.)

8:00 PM: Snack food is being delivered to the Residence Hall kitchen (1st floor)

Saturday morning, July 27, 2024

5:30 AM Breakfast is set in the Residence Hall kitchen (1st floor)

Posters:

1. Amal Vijayalekshmi Sivakumar, *TAMU*, Single photon scattering in a cavity with giant atomic mirrors coupled to a 1D waveguide
2. AmirAli Vanaki Farahani, *TAMU,* The electronic structure calculations of Fe doped monolayer MoS2 using density functional theory
3. Ayla Hazrathosseini, *TAMU*, Development of Photonic Biosensor based on Whispering-gallery Modes
4. Charles Wallace, *TAMU*, Suppression of Wigner Weisskopf Decay by the Acceleration of Entangled Atoms
5. Fan Yang, *TAMU,* Dynamics of Unruh effect and manifestation of Minkowski vacuum entanglement
6. Jiefei Wang, *Zhejiang University*, Quantum Simulator in Room Temperature
7. Jing Yang, *Zhejiang University,* Realization of all-band-flat photonic lattices
8. Joi Malone, *Howard University*, Exploration of Magnetosensitive Proteins with Optically Pumped Quantum Sensors
9. Kevin Chauwinoir, *TAMU,* From Classical Mechanics to Symplectic Manifolds in Mathematics
10. Kyra Frank, *Howard University*, Impacts of Static Magnetic Fields and Roles of Photoreceptors in slime mold Physarum polycephalum
11. Luke Ellert-Beck, *University of Rhode Island*, Power-optimized amplitude modulation for robust trapped-ion entangling gates
12. Ming-Hsun Chou, *TAMU*, Unveiling Molecular Mysteries: Integrating AFM-TERS for Enhanced Raman Spectroscopy and Surface Analysis
13. Nusrat Zahan Tanwee, *Baylor University*, Nanoscale Chemical Sensing Using Optical Fiber-based Near Field Scanning Microscopy (NSOM)
14. Olawale Ayoade, *Baylor University*, Understanding Plasmonic-TiO_2 Interactions: Au Nanoparticles on Single Bulk Crystal TiO_2 Surfaces for Redox Photocatalysis
15. Punyasloka Sahoo, *TAMU*, Detection and Classification of Aerosol Particles using Digital Inline Holography

16. Qingtian Miao, *TAMU*, Quantum Entanglement in the Ground State in Ultrastrong Coupling Regime
17. Riva Salzman, *TAMU*, High Resolution Imaging of Soil Aggregate Pore Space and Microbial Activity using Optical Coherence and Multiphoton Microscopy
18. Sahar Delfan, *TAMU,* Photonic Biosensor in Young Interferometer Configuration
19. Sanjib Thapa, *Baylor University*, Enhancing Optical Fiber Sensitivity with Diatoms and Nanoparticles
20. Sheila Chauwinoir, *TAMU,* Hanbury Brown and Twiss Demonstration: Intensity Autocorrelation Function of a Thermal Light
21. Srila Palanikumar, *Howard University*, Quantum Fourier Transform for Medical Resonance Imaging Data Reconstruction
22. Yanli Shi, *TAMU*, On demand Zeeman Frequency Comb Quantum Memory via reversing the B direction

Summer School is organized by:

Bob Brick, Reed Nessler, Marlan Scully, Anatoly Svidzinsky, Zhenhuan Yi, Aleksei Zheltikov

Afternoon Activities

- This year, we will feature a number of afternoon activities such as hiking, kayaking, swimming, rafting, and others.

- The activities will be divided into three groups: free activities, reserved paid activities that are organized by us beforehand, and other paid activities that you can organize yourselves.

- The sign up sheets for these activities will be in the lobby of the dorms so that you can organize into groups and decide who will go, who will drive, etc.

- If you can drive, put a number to the right of your name in the "Number of seats" column. It is up to those interested in the activity to ensure that there are enough drivers with enough seats.

- Rafting and horseback riding can only accommodate a certain number of people, so do not write in more names than there are on the sign up sheet.

- People generally congregate in the lobby around 1:30-2:00 p.m. after lunch to gather together and depart for the activity (although the reserved activities may start later in the afternoon).

Free Activities

Hiking:
The most common spots to hike around Casper are Rotary Park and Casper Mountain. Both are easily within driving range for an afternoon and feature beautiful views. More trails can be found on sites such as alltrails.com.

Swimming:
Sandy Beach at the nearby Alcova Reservoir features nice, cold water and a relatively large area for swimming.

Tate Geological Museum:
The Tate Geological Museum sits on the Casper College Campus at the top of the hill and features various geology and paleontology exhibits. It is free to enter, and we will attempt to organize either a guided tour with a paleontologist who works at the museum or a fossil dig at some point throughout the duration of the summer school/science camp.

Reserved Paid Activities

To start, the summer school/science camp organizers will reserve only one outing of these paid activities for the first week, but we will not hesitate to reserve more if there is more interest shown than there is capacity for each activity. Additional interest forms will be included with the sign up sheets in case the activity is full.

Rafting (now a free activity–paid for by IQSE and Casper Foundation):
The rafting will take place on the North Platte River which runs through Casper and features a few large rapids on the section of the route inside of the city. Cost is usually $20 per person, but the IQSE and Casper Foundation have graciously decided to pay the costs for all those who wish to attend. The location and time will be on the sign up sheet.

Horseback Riding:
Horseback riding has always been a popular activity during the Casper summer school. For this activity, you will be taken on a trail ride around the area by the barn. The cost will be $65 per person. The location, time, and payment details will be on the sign up sheet.

Other Paid Activities

These activities are activities that people have done in the past, but the summer school/science camp organizers will not make reservations for any groups prior to the start of the summer school/science camp.

Shooting Lessons:
Shooting lessons are offered at Wyoming Gun Company in Casper. They will teach you about gun safety, how to shoot properly, and let you practice some after the lesson. The details can be found at the Wyoming Gun Company's website under the "Events" tab.

Kayaking:
Kayaks can be rented relatively cheaply at the Lake Alcova Resort. They serve on a first come, first serve basis, and rates, availability, and location can all be found at their website alcovaresort.com.

Talk Abstracts

(Listed Alphabetically by Presenter’s Last Name)

Time Reversed Quantum Metrology*

Girish Agarwal**

Texas A&M University

ABSTRACT

It is well recognized that quantum physics can be used to build better sensors. The parameters of special interest are phases, forces, fields that correspond to the unitary evolution of the system or others like absorption, scattering [1] require description in terms open system dynamics. In each case the framework of the quantum Fisher information is especially suited to obtain best estimates of the parameters in terms of the Cramer-Rao bound and then one can design experiments that can saturate Cramer- Rao bounds. I would highlight the importance of the quantum states used as probes, and the importance of the quantum-ness of the measurement schemes. It turns out that in many cases the schemes based on time reversed metrology [2-4] saturate Cramer-Rao bounds. I would discuss the great utility of squeezed states of bosonic systems like photons, ions and cat states of qubits for metrological applications. I will also present preliminary results on multiparameter estimation using multiphoton entangled states.

---

*work done with Jiaxuan Wang, M. Kamble, R. L. De Matos Filho, L. Davidovich

**girish.agarwal@tamu.edu

1. J. Wang, L. Davidovich, and G. S. Agarwal, "Quantum sensing of open systems: Estimation of damping constants and temperature," Phys. Rev. Research 2, 033389 (2020).

2. G. S. Agarwal, and L. Davidovich, Quantifying quantum-amplified metrology via Fisher information, Phys. Rev. Res. 4, L 012014 (2022).

3. J. Wang, R. L. De Matos Filho, G. S. Agarwal, and L. Davidovich, Quantum advantage of time-reversed ancilla-based metrology of absorption parameters, Phys. Rev Res. 6, 013034 (2024).

4. M. Kamble, J. Wang and G. S. Agarwal, Quantum Metrology of Absorption and Gain Parameters using Two-Mode Bright Squeezed Light, Phys. Rev. A 109, 053715 (2024).

Statistical mechanics and laser fusion:
From BGK to BBGKY

Arash Azizi

The Institute for Quantum Science and Engineering,
Texas A&M University, College Station, TX 77843, USA

The National Ignition Facility's 2022 breakthrough [1] is a real game-changer in one of the long-time goals of physics/engineering: fusion. This process is theoretically based on a well-known phenomenon in physics, namely stimulated Brillouin scattering. More fundamentally, the light-matter interaction is a non-equilibrium interaction and obeys the Boltzmann transport equation. However, the collision integral in the latter can be approximated by the relaxation method of Bhatnagar–Gross–Krook (BGK).

In this tutorial talk, we review the kinetic model of Sugawara-Yip [2], which is based on the BGK approximation.

Moreover, the Bogoliubov-Born-Green-Kirkwood-Yvon (BBGKY) hierarchy is a set of equations describing the dynamics of a system of a large number of interacting particles. Since the first term in the hierarchy gives the Boltzmann equation, one aims to generalize the kinetic model of Sugawara-Yip based upon insight from the BBGKY hierarchy.

References

[1] H. Abu-Shawareb *et al.* (The Indirect Drive ICF Collaboration), *Achievement of Target Gain Larger than Unity in an Inertial Fusion Experiment*, Phys. Rev. Lett. 132, 065102 (2024).

[2] A. Sugawara and S. Yip, *Kinetic Model Analysis of Light Scattering by Molecular Gases*, Phys. Fluids 10, 1911–1921 (1967).

Optimizing slime mold solutions to NP-hard problems using synchronization indices

Suyash Bajpai, Sanghita Sengupta and Philip Kurian
Quantum Biology Laboratory, Howard University, Washington, DC, 20060
https://www.quantumbiolab.com/

Despite its simple morphology, *Physarum polycephalum* – an ancient, multinucleate, single-celled slime mold amoeba – possesses sophisticated information-processing capabilities. *Physarum* has solved the shortest path problem in complex mazes (Fig. 1) and demonstrated that it can solve completely or approximately a variety of other optimization problems, including the Boolean satisfiability and traveling salesman problems (TSP). Additionally, it can encode memory of prior periodic stimuli, recapitulating its periodic response when subjected to a similar non-periodic stimulus at much later times. Such intriguing behaviors in nonequilibrium active matter make *Physarum* a rich playground for exploring the relationship between its intrinsic oscillatory dynamics and the computational complexity of problems it can solve.

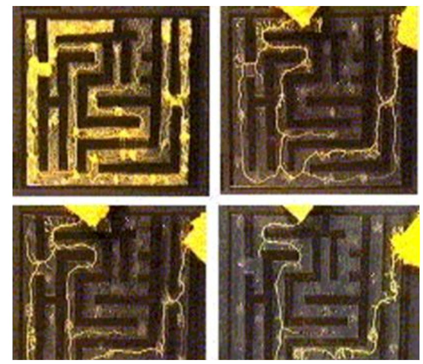

Fig. 1: *Physarum* solving mazes.

Exploiting *Physarum's* shape-changing dynamics and photoavoidance behavior in custom-fabricated stellate chips with a Hopfield neural network controlling the optical feedback, we have instantiated the TSP for *Physarum* using N "neuron" lanes for a $\sqrt{N}$-city problem (Fig. 2). Earlier works demonstrated that *Physarum* provides a high-quality solution for non-trivial TSP instances of up to eight cities with approximately linear dependence of computation time on problem size. In contrast, the best approximate classical algorithms (such as the Lin-Kernighan heuristic, simulated annealing, or genetic algorithm) exhibited only a quadratic dependence at best. We aim to verify if this linear scaling of computation time with the problem size extends to larger TSP instances of up to 20 cities. In order to optimize the correlations among the N branches of *Physarum*, we analyzed an order parameter known as the synchronization index, $S = 1/N \left|\sum_{i=1}^{N} e^{i\phi_i}\right|$, where ϕ_i is the individual phase of a branch at a particular time. When there is no synchronization among the branch phases, S is 0. Otherwise, S takes a positive value, reaching maximum phase synchronization when S is 1. We observed higher synchronization indices for shorter tours, suggesting its potential utility as a metric in selecting high-quality TSP solutions. Synchronization indices in the nonequilibrium steady state exhibit higher (nearly 1) values when *Physarum* reaches a solution. To improve the problem-solving efficiency of *Physarum*, techniques from stochastic resetting and noise-induced transitions will be applied to overcome local energy minima in which the slime mold's optimization algorithm is trapped, thereby enabling it to find the global minimum via "jumps" (resets) outside of the local exploratory phase space.

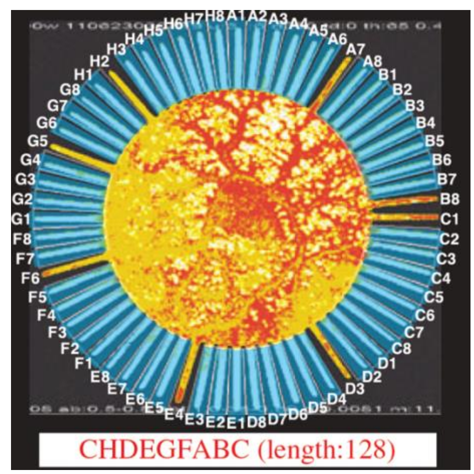

Fig. 2: Solving 8-city TSP employing *Physarum*.

The Hydrogen, Lithium, Boron, and Nitrogen atom fine structure energy levels from electron average-path elliptical orbits and spin

By

Cleo L. Bentley, Jr.

Prairie View A&M University

Abstract: If one takes the average path of an odd-valence electron in hydrogen, lithium, boron, and nitrogen atoms to be elliptical around a spherical force-field porous barrier at a Bohr radius r_n from a proton-source diffraction pattern, improvement in precision of theoretical fine-structure energy values is observed over that found in Schrodinger Quantum Electrodynamics (QED.)

Wave-particle duality and beyond

János A. Bergou

Department of Physics & Astronomy, Hunter College, and the Graduate Center
City University of New York

I'll briefly review the now 100-year-old history of wave-particle duality, which started with the famous Einstein-Bohr debate at the 1927 Solvay conference. Using the device, shown in the figure, Einstein argued that, by measuring the recoil momentum of the first screen, one can have information about which slit on the second screen the photon went through, while also have the interference pattern. Bohr correctly pointed out that measuring the momentum with the required accuracy will inevitably lead to uncertainty in the position of slit in screen 1 which will wash out the interference pattern on screen 3 [1].

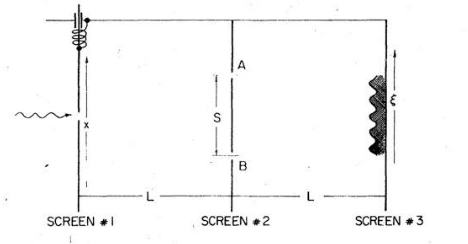

These considerations gradually evolved into quantitative complementarity relations, quantifying wave-particle duality [2]. Wave-like and particle-like realities have their classical analogs. We have shown that entanglement forms a genuine quantum reality with no classical analog. Together, the three realities fully exhaust the information content of a quantum state. The measures of wave-like character, visibility V, particle-like character, predictability P, and entanglement, concurrence C, add up to a complete complementarity relation, $P^2+V^2+C^2 \leq 1$ [3]. Most quantum systems exhibit some wave-like character, some particle-like character, and some entanglement, so they are neither waves, nor particles. They are just that: genuine quantum systems. The actual form of the above complementary relation depends on the measurement used to obtain which path information and we present a generalization of the above formula for arbitrary measurement, and entropic complementarity relations between entropic measures of coherence, path, and entanglement, as well [4]. To close, we discuss the relation between the quantum eraser and complementarity [5].

References

[1] N. Bohr, Das Quantenpostulat und die neure Enrwicklungen der Atomistik, Naturwissenschaften **16**, 245 (1928).
[2] D. M. Greenberger and A. Yasin, "Simultaneous wave and particle knowledge in a neutron interferometer," Phys. Lett. **A128**, 391 (1988); B.-G. Englert, "Fringe Visibility and Which-Way Information: An Inequality," Phys. Rev. Lett. **77**, 2154 (1996); B.-G. Englert and J. A. Bergou, "Quantitative quantum erasure," Opt. Comm. **179**, 337 (2000).
[3] M. Jakob and J. A. Bergou, "Quantitative complementarity relations in bipartite systems: Entanglement as a physical reality," Opt. Comm. **283**, 827 (2010) [also as arxiv:0302075]; M. Jakob and J. A. Bergou, "Complementarity and entanglement in bipartite qudit systems," Phys. Rev. A **76**, 052107 (2007).
[4] E. Bagan, J. A. Bergou, S. S. Cottrell, and M. Hillery, "Relations between Coherence and Path Information," Phys. Rev. Lett. **116**, 160406 (2016).
[5] M.O. Scully and K. Drühl, Quantum eraser: A proposed photon correlation experiment concerning observation and "delayed choice" in quantum mechanics, Phys. Rev. A **25**, 2208 (1982).

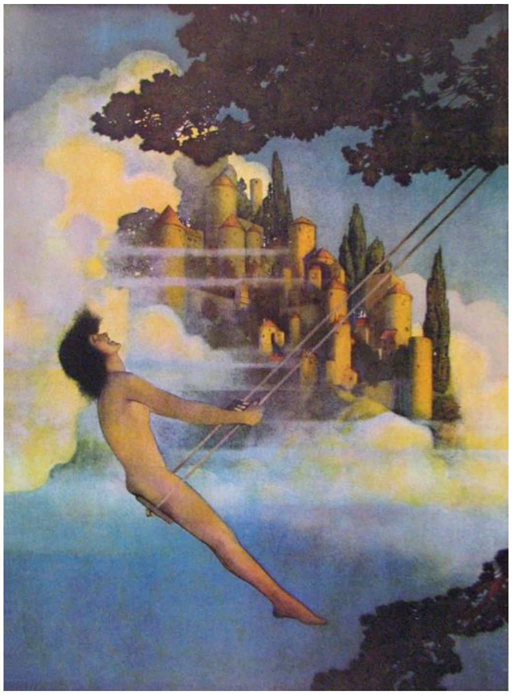

Physics of the Swing

William Case, Grinnell College

The pumping of the playground swing has long been seen as an example of a parametric instability, described by the Mathieu equation. I will argue that this is not true and that the swing is best described as a driven harmonic oscillator. I will present both theoretical and experimental evidence in support of this conjecture.

W. B. Case, M. A. Swanson, Am. J. Phys. 58, 463, ('90)

W. B. Case, Am. J. Phys. 64, 215, ('96)

https://youtu.be/MbWhKFIayp4?si=3m6S2DYqA89sJhWW

The International Atomic Energy Agency: a Central Role in the Development and Promotion of Nuclear Applications for Sustainable Development

Jean-Pierre Cayol

Departmental Programme Coordinator, Department of Nuclear Sciences and Applications, International Atomic Energy Agency, Vienna International Centre, PO Box 100, A-1400 Vienna Austria

Email: j.p.cayol@iaea.org

December 8th, 1953, United Nations General Assembly, New York City. H.E. Dwight Eisenhower, 38th President of the United States of America walks to the podium and takes the floor to deliver what became known as the “Atoms for Peace” speech (photos below).

Such is the genesis of the International Atomic Energy Agency (IAEA), established in 1957, twelve years after the end of World War II, in Vienna, Austria.

Today, almost 61 years after the “Atoms for Peace” speech, the IAEA stands strong, with the support of its 178 Member States, delivering its mandate along three pillars: safeguarding the nuclear fuel worldwide, ensuring the safe and secure use of nuclear sources and equipment, and promoting nuclear sciences, technologies and applications.

Relying on its twelve laboratories dedicated to applied research and development and over 1,000 scientists in Member States working in collaboration with its specialized staff, the IAEA is contributing to making peaceful nuclear applications available in all aspects of basic human needs, contributing directly to nine and indirectly to all 17 Sustainable Development Goals.

The IAEA’s integral role to address some of today’s most pressing global challenges as a science and technology-based Organization has made it indispensable in areas where radiation and nuclear techniques offer solutions where conventional techniques cannot. From providing accurate information on availability of fresh water resources so countries know how many years of water they still have, to diagnosing diseases such as Alzheimer’s, cardiovascular diseases and cancer to recycling plastic waste which would have needed over 100 years to break down, and monitoring the intake of carbon dioxide in the ocean as well as controlling life- and livelihood-threatening insect pests that are transmitting diseases, nuclear applications are in everyday life, even though the public understanding may not reflect that.

All these applications are based on the physical and chemical properties of the atoms, using irradiation to sterilise or modify organisms or materials or using radio- or stable isotopes for tracing biological or physical processes. This lecture will examine the myriad of applications offered through nuclear science and the efforts exerted to ensure that these integral technologies reach the people in need around the world, be it cancer patients in Latin America, rural communities facing limited harvest of wheat due to drought in Sub-Saharan Africa, or the challenges of securing safe food for entire populations in Southeast Asia, while overcoming the “nuclear stigma” in a rapidly evolving global landscape.

Goong Chen

Department of Mathematics and Institute for Quantum Science and Engineering,
Texas A&M University, College Station, TX 77843, USA

Animal shapes and their modal analysis (I): Basic model and properties

ABSTRACT

We develop mathematical and computational models for the analysis of animal shapes, such as horse, camel, duck, goose, giraffe, dinosaur, and eagle. The partial differential equations of linear elastodynamics are studied, and the conservation laws of momentum, angular momentum and energy are established. Eigenmodes of the time-harmonic equations are computed and displayed, and compared with the actual motions of certain of these animals.

Animal shapes and their modal analysis (II): Movie making with AI applications

Abstract

We use movie making of dinosaur motions as motivation to illustrate how to use modal analysis in computational mechanics for movie making purposes. Artificial intelligence (AI) techniques are applied to perform machine training for different models of dinosaurs.

Model for KrF amplifier and laser scaling

Weng Chow

Sandia National Laboratories, Albuquerque, NM 87185-1086

ABSTRACT

This paper discusses a laser model for investigating energy scaling in KrF amplifiers. Of interest are amplifier gain, energy extraction and amplified spontaneous emission loss, especially their dependences on excitation, device geometry and window reflection. The numerical calculations are based on Rigrod analysis as sketched in Figure 1a. The laser transition is between upper and lower KrF states, $|u\rangle = |B, v, J, M\rangle$ and $|l\rangle = |X, v', J', M'\rangle$. A multimode semiclassical laser derivation gives the saturated gain used in the d/dz propagation:

$$G_{sat}(\nu_n) = \frac{G_0(\nu_n, N_u)}{1 + \sum_m \kappa(\nu_n, \nu_m) I(\nu_m)} \quad . \tag{1}$$

In Equation (1), G_0 describes gain resulting from depletion of the entire $|u\rangle$ population by scattering between rotational state populations. N_u is the saturated population determined by d/dt integration. κ is the self- and cross-gain compression factors (borrowing semiconductor notation), which cause further saturation by spectral and spatial hole burnings. The quantum-mechanical polarization at the 4-wave-mixing level gives the optical nonlinear contributions.

Figure 1b shows the two gain saturation contributions for different inject laser power. The dimensionless intensities corresponds to injected laser powers of 73 mJ, 730 mJ and 7.7 J. The left plot shows gain depression from the unsaturated case (dashed spectrum) by reduction in the entire KrF inversion. The right plot shows the additional saturation with hole burning. Figure 1c indicates the resulting amplifier output spectra, amplifier gain and signal-to-noise ratio.

Figures 1b and 1c are chosen to illustrate model capabilities. We look forward to suggestions on the model improvement and application.

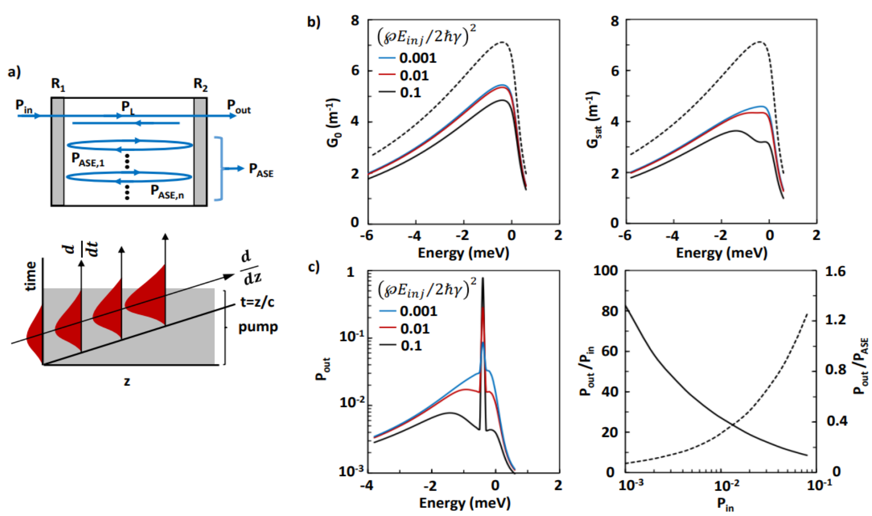

Figure 1. (a) Rigod analysis. Example uses window reflectivities 4%, 1 m amplifier length and excitation giving 10^{19}m^{-3} KrF upper state density. (b) Saturated gain spectra. P_{out} = 0.1 corresponds to 6 Joules. (c) Output behaviors.

Generalization of the Edgeworth and Gram-Charlier series and application to quantum mechanics

LEON COHEN

City University of New York, 695 Park Ave. New York, NY 10065

The main historical purpose of the Gram-Charlier and Edgeworth series is to "correct" a Gaussian distribution when new information, such as moments, is given which do not match those of the Gaussian. These methods relate a probability distribution to a Gaussian by way of an operator transformation that is a function of the differentiation operator. We use the methods of the phase-space formulation of quantum mechanics to generalize these methods. We generalize in two ways. First, we relate *any* two probability distributions by way of a function of the differentiation operator. Second, we generalize to the case where the differentiation operator is replaced by an arbitrary Hermitian operator. The generalization results in a unified approach for the operator transformation of probability densities. Also, when the Edgeworth and Gram-Charlier series are truncated, the resulting approximation is generally not manifestly positive. We present methods where the truncated series remains manifestly positive.

Time-domain quantum light spectroscopy and sensing

Konstantin Dorfman[1,2,3]

[1]Center for Theoretical Physics and School of Sciences, Hainan University, Haikou 570228, China

[2]State Key Laboratory of Precision Spectroscopy, East China Normal University, Shanghai 200062, China

[3]Himalayan Institute for Advanced Study, Unit of Gopinath Seva Foundation, MIG 38, Avas Vikas, Rishikesh, Uttarakhand, India 249201

Email: dorfmank@hainanu.edu.cn

Abstract

I will discuss how new quantum phenomena in complex systems can be studied and controlled using advances in both quantum optics and nonlinear spectroscopy. In particular, I investigate how to probe, control, and image the spectral information of these complex systems using entangled and squeezed quantum state of light reveal the material information, which is not accessible by conventional classical photonics tools. In particular I will share our recent progress in extending the quantum light techniques to time-domain using ultrafast upconversion technique nonlocally mapping the MIR information to the time domain. Broadband MIR photons from spontaneous parametric downconversion are frequency-upconverted to the near-infrared band with quantum correlation preservation. The developed approach circumvents scanning and frequency selection instability, which stands out for its inherent compatibility for evolving environments and scalability for various wavelengths. Because of its high sensitivity and robustness, characterization of biochemical samples and weak measurement of quantum systems are possible to foresee.

Krypton Fluoride (248 nm) As the Laser Driver for Inertial Fusion Energy (IFE)

J. Gary Eden (University of Illinois)

Laser fusion energy (LFE) offers the potential to generate electrical power by the same process that our Sun produces energy. Recent experiments at the Lawrence Livermore National Laboratory (LLNL) have realized the long-sought goal of scientific breakeven - the generation of more energy from a laser-irradiated, deuterium-tritium (DT) target than that delivered to the target by the laser. This breakthrough in LFE suggests that the commercial-generation of electrical power is feasible but the most-challenging goal - realizing an economically viable power plant - lies ahead. This presentation will focus on the krypton-fluoride laser (248 nm) as the most attractive optical driver for the industrial production of power by LFE.

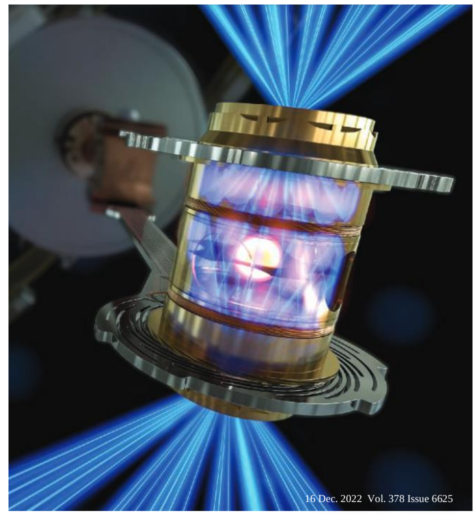

https://www.science.org/doi/epdf/10.1126/science.adg2854

J. Gary Eden has served as a member of the faculty of the University of Illinois (Urbana) for 45 years. After receiving the Ph.D. degree in Electrical Engineering in 1976, he conducted research in the Optical Sciences Division of the U.S. Naval Research Laboratory (Washington, DC) from 1976 to 1979. While at NRL, he co-discovered several lasers, including the KrCl (222 nm) laser and the first proton beam-pumped lasers (Ar-N_2, XeF). Since joining the faculty of the University of Illinois in 1979, he and his students have pursued the discovery of lasers and high-power lamps and their applications, atomic, molecular and ultrafast laser spectroscopy, optical physics in atoms and small molecules, and the science, technology, and commercialization of microcavity plasma devices. He is currently the Intel Alumni Endowed Chair Emeritus in the Department of Electrical and Computer Engineering (ECE) at UIUC, and is a co-Founder of Eden Park Illumination, EP Purification, Cygnus Photonics, EPL Power Electronics, and the Eden Park Foundation. Sixty-five individuals have received the Ph.D. degree under his direction, and his current research focuses on laser fusion energy (LFE), ultrafast optical physics such as the control of atomic coherences, a new generation of optical amplifiers, VUV photochemistry in the solid state, plasma photonic crystals, and the disinfection of drinking water in the developing world. He was elected to the National Academy of Engineering in 2014.

This talk is supported by the U.S. Department of Energy (DOE), Office of Science, Fusion Energy Sciences, under Award No. DE-SC0024882: IFE-STAR.

Deep Super-Resolution Imaging with Three-Photon Image Scanning Microscopy

A. Fernandez[1], A. Classen[1], I.M. Antolovic[2], S. Vitha[1], M. Pacheco[1], D. McCreedy[1], A.V. Sokolov[1], G.S. Agarwal[1], and A.J. Verhoef[1]

[1]Texas A&M University, College Station, TX 77843, USA
[2]Pi Imaging Technology, Lausanne, CH 1015, Switzerland
alma.fernandez@tamu.edu

Laser scanning multiphoton microscopy allows imaging deep in samples, as the nonlinearity causes the excitation to be strongly confined in the axial direction, that is, multiphoton microscopy comes with intrinsic sectioning of the signal. However, the resolution in laser scanning microscopy is given by how tightly one can focus the beam, which is the so-called Abbe limit, given by the wavelength λ, divided by twice the numerical aperture NA of the focusing element (objective). Thus, compared to single photon excited microscopy, for two- and three-photon excited microscopy the resolution worsens by a factor $\sqrt{2}$ or $\sqrt{3}$ respectively. To overcome the Abbe resolution limit, several approaches have been developed for single photon excited microscopy [1–5]. Of those methods, structured illumination microscopy [2] and image scanning microscopy (ISM) [4] can be applied with virtually any fluorescent marker, which makes them the most widely applicable super-resolution methods. ISM is implemented with laser scanning confocal microscopy, and recently it was demonstrated to be applicable to two-photon microscopy [6], achieving deep imaging with a resolution better than what is achieved with confocal microscopy.

In this work we demonstrate 3-photon excited (3PE) ISM experimentally and show the utility of this approach for various imaging scenarios. We achieved resolution enhancements of 1.6 laterally and 1.8 axially for 3PE-ISM over standard 3PE microscopy. We demonstrate that with 3PE-ISM it is possible to surpass the resolution achievable with confocal microscopy for the same fluorophore, despite the three times longer excitation wavelength. Including deconvolution, the resolution enhancements reach factors of 2.5 in the lateral and 3.0 in the axial direction, as is shown in Fig. 1 (left)

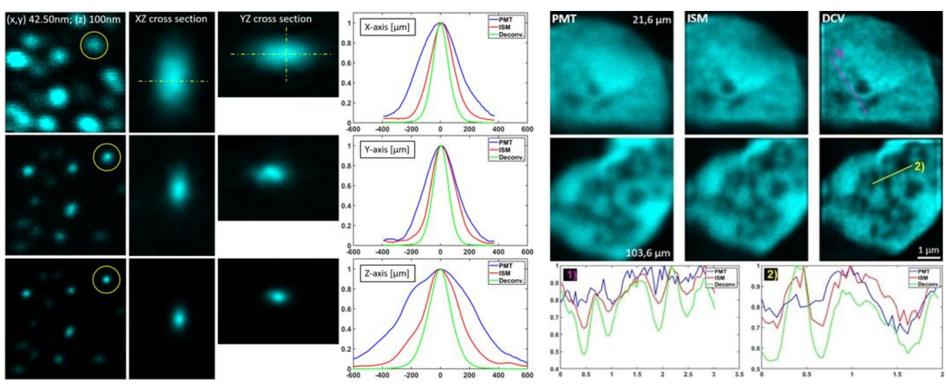

Fig. 1. (left) Results of measurements of a sample with dispersed QD450 quantum dots. The yellow circle indicates the sub-diffraction-limited emitter used to extract the 3-dimensional PSF for NDD (top row), ISM (middle row) and ISM combined with deconvolution (bottom row). (Right): 3PE of DAPI from thick cleared mouse spinal cord samples, demonstrating the ability of 3PE ISM to image with sub-diffraction limited resolution deep into samples (bottom row).

Finally, we use the system for in-depth imaging of fixed biological samples. The right panel of Fig. 1 shows images obtained from a sample containing mouse spinal cord tissue stained with the DNA marker DAPI (thus highlighting the cell nuclei). The resolution and contrast enhancement offered by ISM over standard PMT detection is clearly observed.

References:

1. S. Hell, J. Wichmann, Breaking the diffraction resolution limit by stimulated emission: stimulated-emission-depletion fluorescence microscopy, Opt. Lett. 19, 11, 780 (1994).
2. M. Gustafsson, Surpassing the lateral resolution limit by a factor of two using structured illumination microscopy, J. Microsc. 198, 2, 82 (2000).
3. E. Betzig, et al., Imaging Intracellular Fluorescent Proteins at Nanometer Resolution, Science 313, 5793, 1642 (2006).
4. C. Müller, J. Enderlein, Image Scanning Microscopy, Phys. Rev. Lett. 104, 198101 (2010).
5. A. Alva, et al., Fluorescence fluctuation-based super-resolution microscopy: Basic concepts for an easy start, Journal of Microscopy 288, 3, 218 (2022),
6. S. Koho, et al., Two-photon image-scanning microscopy with SPAD array and blind im- age reconstruction, Biomed. Opt. Express 11, 6, 2905 (2020).

Post-Ignition Physics and Engineering of Target Chambers in Inertial Fusion Energy Systems

Carlo Fiorina

Texas A&M University

This lecture is an overview of the post-ignition physics within inertial fusion energy chambers, with a focus on the engineering challenges and implications of these phenomena. Key topics include the outcomes of target ignition, the impact of neutrons and x-rays, the behavior of thick liquid walls under extreme conditions, the management of ablation and vapor transport. We will explore the theoretical foundations of these processes and their practical implications for the design and operation of inertial fusion reactors. The session is designed to provide an understanding of how post-ignition phenomena impact the development and optimization of fusion energy systems.

Recent Nobel Prize and the Bell Inequality

Edward S. Fry

Department of Physics and Astronomy
Texas A&M University, College Station TX 77843-4242

Abstract

The Nobel prize in 2022 was awarded to John Clauser, Alain Aspect and Anton Zeilinger for their experimental tests of the Bell Inequalities. The conceptual foundations of quantum mechanics and Bell Inequalities will be discussed. And the decades long history of the contentious problem will be reviewed together with some of the associated quotes; *e.g* Einstein believed that quantum mechanics was an incomplete theory and is famously quoted from a letter he wrote to Max Born in 1944: "You believe in God playing dice and I in perfect laws in the world of things existing as real objects . . ." A breakthrough analysis by John Bell in 1964 and the resulting Bell Inequality that made it possible to experimentally test these heretofore philosophical arguments will be discussed. Results of many experimental tests of the Bell inequalities will be presented and one surprising result is that Einstein was wrong. Results (agreement or not with QM) of the five earliest experiments, and the Zeilinger experiment will be provided:

1) 1972: **Clauser** (& Freedman); QM-Yes; data collection ~200 hours
2) 1973: Holt (& Pipkin); QM-No; data collection ~200 hours
3) 1976: **Clauser**; QM-Yes; data collection ~200 hours
4) 1976: Fry (&Thompson); QM-Yes; data collection ~60 minutes
5) 1981: **Aspect** (& Grangier, Roger) QM-Yes; data collection ~13 minutes
6) 1998: **Zeilinger** (& 4 others) QM-Yes; data collection ~10 seconds

Scattering Singularities & Metasurfaces

Patrice Genevet

Colorado School of Mines, Golden CO, USA

Optical singularities are points at which a physical quantity, such as the phase, polarization, polarization ellipticity, etc., is not defined, but around which this same physical quantity can take almost any value. Singularities are ubiquitous in nanophotonics as they generically occur when varying at least two optical or geometrical parameters of the system. Here, we present approaches to design nanophotonic building blocks with desired optical responses via singularity position engineering[1]. We show that the control of the positions of zeros and poles of optical response functions (e.g., reflection, transmission coefficient or scattering, and Jones matrices), the so-called singularities, can be used to design optical metasurfaces with desired amplitude and phase behaviors[2]. Additionally, breaking the in-plane symmetries of the metasurface is shown to achieve a phase singularity for only one circular polarization state, while its orthogonal counterpart remains unmodulated, thereby opening new avenues for the information multiplexing with nanophotonic designs[3]. Sharing similarities and inspiration from established works in signal processing and control theory, it is expected that the control of the position of complex-valued singularities in the "pole-zero complex-plane," for example relying on symmetries, would provide new design methodologies in photonics.

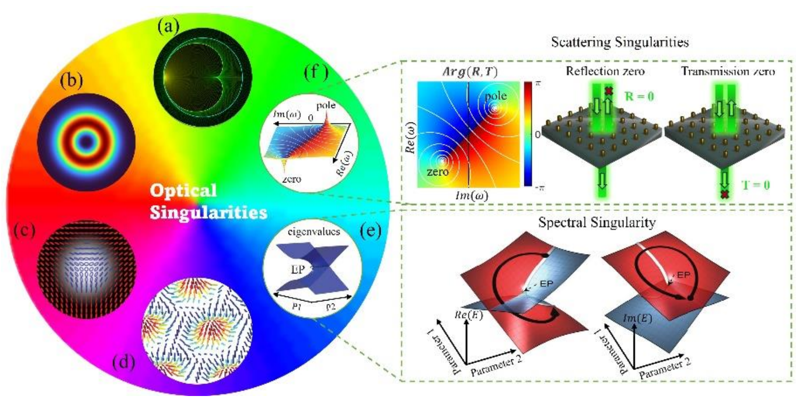

Figure: Optical singularities and their topological features, reproduced from [4].

[1] Plasmonic topological metasurface by encircling an exceptional point ***Science*** 373 (6559), 1133-1137 (2021)
[2] Crossing of the Branch Cut: The Topological Origin of a Universal 2π-Phase Retardation in Non-Hermitian Metasurfaces ***Laser & Photonics Reviews*** 17 (6), 2200976 (2023)
[3] Asymmetric phase modulation of light with parity-symmetry broken metasurfaces ***Optica*** 10 (10), 1287-1294 (2023)
[4] Roadmap on photonic metasurfaces, ***Appl. Phys. Lett.*** 124, 260701 (2024)

From planetary interiors to harnessing star power: exploring the frontier matter at extreme conditions

A. Gleason *(SLAC/Stanford University)*

The study of matter under extreme conditions is a highly interdisciplinary subject with broad applications to materials science, plasma physics, geophysics and astrophysics. Understanding the processes which dictate physical properties in warm dense plasmas and condensed matter requires studies at the relevant length-scales (e.g., interatomic spacing) and timescales (e.g., phonon period). Experiments performed at XFEL light sources across the world, combined with dynamic compression, provide ever-improving spatial- and temporal-fidelity to push the frontier. This talk will cover a very broad range of conditions, intended to present an overview of important recent developments in how we generate extreme environments and then how we characterize and probe matter at extremes conditions– providing an atom-eye view of transformations and the fundamental physics dictating plasma and materials properties. Examples of case-studies closely related to planetary sciences and inertial fusion energy, as enabled by ultrafast X-ray imaging, diffraction and spectroscopy, will be discussed.

Photon number squeezed states in semiconductor quantum dot lasers

Frédéric Grillot

Institut Polytechnique de Paris, France & University of New-Mexico, USA

ABSTRACT

Squeezed states of light have become a versatile tool in quantum optics, significantly advancing optical information technology and precision measurements. Various methods exist to generate these states, including cavity-enhanced nonlinear processes using nonlinear crystals, optical fibers, and integrated photonics platforms.[1] Additionally, quiet pump-driven semiconductor lasers, utilizing quantum dots (QDs) as gain media, show promise for producing non-classical states of light. In this study, we demonstrate photon number squeezed states from a single-mode QD gain chip operating under quiet pumping conditions, and achieving 1 dB squeezing with a 9 GHz bandwidth at room temperature.[2] After noise correction, the squeezing level improves to 3.1 dB, highlighting the QD potential for quantum PIC.

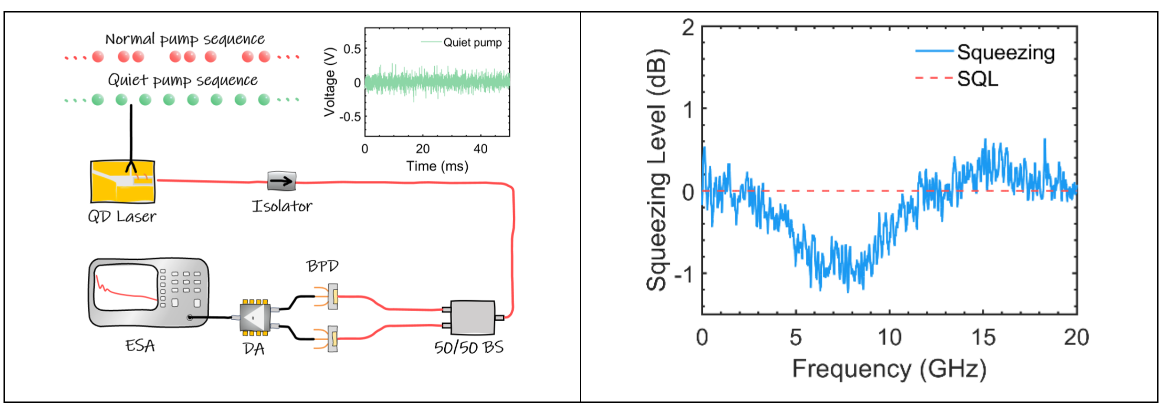

Figure: Noise spectrum measured using a self-homodyne detection with the QD laser driven by a quiet pump. The squeezing level achieved is 1 dB. The red dashed line indicates the shot noise level.

1. U. L. Andersen et al., 30 years of squeezed light generation, IOP Physica Scripta (2016).
2. S. Zhao et al., Accepted, Physical Review Research (2024).

Complex Plasma Physics

Truell W. Hyde

Director, Center for Astrophysics, Space Physics & Engineering Research (CASPER)
Professor of Physics, Baylor University

ABSTRACT

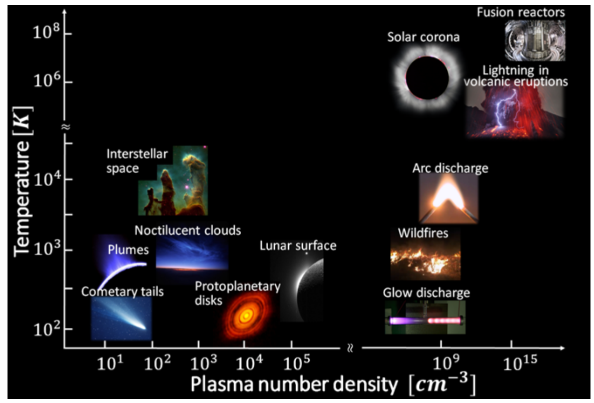

A large percentage of the visible matter in the Universe can be considered to be in a complex plasma state. Within this parameter space, nanometer to micron size particles comprise the solid component of the complex plasma with these particles acting either as probes of the local environment or integral components of the complex plasma itself. This combination produces novel physics as evidenced by the formation of both symmetric and/or asymmetric structural 'states' and 'state changes' as well as new physics such as that embodied in the formation of 'torsions,' systems which exhibit non-Hamiltonian physics. This talk will discuss a small sample of recent research from the Hyde lab at Baylor University and the PK-4 on board the International Space Station.

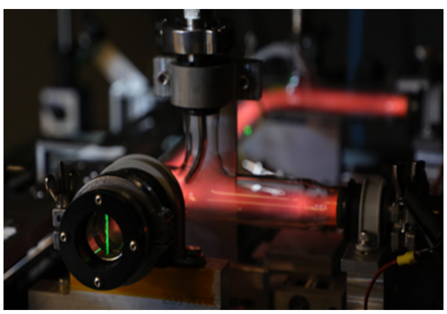

Recent References

[1] The Planetary Science Journal, 4:113 (14pp), 2023 June [2] The Astrophysical Journal, 950:11 (14pp), 2023. [3] Physics of Plasmas 29, 023701 (2022) [4] Plasma Phys. Control. Fusion 65 044006 (2023) [5] Physics of Plasmas 28, 073705 (2021) [6] Icarus Volume 354, 15 January 2021, 114053 [7] Phys. Rev. Research **2**, 043375 (2020) [8] Nature Research 10:13653 (2020)

Funding Support

Financial support from NSF grants No.1740203 and AAG-2008493, the US Department of Energy DE-SC-0021334, NASA Emerging Worlds grants 20-EW20_2-0053 and 80NSSC21K0381 and JPL Contracts 1647194 and 1571701 is gratefully acknowledged.

Nambu Mechanics as a Generalization of Hamiltonian Mechanics – A Framework for Non-equilibrium Dynamics

Tuo Jia

Institute for Quantum Science and Engineering and Department of Physics and Astronomy, Texas A&M University, College Station, TX 77843, USA

Studying physical systems which are not in the states of equilibrium has always been fascinating. Here we review Nambu mechanics and its role as a framework for studying non-equilibrium physics.

From Hamilton to Nambu. In 1973, Yoichiro Nambu published his seminal work "Generalized Hamiltonian Dynamics". Starting from the *Liouville's theorem* in Hamiltonian dynamics, the volume of phase space occupied by an ensemble of systems is conserved. One can readily generalize the two canonical variables (let us consider only one pair of (p, q) for simplicity) in Hamiltonian dynamics to a triplet and more and Liouville's theorem still holds true, and then they will span a three-dimensional or multi-dimensional phase spaces,

$$\frac{\mathrm{d}x_i}{\mathrm{d}t} = \frac{\partial(x_i, H_1, \ldots, H_{n-1})}{\partial(x_1, x_2, \ldots, x_n)} = \sum_{jk\ldots l} \epsilon_{ijk\ldots l} \frac{\partial H_1}{\partial x_j} \frac{\partial H_2}{\partial x_k} \cdots \frac{\partial H_{n-1}}{\partial x_l}, \tag{1}$$

where x_i is an n-dimensional vector, and H_k are $n-1$ "Hamiltonians". Similarly, we can define the Nambu brackets

$$[F, H_1, H_2, \ldots, H_{n-1}]_{NB} \equiv \frac{\partial(F, H_1, \ldots, H_{n-1})}{\partial(x_1, x_2, \ldots, x_n)}. \tag{2}$$

Examples of Nambu mechanics include rigid body systems, fluid dynamics, the membrane action in string theory and M(atrix) theory.

Nambu Non-equilibrium Thermodynamics. Katagiri et al. applied Nambu mechanics to non-equilibrium thermodynamics. The Nambu non-equilibrium thermodynamic equation is

$$\frac{\mathrm{d}F}{\mathrm{d}t} = -[F, H_1, \ldots, H_{n-1}]_{NB} + [F, x_{i_1}, \ldots, x_{i_{n-1}}]_{NB}[S, x_{i_1}, \ldots, x_{i_{n-1}}]_{NB}. \tag{3}$$

BZ reaction as a typical case of time-oscillating reactions can be well described by the Nambu time-evolving equations. Onsager's non-equilibrium thermodynamics cannot be applied to the BZ reaction since it is formulated near the equilibrium point of the entropy.

More Potential Applications. Both classical and quantum Nambu mechanics have drawn a lot of attention from mathematical physicists. However, instead of being a mathematical playground, the toolbox of Nambu mechanics perhaps need to be developed and utilized more in the field of optics, condensed matter physics and plasma physics.

Mitigation of Scattering in a Quantum System Using an Integrating Sphere

Zhenfei Jiang

Institute for Quantum Science and Engineering and Department of Physics and Astronomy, Texas A&M University, College Station, TX, USA 77843.

Abstract: Strong quantum-correlated sources are essential but delicate resources for quantum information science and technology protocols. Decoherence and loss are the two main disruptive processes that cause quantum correlations to lose their nonclassical behavior. In quantum systems, scattering can contribute to both decoherence and loss. In this work, we present an experimental scheme capable of significantly mitigating the adverse impact of scattering in quantum systems. Our quantum system is composed of a two-mode squeezed light generated with the four-wave mixing process in hot rubidium vapor, and a scatterer introduced to one of the two modes. An integrating sphere is then placed after the scatterer to recollect the scattered photons. We use mutual information between the two modes as the quantum correlation measure, and demonstrate a 47.5% mutual information recovery from scattering, despite an enormous photon loss of greater than 85% . Our scheme is the very first step towards recovering quantum correlations from disruptive random processes, thus has the potential to bridge the gap between proof-of-principle demonstrations and practical real-world implementations of quantum protocols.

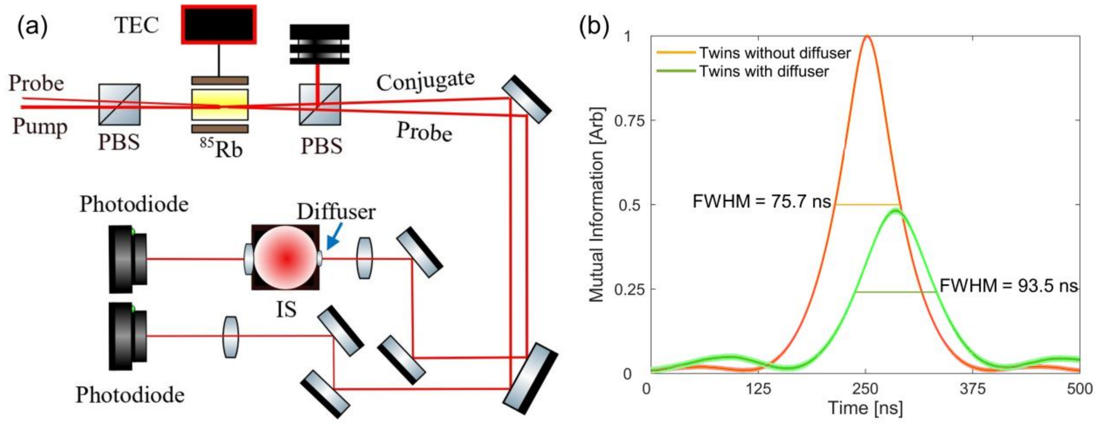

Figure 1 (a) Experimental setup in which a seeded ^{85}Rb vapor cell generates strong quantum-correlated twin beams via FWM. The probe beam is propagating through a 5-cm-diameter integrating sphere (IS). A scatterer, half-inch-diameter ground glass diffuser, is placed at the entrance port of IS. The probe beam is incident on the specular-reflection side of the diffuser. And the other side of the diffuser has 120 grits which can produce a large scattering pattern. A lens is closely attached to the back port of IS to collect scattered probe photons. PBS: polarizing beam splitter, IS: integrating sphere. (b) Mutual information between the probe and conjugate beam as a function of relative delay. The smooth shape of the curves results from the large amount of data used to calculated the mutual information. Each curve is a statistic result averaging 10 time traces. Orange curve: mutual information of the twin beams without scatterer. Green curve: mutual information of the twin beams with the scatterer. The shadow shows the error bar for each curves. The peak difference between two curves τ_0 is 32.7 ns. And the peak height ratio between green and orange curves is ~ 0.475/1.

An Introduction of High-Power Laser Systems for Inertial Fusion Energy (IFE)

Speaker: Kavita Desai Kabelitz (University of Illinois)

One important component for internal fusion energy (IFE) is the laser driver. For IFE, there are several goals for the laser such as having an output power on the order of megawatts, operating in the ultraviolet, and a high wall-plug efficiency. In order to scale up the laser energy, there are several important parameters which must be considered during the engineering process. This presentation will focus on laser physics and the parameters paramount to high power systems. A comparison of different high-power systems including the rare gas-halide systems and Nd:Glass will be provided along with an overview of their operation. Examples of other laser systems will also be shown including helium neon systems, argon ion lasers (see Fig. 1), and the Nd:YAG laser.

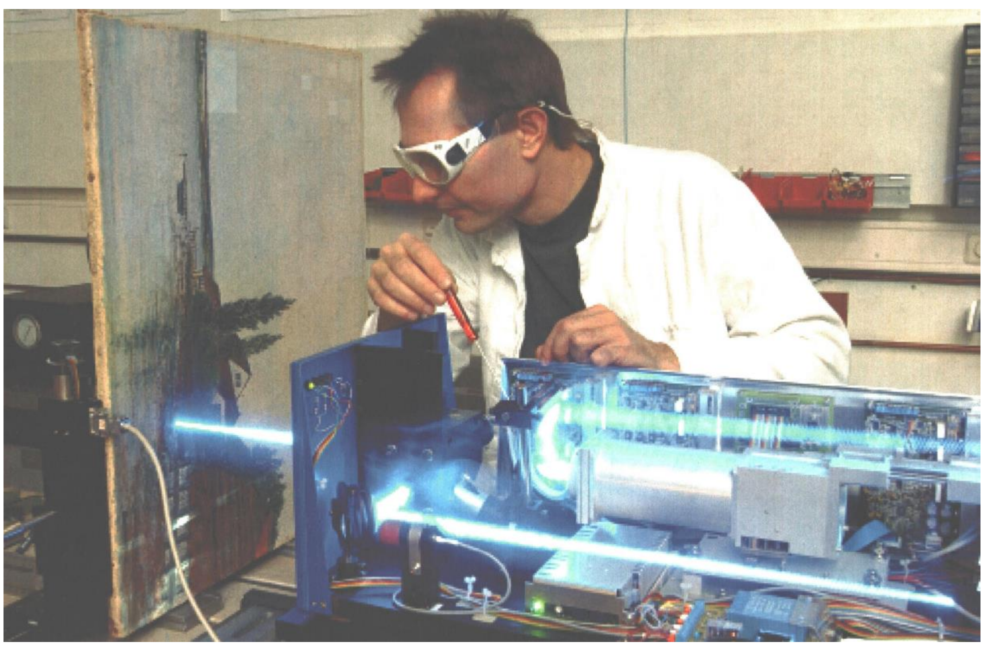

Fig. 1: An argon ion laser in operation reconstructing a painting (from UIUC ECE 455 course notes).

This talk is supported by the U.S. Department of Energy (DOE), Office of Science, Fusion Energy Sciences, under Award No. DE-SC0024882: IFE-STAR.

Nano-Focusing and Characterization of the OAM Beam through an Optical Fiber Using Plasmonic Nanostructure

Rohil Kayastha[1], Wei Zhang[2], Blake Birmingham[1], Zhi Gao[3], Jonathan Hu[2], Rafael Quintero-Torres[3,4], Alexei V. Sokolov[3] and Zhenrong Zhang[1]

[1]Department of Physics, Baylor University, Waco, TX 76798-7316, USA
[2]Department of Electrical and Computer Engineering, Baylor University, Waco, TX 76798-7356, USA
[3]Institute for Quantum Science and Engineering, Department of Physics and Astronomy, Texas A&M University, College Station, TX 77843-4242, USA
[4] Centro de Física Aplicada y Tecnología Avanzada, UNAM Juriquilla, Boulevard Juriquilla 3001, 76230 Querétaro, México

Optical vortex beam has been used in many applications such as nanoscale imaging, telecommunication, sensing, and so on due to its unique azimuthal phase distribution. Many of these applications utilize optical fibers as sensors or to propagate the beam to transmit data and information. The vortex beam carrying an orbital angular momentum (OAM) has a phase singularity, giving the beam a doughnut intensity profile (Figure 1 a and b). Due to its helical wavefront nature, the vortex beam carrying OAM has also been used to distinguish the enantiomers of the chiral molecule. However, coupling efficiency remains a problem due to the size mismatch of the beam and the molecule. Our work uses vortex fibers with plasmonic nanostructures to nano-focus the vortex beam to enhance the coupling between light and chiral matter. To achieve this goal, the vortex beam was characterized in free space and through vortex fiber (a polarization-maintaining ring core optical fiber), and the nanostructure on the fiber facet was fabricated.

Our research involved generating and propagating OAM beams characterized in free space and through a vortex fiber. The free-space OAM beam was successfully coupled and transmitted through the vortex fiber, resulting in a pure and stable output beam as shown in Figure 1. The helicity characterization and polarization analysis of the free-space and fiber-coupled output vortex beams showed consistent polarization and OAM. The direction of the phase front was maintained after propagation of the OAM through the vortex fiber, as observed from the spiral interference pattern (Figure 1 d). We also observed the nano-focusing of the OAM beam using a nanostructure on the fiber facet through simulation. The plasmonic nanorods were fabricated on the fiber facet core, and the far-field image of the output OAM beam was observed after transmission through the fiber with the nanostructure. The near-field image of the nano-focused OAM beam on the fiber will be investigated using a near-field scanning optical microscope (NSOM). The focusing of the OAM beam on a fiber facet with the nanostructure could enhance the coupling efficiency of the beam with chiral molecules, making it a potential scanning and sensing probe for single-molecule chirality detection.

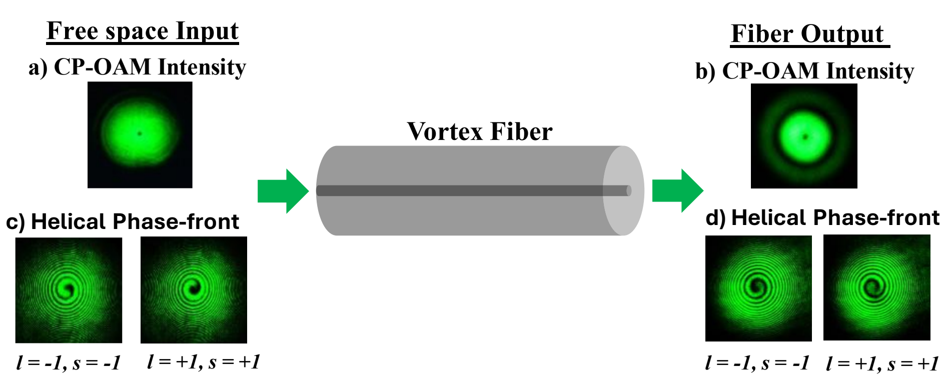

Figure 1: The free-space input circularly polarized OAM (CP-OAM) beam coupled and transmitted through to the vortex fiber. The intensity profile of **a)** input and **b)** output CP-OAM beam. Spiral interference showing helical phase front of the **c)** input and **d)** output CP-OAM beam.

Generating Einstein–Podolsky–Rosen correlations for teleporting collective spin states in a two-dimensional trapped ion crystal

Muhammad Miskeen Khan,[1, 2] Edwin Chaparro,[1, 2] Bhuvanesh Sundar*,[1] Allison Carter,[3] John Bollinger,[3] Klaus Molmer,[4] and Ana Maria Rey[1, 2]

[1]JILA, National Institute of Standards and Technology and University of Colorado, 440 UCB, Boulder, Colorado 80309, USA; [2]Center for Theory of Quantum Matter, University of Colorado, Boulder, Colorado 80309, USA; [3]National Institute of Standards and Technology, Boulder, Colorado 80309, USA; [4]Niels Bohr Institute, University of Copenhagen, 2100 Copenhagen, Denmark.

Quantum teleportation is one of the hallmarks of quantum information science, that unlocks the potential of entanglement and plays a crucial role in modern quantum communication and information processing. Traditional quantum teleportation with large atomic ensembles has focused on transporting spin-coherent states [1]. Here we proposed a teleportation protocol that allows to transport entangled collective spin-squeezed and Dicke-states [2]. Our scheme is realized using a two-dimensional trapped ion quantum simulator in Penning trap. The strong magnetic field native to the Penning trap generates large enough energy splitting of internal electronic and nuclear spin states. The ions prepared in different spin states forms energetically separated spin ensembles.

Our proposed teleportation protocol leverages both phonon-mediated collective spin-spin interactions among three energetically separated spin-ensembles together with measurements and local operations on these ensembles. The success of our teleportation circuit lies in its ability to emulate the continuous variable teleportation schemes at different stages of the protocol. Exact numerical simulations of the teleportation circuit confirm the teleportation (see Fig. 1) of the collective entangled spin states with good fidelity for realistic experimental conditions in arrays from a few tens to a few hundred ions.

This proposed protocol advances our understanding of non-local aspects of quantum mechanics and to explore the practical implications of teleporting substantial amount of many-body entanglement. This capability could be advantageous for future quantum networks and experiments by enabling the creation of on-demand entangled states across distant atomic ensembles. Our research pushes the boundaries of quantum teleportation beyond simple spin-coherent states to non-trivial many-body collective entangled spin states.

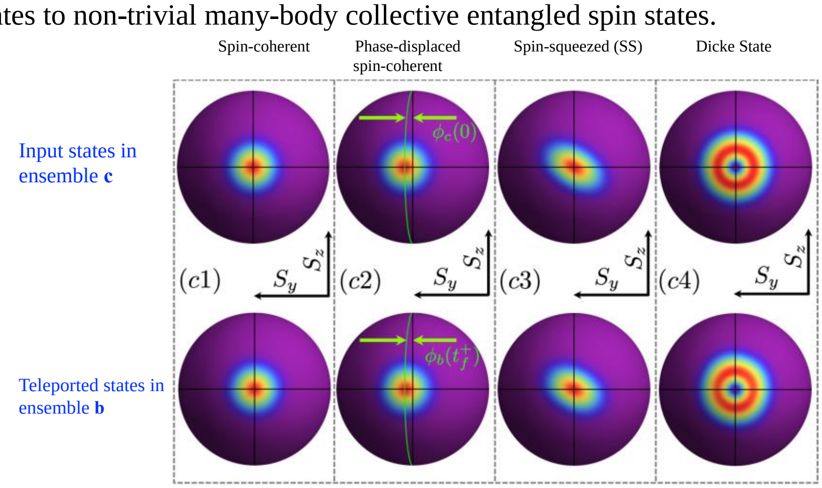

Fig. 1: (Top row)- Husimi-Q function of the four input states encoded in the ensemble c. (Bottom row)-The same function is shown for the corresponding teleported stated as imprinted on the targeted ensemble b. For all cases, the mean orientations and noise distributions of the teleported states match the ones of the input.

References:

[1] H. Krauter, D. Salart, C. A. Muschik, J. M. Petersen, H. Shen, T. Fernholz, and E. S. Polzik, Nature Physics **9**, 400 (2013).

[2] Muhammad Miskeen Khan, Edwin Chaparro, Bhuvanesh Sundar, Allison Carter, John Bollinger, Klaus Molmer, Ana Maria Rey, arXiv:2405.19536 (2024).

***Title: Photonic Integrated Circuits for applications in biosensing**

Authors: Mohit Khurana(1,2), Sahar Delfan(1,2), Ayla Hazrathosseini(1,2), Lanyin Luo(1,2), Zhenhuan Yi(1,2), Alexei Sokolov(1,2), Philip R. Hemmer(1,2), Marlan O. Scully(1,2,3,4)

Affiliations:
1- Department of Physics and Astronomy, Texas A&M University, College Station, TX 77843, USA.
2- Institute of Quantum Science and Engineering, Texas A&M University, College Station, TX 77843, USA.
3- Baylor University, Waco, Texas 76704, USA.
4- Princeton University, Princeton, New Jersey 08544, USA.

Photonic Integrated circuit (PIC) is a rapidly growing field in academia and industry for its applications in biosensing, non-linear photonics, quantum photonics, coherent optics, optical computing, opto-electronic devices, optical communication, data-center optical interconnects, lidar and many more[1,2,3,4]. In this talk, I will discuss various platforms for development of PIC such as Silicon, Silicon Nitride, Lithium Niobate, Indium Phosphide in general and one application in the biosensing field using Silicon Nitride waveguide based interferometer and whispering gallery modes resonator as shown in fig.(1). I will discuss the finite domain time difference (FDTD) method to simulate the waveguides and photonic elements for a PIC. I will also give a short tutorial on how to design, develop architecture, optimization methods, fabrication process and characterization of a PIC for a given application.

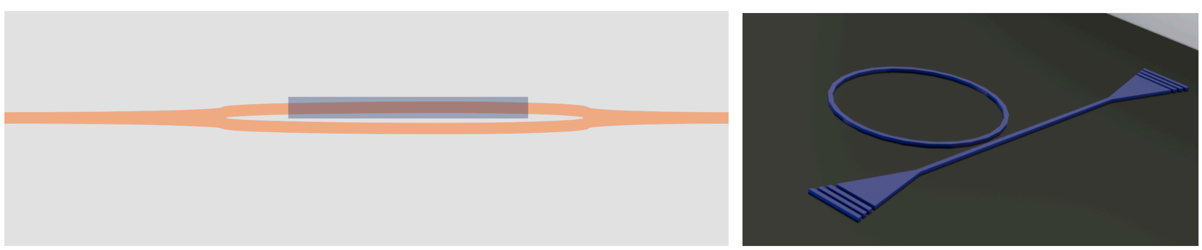

Fig. 1). Schematic diagrams: a) Waveguide based Mach-Zehnder interferometer, with a sensing arm (light gray color) b) Resonator coupled to a waveguide.

It is critical to optimize each element of a PIC to achieve its optimal operation. As in sensing application, sensitivity(S) is optimized by increase in mode overlap with the surrounding material, interaction length and high signal-to-noise ratio measurements with the trade-offs in mode confinement in waveguide, scattering, radiative losses and fabrication errors.

References:

1. Galan Moody et al 2022 J. Phys. Photonics 4 012501
2. D. M. Lukin, M. A. Guidry, and J. Vučković, Integrated quantum photonics with silicon carbide: Challenges and prospects, PRX Quantum 1, 020102 (2020)
3. Lukashchuk, A., Yildirim, H.K., Bancora, A. et al. Photonic-electronic integrated circuit-based coherent LiDAR engine. Nat Commun 15, 3134 (2024). https://doi.org/10.1038/s41467-024-47478-z
4. Shekhar, S., Bogaerts, W., Chrostowski, L. et al. Roadmapping the next generation of silicon photonics. Nat Commun 15, 751 (2024). https://doi.org/10.1038/s41467-024-44750-0

Introduction to the BGK relaxation model for the Boltzmann transport equation

Barnabas Kim

IQSE, Texas A&M University, College Station, TX, USA 77843

In kinetic theory, Boltzmann has introduced a transport equation for a dilute gas [1]. Since this equation is very difficult to get a solution even in a simple system, many attempts have been tried to get a physically reasonable solution, e.g., works done by Wang Chang and Uhlenbeck [2]. One of notable approximations about the troublesome collision integral is introduced by Lorentz through relaxation time. Bhatnagar, Gross, and Krook [3] have developed into a proper model for the collision integral, and presented a systematic way to get a dynamical description on the system, which is known as BGK model, and gave a solution of the Boltzmann equation. After a brief derivation for the Boltzmann equation, I will introduce the main strategies of BGK model with their views on the problem: note that the collision process in BGK model conserves particle numbers, momentum, and energy upto first order. This tutorial will improve the understanding for the gas dynamics in the stimulated Brioullion Scattering [4].

[1] Huang, Stat. Mech. (2nd).
[2] Wang Chang and Uhlenbeck, CM-443 (1948); CM-681 (1951).
[3] Bhatnagar, Gross and Krook, Phy. Rev. 94, 511 (1954).
[4] Averbakh, Makarov, and Talanov, Sov. J. QE 5, 1201 (1975).

TAMU-Princeton Summer School, July 15-26, 2024

Towards Nuclear Clocks and Nuclear Memories

Xiwen Wang, Yanli Shi, and Olga Kocharovskaya

Institute for Quantum Science & Engineering
Department of Physics & Astronomy, Texas A&M University

Nuclear oscillators have some natural advantages over the atomic ones for building superior clocks and quantum memories. They are less sensitive to perturbations of electric and magnetic fields due to the tiny size of a nucleus compared to atom. Besides, contrary to atomic transitions, spectrally narrow nuclear transitions are available even at a high solid-state density and room temperature. These benefits give promise for building compact room temperature solid-state nuclear clocks which are expected to outperform atomic clocks both in terms of accuracy and stability. They would redefine the standards of time and other base units, be used in advanced searches for new physics beyond the Standard Model, such as dark matter and time-dependence of fundamental constants, as well as for applications in navigation, chronometric geodesy, geology, seismology and climatology.

Last year experimental demonstrations of the resonant laser excitation of the two most promising nuclear clock isomers: Sc-45 (12.4 keV, 0.46 s lifetime) [1] and Th-229 (8.4 eV, 630 s lifetime) [2] present an important step toward realization of the Mössbauer nuclear clock. We will discuss the next important step to be made in this direction, an experiment to be performed this year at EuXFEL, aimed at observation of the coherent nuclear forward scattering and measuring the actual linewidth of the Sc-45 nuclear transition. Measuring of the actual linewidth (or coherence time of a nuclear transition) is crucially important for its various applications (nuclear clock, nuclear memory, spectroscopy, search for dark matter, fundamental constants time dependence, etc.).

Narrow nuclear resonances in solids are also promising for realization of compact, long-lived nuclear quantum memories. Very recently nuclear quantum memory for the hard X-ray 14.4 keV photons was demonstrated for the first time [3]. It was based on realization of an absorption frequency comb in a set of the moving nuclear resonant absorbers, as it was earlier suggested in our work [4]. However, the moment of the photon wave packet retrieval in this protocol was predetermined by the frequency comb interval. We will discuss various ways to achieve on-demand quantum nuclear memory.

[1] Yu. Shvyd'ko, R. Röhlsberger, O. Kocharovskaya, J. Evers et al., Resonant X-ray excitation of the nuclear clock isomer 45Sc, *Nature* **622**, 471(2023), DOI:10.1038/s41586-023-06491-w.
[2] J. Tiedau *et al.*, Laser excitation of the Th-229 nucleus, Phys. Rev. Lett. **132**, 182501 (2024).
[3] S. Velten, L. Bocklage, X. Zhang, K. Schlage, A. Panchwanee, I. Sergeev, O. Leupold, A.I. Chumakov, O. Kocharovskaya, R. Röhlsberger, Nuclear quantum memory for hard X-ray photons, Science Advances, **10**, 26 (2024) DOI: 10.1126/sciadv.adn9825.
[4] X. Zhang, W.-T. Liao, A.A. Kalachev, R.N. Shakhmuratov, M.O. Scully, O. Kocharovskaya, Nuclear quantum memory and time sequencing of a single γ photon, Phys. Rev. Lett. **123**, 250504 (2019).

Universal mechanism behind quantum supremacy of many-body systems

Vitaly Kocharovsky (Texas A&M University)

The universal mechanism behind quantum supremacy and #P-hard complexity of many-body systems is revealed. Its complexity is equivalent to multivariate Fourier-series integration that is #P-hard for classical computers. It occurs even in equilibrium systems, via interference through eigen-squeeze modes and eigen-energy quasiparticles but requires interaction beyond the rotation-wave approximation. Applying the newly found hafnian master theorem and referring to the Toda's theorem on a ♯P-complete oracle, it is shown that this mechanism constitutes the universal base for the computational #P-hardness and quantum supremacy.

The mechanism is described via an example of boson sampling of interacting atoms from a noncondensed fraction of Bose–Einstein-condensed (BEC) gas confined in a box trap. The characteristic function and statistics of atom numbers are calculated. Using Bloch–Messiah reduction, it is shown that atom interactions give rise to two equally important entities—eigen-squeeze modes and eigen-energy quasiparticles—whose interplay with sampling excited atom states determines the quantum statistical properties of the BEC gas. The two necessary ingredients of #P-hardness, squeezing and interference, are self-generated in the gas and, contrary to the Gaussian boson sampling in linear interferometers, external sources of squeezed bosons are not required. Furthermore, the major limitation factor for achieving quantum supremacy via boson sampling in a deep linear interferometer - an exponential loss of photons due to scattering and absorption on coupling elements (beam splitters and phase shifters) - is not an issue for the atomic boson sampling.

Proof-of-principle pioneering experiments on atomic boson sampling in the trapped BEC gas are proposed.

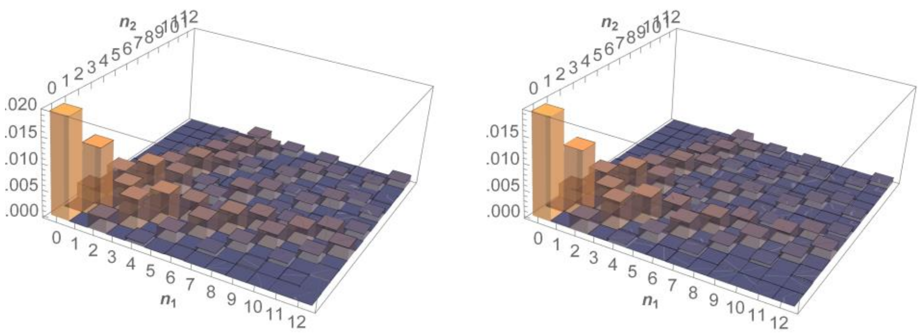

Fig. 1. Joint occupation probabilities for two interfering squeezed excited atom states. A messy quantum supremacy statistics shows up starting from a few samplings modes but only if thermal noise does not hide it when thermal occupations exceed one quantum per mode (left $N_{th}=0$, right $N_{th}=1$).

1. V. V. Kocharovsky, Vl. V. Kocharovsky, S. V. Tarasov, The Hafnian Master Theorem, Linear Algebra Appl. **651**, 144–161 (2022).
2. V. V. Kocharovsky, Vl. V. Kocharovsky, W. D. Shannon, S. V. Tarasov, Towards the simplest model of quantum supremacy: Atomic boson sampling in a box trap, Entropy **25**, 1584 (2023).
3. V. V. Kocharovsky, Vl. V. Kocharovsky, S. V. Tarasov, Atomic boson sampling in a Bose-Einstein-condensed gas, Phys. Rev. A **106**, 063312 (2022).
4. V. V. Kocharovsky, Vl. V. Kocharovsky, W. D. Shannon, S. V. Tarasov, Multi-Qubit Bose–Einstein Condensate Trap for Atomic Boson Sampling, Entropy **24**, 1771 (2022).
5. V.V. Kocharovsky, Vl.V. Kocharovsky, S.V. Tarasov, Unification of nature's complexities via a matrix permanent – critical phenomena, fractals, quantum computing, ♯P-complexity, Entropy **22**, 322 (2020).
6. V. V. Kocharovsky, Vl. V. Kocharovsky, M. O. Scully, Condensation of N bosons. III. Analytical results for all higher moments of condensate fluctuations in interacting and ideal dilute Bose gases via the canonical ensemble quasiparticle formulation, Phys. Rev. A **61**, 053606 (2000).

Observers, Controllers And The World: What Has Quantum Mechanics Changed?

Gershon Kurizki

Weizmann Institute of Science, Rehovot 7610001, Israel

ABSTRACT

I will survey the concept of observation that has preoccupied thinkers since ancient times. I will then dwell on a key notion in thermodynamics and quantum mechanics, that of observers-controllers that actively affect the outcome of observations by the information they acquire, as in Scully's Quantum Eraser. I will then discuss theoretical and experimental results on the interplay of observation, control and the environment in quantum measurements and thermodynamics.

Detecting multimode entanglement from classical-nonclassical polarity

Jiru Liu[1], Wenchao Ge[2], and M. Suhail Zubairy[1]

[1]Institute for Quantum Science and Engineering (IQSE) and Department of Physics and Astronomy, Texas A&M University, College Station, TX 77843-4242, USA

[2]Department of Physics, University of Rhode Island, Kingston, Rhode Island 02881, USA

Abstract

Recent research in continuous-variable systems introduces the concept of classical-nonclassical polarity (CNP), which unifies various classical-nonclassical features of Gaussian states and reveals a precise conservation relation under linear optical transformations [1]. We demonstrate that the CNP of a given state correlates with the average number of photons induced by various Gaussian operations during state preparation: squeezing operations increase overall nonclassicality, displacement operations have no impact, and thermal noise detracts from it. Our findings contribute to a novel quantification of nonclassicality and provide valuable insights into detecting multimode entanglement within quantum networks.

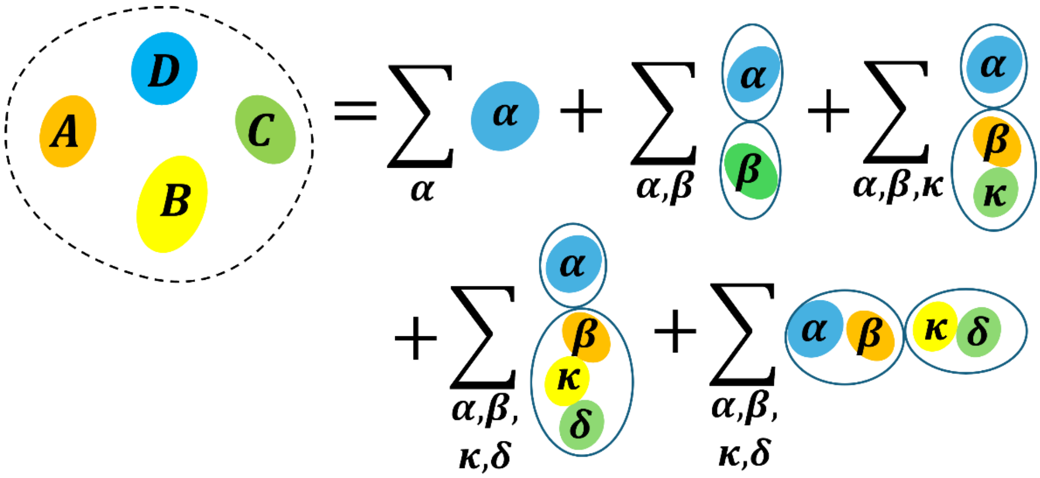

Figure 1: The cluster-expansion structure of the CNP within a four-mode Gaussian states, where $\alpha, \beta, \kappa, \delta \in \{A, B, C, D\}$.

Reference

[1] Jiru Liu, Wenchao Ge, and M. Suhail Zubairy, “Classical-Nonclassical Polarity of Gaussian States”, Physical Review Letters 132, 240201 (2024).

Lidar in entomological studies

Yiyun Li[1], Robert Brick[1], Alexei V. Sokolov[1, 2] and Marlan O. Scully[1, 2]

[1]Institute for Quantum Science and Engineering, Department of Physics and Astronomy, Texas A&M University, 578 University Drive, 77843–4242, College Station, Texas, USA
[2]Department of Physics, Baylor University, Baylor Sciences Building D.311, 76798-7316, Waco, Texas, USA

Abstract

Entomological lidar is a research field that explores two questions: what insect species are in the field, and what are insects doing in the field? To answer the first question, we conducted an indoor study on flying native solitary pollinators employing an optical multiband polarimetric modulation sensing system. This study included individuals of both genders of three native solitary pollinator species, *Osmia californica*, *Osmia lignaria*, and *Osmia ribifloris*. Properties including optical cross-section, degree of linear polarization, and wingbeat power spectra at all three wavelengths have been extracted from the insect signals. These properties are then used in the classification analysis. For species with temporal and spatial overlap, the highest accuracies of our method exceed 96% (*O. ribifloris* & *O. lignaria*) and 93% (*O. lignaria* & *O. californica*). Efforts have also been made to measure the flying velocity of insects in the field to describe their behavior. We proposed a novel scheme for the 1-D flight velocity measurement of flying insects by using a Scheimpflug lidar system. We implemented this new technique and applied it to study insects at the Salter Research Farm, Robertson County, Texas. We observed a shift in wingbeat frequency distribution, indicating new insect species' presence during the multi-day measurement. The study on 1-D flight velocity reveals a net directional movement of insects, providing supportive evidence of the arrival of a new species. Our plans in this field will also be briefly discussed.

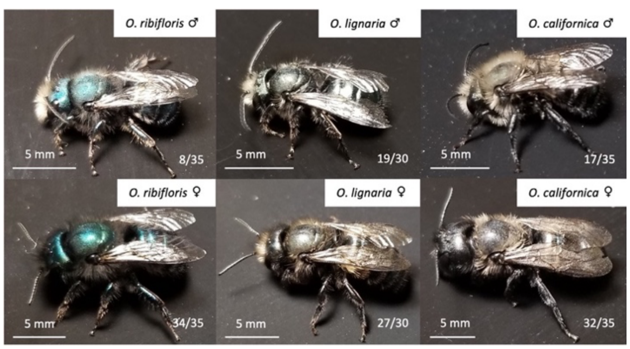

Fig. 1. Images of the solitary bees used in the study.

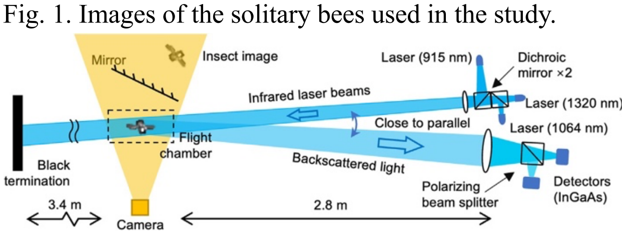

Fig. 2. Schematic diagram of the indoor stand-off sensing setup for collecting optical multi–band polarimetric properties of flying solitary pollinators.

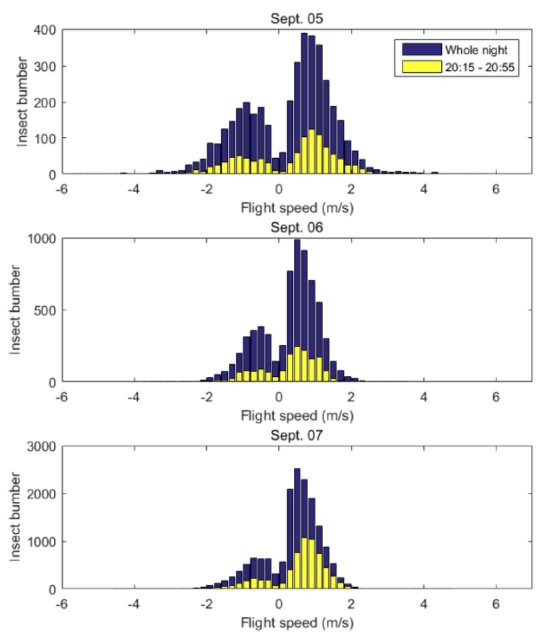

Fig. 3. Insects' 1-D flight velocity distribution during the field measurement on Salter farm.

References

1. Li, Y., Wang, K., Quintero-Torres, R., Brick, R., Sokolov, A.V. and Scully, M.O., 2020. Insect flight velocity measurement with a CW near-IR Scheimpflug lidar system. *Optics Express*, *28*(15), pp.21891-21902.
2. Li, Y., Han, Z., Nessler, R., Yi, Z., Hemmer, P., Brick, R., Sokolov, A.V. and Scully, M.O., 2023. Optical multiband polarimetric modulation sensing for gender and species identification of flying native solitary pollinators. *Iscience*, *26*(11).

Exploring quantum computing frontier with programmable atom arrays

Mikhail Lukin

Harvard University

ABSTRACT

A broad effort is currently underway to develop quantum computers that can outperform classical counterparts for certain computational or simulation tasks. Suppressing errors is one of the central challenges for useful quantum computing, requiring quantum error correction for large-scale processing. However, the overhead in the realization of error-corrected “logical” qubits, where information is encoded across many physical qubits for redundancy, poses significant challenges to large-scale logical quantum computing. In this talk, we will discuss how the early theoretical research starting in the 1990s and early 2000s resulted in the recent exciting developments that redefined the cutting edge frontier of quantum information science and quantum computing.

Specifically, we will discuss the recent advances involving programmable, coherent manipulation of quantum systems based on neutral atom arrays excited into Rydberg states, allowing the control over several hundred qubits in two dimensions. In particular, we use this platform to explore quantum algorithms with encoded logical qubits and quantum error correction techniques. Using this logical processor with various types of error-correcting codes, we demonstrate that we can improve logical two-qubit gates by increasing code size, outperform physical qubit fidelities, create logical GHZ states, and perform computationally complex scrambling circuits using 48 logical qubits and hundreds of logical gates. These results herald the advent of early error-corrected quantum computation, enabling new applications and inspiring a shift in addressing both the challenges and opportunities that lay ahead.

Gravitational Quantum Eraser

Yusef Maleki

Institute for Quantum Science and Engineering (IQSE) and Department of Physics and Astronomy,
Texas A&M University, College Station, TX 77843-4242, USA

Pursuing a quantum mechanical description of gravity is an important endeavor in modern physics, promising insights into profound unresolved mysteries in the field. Any comprehensive theory aiming to unify gravity with quantum physics must integrate key quantum principles such as the uncertainty principle, quantum superposition, and wave-particle duality. Exploring the concept of wave-particle duality, the quantum eraser exposes a fundamental distinction between quantum mechanics and classical theory. In this presentation, I will discuss how the intrinsic quantum properties of gravity facilitate the emergence of a quantum eraser phenomenon within the framework of quantum gravity. I will demonstrate that the gravitationally induced quantum eraser may provide a direct and potentially feasible means to investigate the quantum characteristics of gravity.

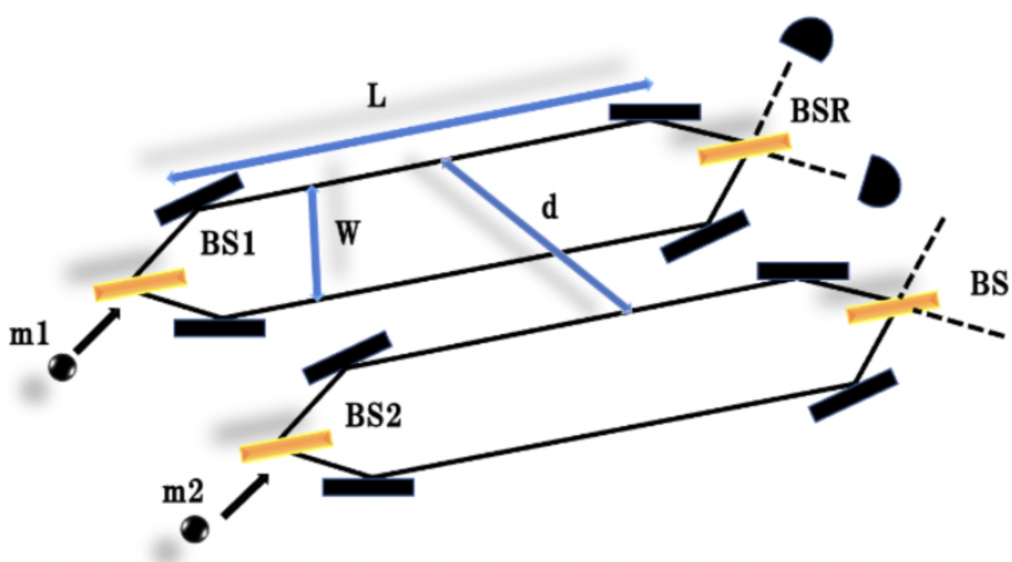

Exploration of Magnetosensitive Proteins with Optically Pumped Quantum Sensors

Joi Malone†, M. Cristina Marchetti*, Zvonimir Dogic*, and Philip Kurian†
*Department of Physics, University of California at Santa Barbara, Santa Barbara, CA 93106
†Quantum Biology Laboratory, Howard University, Washington, DC 20060
https://quantumbiolab.com

Nematic liquid crystals are in a hybrid state of matter between liquid and solid. Like solids, they possess a certain positional order, but like liquids they demonstrate little average orientational order. Defects—certain places in liquid crystals where there is no positional or orientational order—have been tracked using a variety of experimental, computational, and mathematical methods, comparing their movements to Brownian and ballistic motions [1]. Janus particles (synthetic beads with two distinct physicochemical surfaces, see Fig. 1) in a water solution were employed because they could be self-propelled like biological systems by illumination with blue light (430-490 nm), but only at the surface of the sample [2]. They were imaged and tracked computationally, and their trajectories were used to calculate each particle's mean squared displacement from its origin in time (diffusion rate): $MSD(t) = \langle [x(t + t_0) - x(t_0)\ ]^2 \rangle$. The results from this experiment have been crucial to understanding "simple" living systems, including bacteria and more complex unicellular protists.

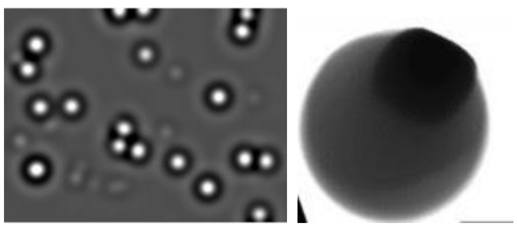

Figure 1: Synthetic Janus particles in a water solution (left). Single Janus particle with two physiochemical surfaces (right). Adapted from [2].

Quantum sensors exploit quantum coherence and entanglement to enhance sensitivity and precision of measurement, and they can detect very small changes to a system caused by an external magnetic field. In the biomedical world, they have been used in magnetoencephalography (MEG) to study brain activity by detecting the magnetic fields produced by electric currents from neuronal ionic flows [3]. Optically pumped magnetometers (OPMs) use electromagnetic pumping to create magnetically sensitive states. Because of the Zeeman affect, when a magnetic field is applied, the quantized energy levels split into more levels corresponding to the orientation of the angular momentum. However, when the laser cannot increase the total angular momentum past a particular point, certain excited atoms become trapped. Because the light can no longer transfer energy to the system, the material will be transparent to the laser light and the photodiode will detect higher photon counts; this process provides highly sensitive and functional measurements in clinical settings [4].

The observation of significant terahertz modes resulting from phonon condensation [5] (per Fröhlich) in optically pumped model proteins, most notably bovine serum albumin [6], opens the tantalizing possibility that such systems could be engineered for *in vivo* OPMs in neurons. Proteins like cryptochrome, a circadian photoreceptor that is magnetosensitive upon activation with blue-green light, would be prime targets as intrinsic reporters for tracking neuron states without the addition of an exogenous probe. However, efforts to enhance the weak but detectable changes in the fluorescence emission of flavins within cryptochrome is the subject of ongoing research.

References

[1] **Malone, J.** (2021). A New Type of Motion: Active Materials. Physics REU: September 24, 2021. https://reu.physics.ucsb.edu/sites/default/files/sitefiles/REUPapersTalks/2021-REUPapersTalks/Dynamic_of_Active_Materials-Joi-Paper.pdf
[2] Palacci, J., et al. (2013). Living crystals of light-activated colloidal surfers. *Science* **339,** 936-940.
[3] Aslam, N., et al. (2023). Quantum sensors for biomedical applications. *Nature Reviews Physics* **5,** 157–169.
[4] Tierney, T. M., et al. (2019). Optically pumped magnetometers: From quantum origins to multi-channel magnetoencephalography. *NeuroImage* **199,** 598-608.
[5] Zhang, Z., Agarwal, G. S. & Scully, M. O. (2019). Quantum Fluctuations in the Fröhlich Condensate of Molecular Vibrations Driven Far From Equilibrium. *Physical Review Letters* **122**, 158101.
[6] Azizi, K., Gori, M., Morzan, U., Hassanali, A., & **Kurian, P.** (2023). Examining the origins of observed terahertz modes from an optically pumped atomistic model protein in aqueous solution. *PNAS Nexus* **2,** pgad257.

Title:

Hyper-Raman Spectroscopy of Biomolecules

Author's Names:

Christopher B. Marble,[1,2] Kassie S. Marble,[2] Xingqi Xu,[2,3] Ethan B. Keene,[1,2] Georgi I. Petrov,[2] Dawei Wang,[3] and Vladislav V. Yakovlev[2]

Affiliations:

[1]Tarleton State University

[2]Texas A&M University

[3]Zhejiang University

Summary of Findings:

We report on our success in developing hyper-Raman scattering (HRS) spectroscopy for biomolecules in response to the existing limitations of Infrared (IR) absorption spectroscopy. IR absorption and Raman scattering (RS) spectroscopy are two traditional techniques that provide insight into the structure of biomolecules. IR absorption and RS are complementary techniques by nature of having different selection rules, which determine which molecular vibrations are detectable. RS has enjoyed considerable success for biomolecule detection while IR absorption is rarely employed. This is primarily because IR absorption spectroscopy below 1000 cm^{-1} is functionally impossible in "wet" samples due to extremely strong water absorption in that range.

HRS provides access to the IR active molecular vibrations including sub-1000 cm^{-1} vibrations in aqueous solution while retaining many of the practical advantages of traditional RS. To demonstrate the value of HRS as a complementary technique to RS for biomolecules, we built a 532 nm, ps laser system that can perform dual detection of RS and HRS. High signal-to-noise HRS spectra of biologically significant molecules including D-glucose, L-alanine, L-arabinose, and L-tartaric acid in aqueous solution were captured using the system in minutes. We verified that HRS detects the known IR active molecular vibrations of the target molecules, but that the HRS spectra showed substantially different peak intensities compared to IR absorption spectroscopy.

Finally, we demonstrated that HRS can be applied to help resolve major points of contention regarding hydrogen bonding between water and polar organic molecules. Using the model system of dimethyl-sulfoxide (DMSO) and water, we exploited the sensitivity of HRS to the low frequency librations of H_2O to show HRS can detect changes in the coordination of H_2O around DMSO molecules and the formation of hydration shells around DMSO molecules. Furthermore, we found evidence of intermolecular bonding between H_2O and DMSO methyl groups for DMSO concentrations below 33 mol %.

Cosmic Dust Bunnies and Laboratory Dust Crystals: Modeling Complex Interactions in a Complex Plasma

Lorin Swint Matthews

Baylor University, Waco, Texas USA

E-mail: lorin_matthews@baylor.edu

99.99% of the matter in the universe is in the plasma state. Plasma is the material that forms our sun, candle flames and neon lights. Plasma flows through our solar system and fills the space between stars– it's everywhere. Dust is everywhere, too. What happens when dust and plasma get together?

A complex, or dusty, plasma consists of tiny pieces of solid material a hundred times smaller than the width of a human hair immersed in a plasma environment. The phenomena I study range from how the dust in cosmic gas clouds starts to clump together to form new planets (the formation of cosmic dust bunnies) to how these small particles can assemble themselves into incredibly ordered structures like crystals and helical strings.

Charged dust is the primary component of many beautiful astrophysical phenomena such as comet tails, planetary rings, protoplanetary disks, and noctilucent clouds. It can also be a problem. The Apollo astronauts found lunar dust a nuisance, obscuring visors and instrument readouts, degrading seals, and abrading materials. The Mars Rovers stopped working when their solar panels became covered with dust. Dust created when plasma in tokamaks interacts with the walls can kill the fusion process.

Understanding the charging and dynamics of dust is important to understanding our universe as well as exploring our solar system. Numerical modeling of the coupled charging and transport processes allows exploration of environments which can't be easily probed. This talk will provide a brief overview of numerical modeling of particle charging, ion wakes, and charged particle transport in plasmas.

Support for this work from the US Department of Energy, Office of Science, Office of Fusion Energy Sciences under awards DE-SC0021334 and DE-SC0024681, and National Science Foundation under awards PHY-2308742 and PHY-2308743.

Calculate dust charge from balance of electron and ion currents to the grain surface

$$I_j = n_j q_j \int_{v_{min}}^{\infty} \pi\left(1-\frac{2q_j\Phi_s}{m_j v^2}\right) f(v)\, v^3 dv \boxed{\int \cos\theta \, d\Omega}$$

Numerical integration over angles open to incoming electrons and ions

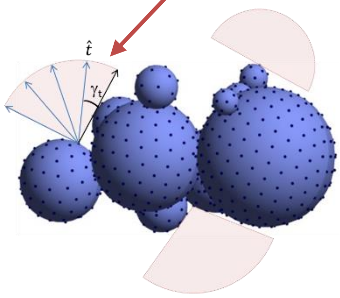

Sum the currents

$$\frac{dQ}{dt} = \sum_j I_j(\phi_s)$$

Iterate to reach equilibrium charge

$$Q = C\phi_s$$

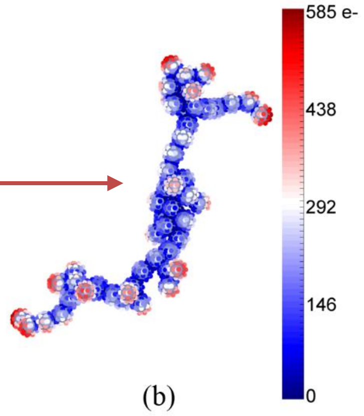

t = 0.005 s
Spin = (3, -0.3, 9.7)

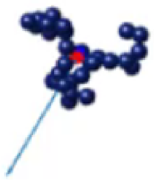

Simulate the dust dynamics

The demands on optical materials in high power lasers for inertial fusion energy

Carmen S. Menoni

Department of Electrical and Computer Engineering

Colorado State University

Laser technologies have played a pivotal role in advancing science. Ultrafast lasers focused to ultra-high intensities (> 10^{21} W/cm^2) make it possible to generate high density plasmas at [1] which produce intense sources of x-rays rays and drive fusion reactions [2], and to accelerate electrons to GeV energies in a few tens of centimeters [3]. Simultaneous advances in laser and target technologies were key to demonstrate laser driven fusion with net energy gain at the Lawrence Livermore National Laboratory (LLNL) National Ignition Facility (NIF) in Dec. 2022 [4].

In large part, advances in laser technologies rely on advances in materials. In this presentation I will describe basic laser architectures that are being developed as drivers for laser fusion. In particular I will emphasize the role of dielectric coatings which are ubiquitous in high power laser systems and will layout the opportunities that exist to advance these materials to the next level. In a second part of this talk I will provide a glimpse of parallel efforts in materials' studies which are fundamental to support and advance laser fusion.

This work is supported by the U.S. Department of Energy (DOE), Office of Science, Fusion Energy Sciences, under Award No. DE-SC0024882: IFE-STAR.

[1] M. Purvis et al., Nature Photonics, **7**: 796–800, (2013).

[2] A. Curtis et al., Nature Communications, **9**: 7, (2018).

[3] B. Miao et al., Physical Review X, **12**: 031038, (2022).

[4] H. Abu-Shawareb et al., Phys. Rev. Lett. **129**, 075001, (2023).

Multidimensional spectroscopy with quantum light, entangled photons, and X ray pulses

Shaul Mukamel

Dept. of Chemistry and Physics & Astronomy, University of California, Irvine, CA 92697, USA
Email: smukamel@uci.edu

Multidimensional spectroscopy has been instrumental for probing dynamical processes in a wide variety of material systems ranging from atoms, molecules to biological complexes. These techniques traditionally rely on sequences of coherent laser pulses with electric fields with well-defined envelopes and phases. Quantum light sources have been developed for broad applications such as quantum information processing, secure communication, and lithography. Employing quantum light in multidimensional spectroscopy is opening up many exciting opportunities to enhance the signal-to-noise ratio, improve the combined temporal, spatial, and spectral resolutions, and simplify nonlinear optical signals by selecting desired transition pathways. In second and third order signals, we show how photoelectron signals generated by time-energy entangled photon pairs can monitor ultrafast excited state dynamics of molecules with high joint spectral and temporal resolutions, not limited by the Fourier uncertainty of classical light. Two-entangled-photon absorption scales linearly with the pump intensity, allowing the study of fragile biological samples with low photon fluxes. We present a quantum dynamical study on the charge migration in molecules by coupling to an optical cavity, which can activate and enhance the targeted charge migration modes that are suppressed in the bare molecule.

Novel X-ray pulse sources from free-electron lasers and high-harmonic generation setups enable the monitoring of molecular events on unprecedented temporal, spatial and energetic scales. The attosecond duration of X-ray pulses, their large bandwidth, tunable energy range, and the atomic selectivity of core X-ray excitations offer a uniquely high spatial and temporal selectivity for non-linear spectroscopies. We show how the orbital angular momentum of twisted X-ray light can be leveraged to detect electronic and vibrational coherences and time evolving chirality emerging at conical intersections.

1. Kizmann, M., Yadalam, H. K., Chernyak, V. Y., Mukamel, S.: Quantum interferometry and pathway selectivity in the nonlinear response of photosynthetic excitons. *PNAS* 120, e2304737120 (2023). https://doi.org/10.1073/pnas.2304737120

2. "Ultrafast X-ray Probes of Elementary Molecular Events," Daniel Keefer, Stefano M. Cavaletto, Jérémy R. Rouxel, Marco Garavelli, Haiwang Yong, Shaul Mukamel, Annual Review of Physical Chemistry 2023 74:1, 73-97. https://doi.org/10.1146/annurev-physchem-062322-051532

3. "Manipulating two-photon-absorption of cavity-polaritons by entangled light," Bing Gu and Shaul Mukamel. Journal of Physical Chemistry Letters, 11, 19, 8177–8182 (2020) https://pubs.acs.org/doi/abs/10.1021/acs.jpclett.0c02282

4. "Cavity control of molecular spectroscopy and photophysics," Bing Gu, Yonghao Gu, Vladimir Y. Chernyak, and Shaul Mukamel, *Accounts of Chemical Research* (2023). https://doi.org/10.1021/acs.accounts.3c00280

5. "Distinguishability and "which pathway" information in multidimensional interferometric spectroscopy with a single entangled photon-pair," Shahaf Asban and Shaul Mukamel. Science Advances, 7: eabj4566 (2021) DOI: 10.1126/sciadv.abj4566

Boltzmann equation and BGK for stimulated Brillouin scattering

Reed Nessler

IQSE, Texas A&M University, College Station TX 77843

In the study of stimulated scattering of light by density fluctuations in gases (stimulated Brillouin scattering, SBS) a range of conditions are encountered when varying gas pressure. At high pressures, hydrodynamic approaches apply, but lower pressures require kinetic theory, particularly using models like the Bhatnagar–Gross–Krook (BGK) relaxation operator. This model effectively spans the intermediate range and aligns with collisionless gas theory (i.e., Vlasov equation) at low densities, making it suitable for analyzing SBS in gases.

We review the work of Talanov et al.[1], which builds upon Sugawara and Yip's linearized BGK theory of Brillouin light scattering[2] by including a force term. The research involves calculating frequency dependencies of backward SBS increments in monatomic and diatomic species of gas, and includes experimental findings on nitrogen near atmospheric pressures.

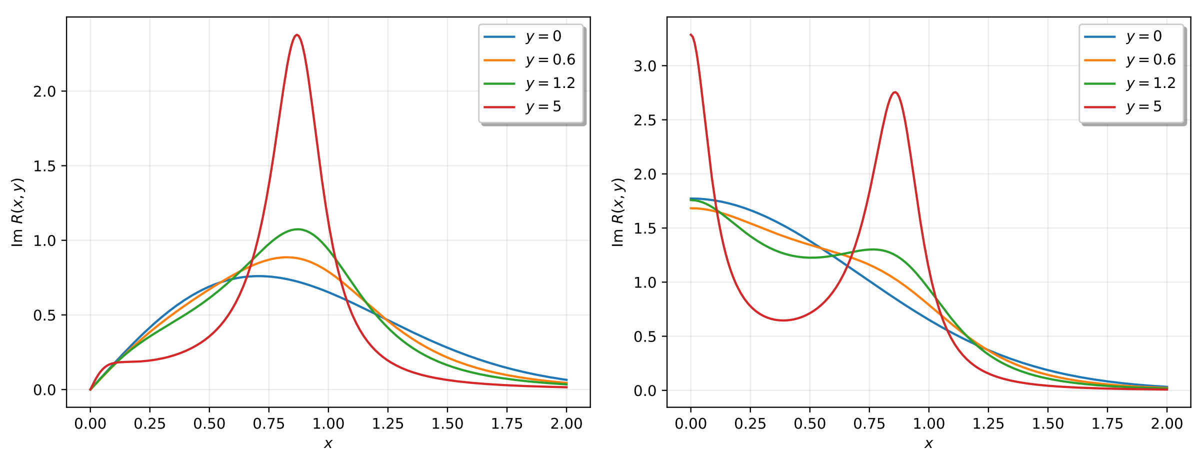

Gain in N_2 gas for stimulated (left) and spontaneous (right) Brillouin scattering. x corresponds to frequency difference between pump and scattered waves, y to collision frequency.

---

[1] V S Averbakh, A I Makarov, and V I Talanov, *Sov. J. Quantum Electron.* **5**, 1201–1206 (1975)

[2] A Sugawara and S Yip, *Phys. Fluids* **10**, 1911–1921 (1967)

Progress in the Vector Diagram for Maxwell's Equations

R. Nevels[(1)], D. R. Wilton[(2)], and K.-H. Yang[(3)]

(1) Dept. of ECE, Texas A&M University, College Station, Tx
(2) Dept. of ECE, University of Houston, Houston, TX
(3) Physics Dept., St. Ambrose University, Davenport, IA

The vector relationship between Maxwell's equations and the electromagnetic field potentials can be presented in a vector diagram based on transverse and longitudinal properties of the fields and potentials. This diagram provides a unique visual comparison of different gauges, largely in a two-dimensional plane. One of the most interesting aspects of the diagram is that it is constructed with axes based on the longitudinal and transverse properties of vectors rather than with the typical dimensional coordinates. Because the curl, gradient and divergence that define the axes in a transverse/longitudinal coordinate system are fundamental operations in the mathematical description of the electromagnetic field, a unique picture of the fields and potentials arises that emphasizes the differences between gauges. We present a brief review of the construction of the diagram and apply it to the fields and potentials obtained with several gauges.

In a transverse/longitudinal coordinate system the three axes represent the one longitudinal and two transverse parts of a vector. Any vector in this coordinate system can have x-, y-, and z-components and any vectors parallel to each other in cartesian coordinates are also parallel in this system. Any vector $\mathbf{U}$ parallel to the longitudinal axis must have the properties $\nabla\cdot\mathbf{U}\neq 0$ and $\nabla\times\mathbf{U}=0$, and for any vector parallel to the transverse axes $\nabla\cdot\mathbf{U}=0$ and $\nabla\times\mathbf{U}\neq 0$. Maxwell's equations then lead to the gauge independent equation $\left(\nabla^2-\frac{1}{c^2}\frac{\partial^2}{\partial t^2}\right)\mathbf{A}(r,t)=-\mu\mathbf{J}(\mathbf{r},t)+\nabla\left(\nabla\cdot\mathbf{A}(\mathbf{r},t)+\frac{1}{c^2}\frac{\partial}{\partial t}\Phi(\mathbf{r},t)\right)$. A gauge is obtained either by specifying the divergence of $\mathbf{A}$ or in placing a requirement on the scalar potential Φ, or both. These choices determine a variety of gauges whose resulting potentials, when plotted on the diagram, provide a concrete picture of differences between them as well as their advantages and limitations. We present a few of these of these gauge diagrams and describe how they can be used both in teaching and research.

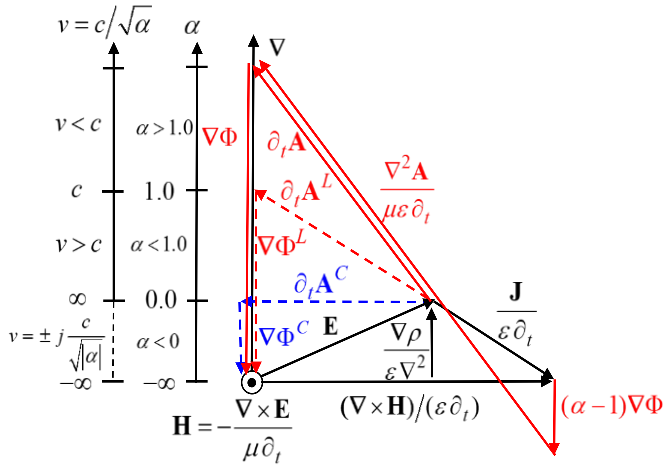

Radio and the Science of Wireless Transmission

Robert Nevels
Texas A&M University
College Station, TX

Radio transmission brought great changes to society. First to ships at sea that prior to the 20th century were completely isolated from land contact for months at a time. Then to people on land in a world where news previously spread slowly to a population mostly living on farms. But radio brought some serious challenges to society and science including, a need understand what electrical current is made of on a fundamental level, how electrical components could control current, how the current interacted with the electromagnetic field inside these components, how the field could be efficiently launched and received by the antenna and what form the signal itself should take. In this presentation we will see how a sinusoidal field gains its polarization, and how information is impressed on the field. We will look at how the field propagates and is received by the radio and how the radio circuit pulls the information off the signal, and finally amplifies it and sends it to the speaker.

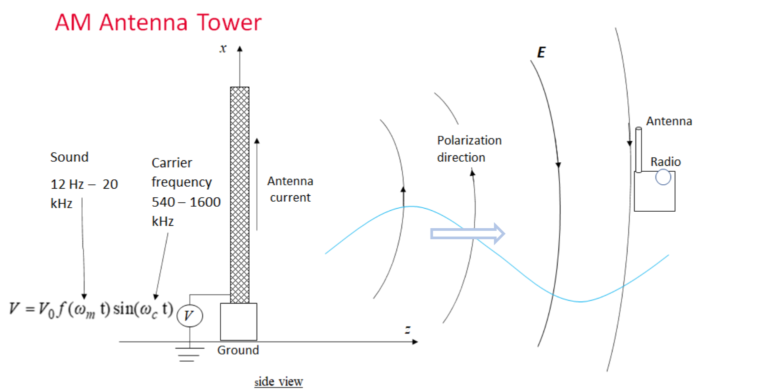

The figure on the right shows a generator sending an amplitude modulated (AM) signal into an antenna tower which launches an electromagnetic wave traveling outward from the antenna and polarized in the direction of the curved lines. The blue sinusoid line shows the amplitude of the wave as it travels in the z-direction and excites a current on the receiving antenna.

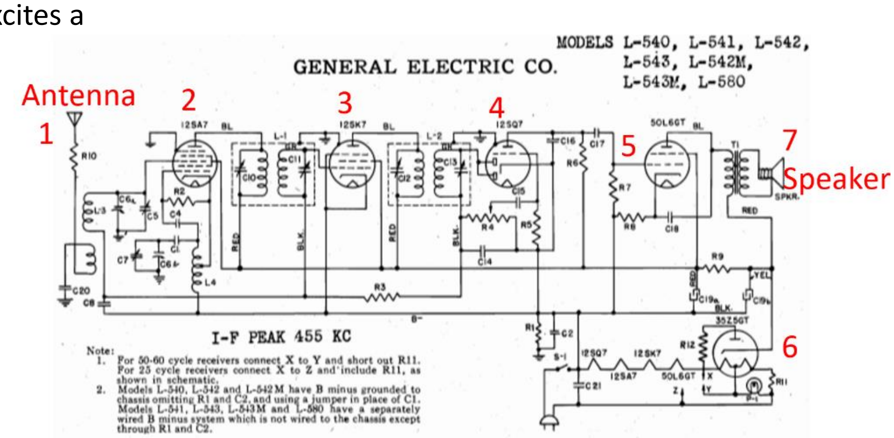

On the right is the schematic for a General Electric L-542 radio made in 1942. The circles are vacuum tubes, which are labeled according to their function. In the order they interact with the input signal: (1) Antenna, (2) Variable frequency oscillator, (3) Mixer, (4) Detector, (5) Audio amplifier, (6) Rectifier, and (7) Speaker. The property of each tube will be explained in the presentation which will conclude with a schematic and explanation of the transistor radio receiver similar to the one you will construct.

Ultra-intense laser interactions with nanostructures: creating extreme plasma conditions and high energy ions for fusion energy with ultrafast lasers

Jorge J. Rocca
Department of Electrical and Computer Engineering
Department of Physics
Colorado State University
jorge.rocca@colostate.edu

The interaction of ultrafast laser pulses of relativistic intensity with high aspect ratio nanostructures can efficiently volumetrically heat matter to an ultra-high-energy-density regime encountered in the center of stars and within the core of fusion capsules compressed by the world's largest lasers [1]. It also generates gigantic quasi-static electromagnetic fields that accelerate particles. Here we present an overview of the physics and applications of these dense relativistic plasmas that can be created with pulses of relatively modest energy from lasers that can operate at high repetition rate. Recent nanowire array experiments produced near-solid density plasmas with an extreme degree of ionization (eg Au^{+72}) which can serve as a platform for understanding atomic processes in extreme environments, and converted ultrafast pulses of laser light into intense x-ray flashes with record efficiency. The irradiation of nanostructures at intensities of > 1×10^{22} W cm^{-2} is predicted to lead to an extreme Ultra High Energy Density plasma regime characterized by Terabar pressures that is virtually unexplored.

Nanowire arrays irradiated at relativistic intennsity act a micro-accelerators that accelerate ions to MeV energies efficiently driving micro-scale fusion reactions. The acceleration of deuterons from deuterated nanowire arrays to multi-MeV energies by the ALEPH Petawatt-class femtosecond laser resulted in quasi-monochromatic fusion neutron production 500 times larger than that from flat solid targets of the same material [2]. These results has been followed by the development of fusion energy concepts by Marvel Fusion that rely on the efficient conversion of laser energy into ion kinetic energy and its subsequent deposition into fusible materials [3], opening a new pathway to laser-driven fusion energy.

Work supported by the U.S. Department of Energy (DOE), Office of Science, Fusion Energy Sciences, under Award No. DE-SC0024882: IFE-STAR, Air Force Office of Scientific Research under award FA9550-17-1-0278, and a DoD Vannevar Bush Faculty Fellowship ONR award N000142012842, using facilities supported by LaserNet US grant US DE- SC0021246

1. J. J. Rocca, M. G. Capeluto, R. C. Hollinger, S. Wang, Y. Wang, G. R. Kumar, A. Lad, A. Pukhov, and V. N. Shlyaptsev, "Ultra-intense femtosecond laser interactions with aligned nanostructures," OPTICA, **11**, 437 (2024)

2. A. Curtis, C. Calvi, J. Tinsley, R. Hollinger, V. Kaymak, A. Pukhov, S.J. Wang, A. Rockwood, Y. Wang, V.N. Shlyaptsev, and J.J. Rocca, *Micro-scale fusion in dense relativistic nanowire array plasmas,* Nature Communications, **9**: 7, (2018).

3. H. Ruhl and G. Korn, "High current ionic flows via ultra-fast lasers for fusion applications," arXiv:2212.12941 (2022).

A gravitational wave detector with atoms: an intriguing precursor

Wolfgang P. Schleich

Institut für Quantenphysik and Center for Integrated Quantum Science and Technology (IQST), Universität Ulm, Albert-Einstein-Allee 11, D-89069 Ulm, Germany;
Texas A&M AgriLife Research, Texas A&M University, College Station, Texas 77843-4242, USA;
Hagler Institute for Advanced Study and Department of Physics and Astronomy, Institute for Quantum Science and Engineering (IQSE), Texas A&M University, College Station, Texas 77843-4242, USA

It is interesting that as early as 1978 a suggestion [1] for the detection of gravitational waves employed atoms. Obviously, they were not cold but at room-temperature. For this reason, this proposal did not rely on the wave nature of the motion, but of light. In this talk we show that an intriguing interference effect of the radiation appears in this proposal of gravitational wave-detector based on non-linear absorption spectroscopy.

Due to its oscillatory motion, enforced by the gravitational wave, the atom interacts with the strong monochromatic electromagnetic pump wave, not only at its frequency, but also at the motional side bands. Since the same behavior occurs also for the probe field, two interfering terms give rise to a dispersive curve [2,3] in the velocity space of the atoms, determining the strengths of the absorption at a single side-band frequency. A similar interference effect is at the very heart of the phenomenon of lasing without inversion [4,5,6].

The Doppler motion of the atom averages out this first order effect due to the dispersion curve. However, hole burning creates a narrow velocity distribution and restores the first order term in the absence of Doppler broadening.

Estimates [1,2,3] of the non-linear term showed that this type of detector would be sensitive to gravitational waves in the frequency regime of 100Hz and an amplitude of $10^{-18} – 10^{-21}$. Despite these promising prospects, we are not aware of more research on this quantum optical approach towards gravitational detection.

References:

[1] Yu. E. Nesterikhin, S. G. Rautian, and G. I. Smirnov, *Laser detector of gravitational waves*, [Zh. Eksp. Teor. Fiz. 75, 3-8 (1978)] Sov. Phys. JETP **48**, 1-3 (1978)

[2] Ch. J. Bordé, J. Sharma, P. H. Tourrenc, and T. Damour, *Theoretical approaches to laser spectroscopy in the presence of gravitational fields*, J. Physique Letters **44**, L983-990 (1983); see also: P. Tourrenc, T. Damour, J. Sharma and Ch. J. Bordé, *Ultra-high laser spectroscopy of atoms as a probe of gravitational fields including gravitational radiation*, in: *General Relativity and Gravitation*, edited by B. Bertotti, F. de Felice, N. A Pascaloni, Vol. **2**, 933-935 (1983).

[3] W. P Schleich, Optische Tests der Allgemeinen Relativitätstheorie, MPQ Report **89** (1984): W. P. Schleich and M. O. Scully, *Non-linear absorptions spectroscopy in an accelerated frame with application to gravity wave detection*, (unpublished manuscript, 1984)

[4] O. A. Kocharovskaya, and Ya. I. Kahanin, *Population trapping and coherent bleaching of a three-level medium by a periodic train of ultra-short pulses*, [Zh. Eksp. Teor. Fiz. **90**, 1610-1618 (1986)] Sov. Phys. JETP **63**, 945-950 (1986)

[5] S. E. Harris, *Lasers without inversion: interference of lifetime-broadened resonances*, Phys. Lett. **62**, 1033-1036 (1989)

[6] M. O. Scully, Shi-Yao Zhu, and A. Gavrielides, *Degenerate quantum beat laser: lasing without inversion, an inversion without lasing*, Phys. Rev. Lett. **62**, 2813-2816 (1989).

Entanglement in Unruh and Hawking radiation from a quantum optical perspective*

Marlan O. Scully

Texas A&M University, College Station, TX; Princeton University, Princeton, NJ

Free quantum field theory in flat space-time is often believed to be well established, holding no surprises. However, in recent work we show that a uniformly accelerated atom in Minkowski space-time emits entangled photon pairs into a squeezed state which mimics entanglement between Minkowski modes which are dominantly in opposite causal wedges of the space-time. Similar emission of photon pairs occurs if an atom is held above the black hole event horizon. Namely, a ground-state atom becomes excited by emitting a “negative”-energy photon under the horizon and then spontaneously decaying back to the ground state by emitting a positive-energy photon outside the horizon, which propagates away from the black hole.

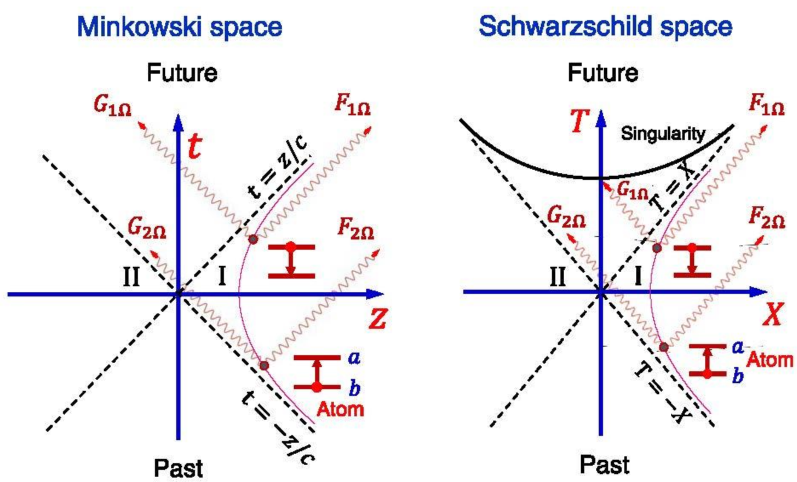

(a) (b)

A ground-state atom accelerated in wedge I goes to the excited state $|a\rangle$ while emitting a photon into a right-propagating Unruh-Minkowski (UM) mode $F_{2\Omega}$, and a left-propagating mode $G_{2\Omega}$. Then, the atom spontaneously decays to the ground state $|b\rangle$ emitting a photon into the UM modes $F_{1\Omega}$ and $G_{1\Omega}$. (b) A ground-state atom held fixed above the horizon of a Schwarzschild black hole goes to the excited state while emitting a photon into the Unruh-Schwarzschild (US) mode $F_{2\Omega}$. Then, the atom spontaneously decays to the ground state emitting a photon into the US modes $F_{1\Omega}$ and $G_{1\Omega}$ which are located mostly above the horizon.

*M. Scully, A. Svidzinsky, and W. Unruh, Phys. Rev. Res. **4**, 033010 (2022).

Can a coherent CW laser beam produce intensity correlation like thermal light?

Yanhua Shih
Department of Physics, University of Maryland Baltimore County, MD 21250

Since Hanbury Brown and Twiss (HBT) discovered intensity correlations in light from thermal (chaotic) sources, it is well-accepted that intensity correlations, i.e. second-order coherence, can be used to characterize the quantum state of light. Specifically, correlations are obtained from light in a thermal state, and it is thus considered a correlated state. Contrarily, light in a coherent state, is free from intensity correlations and thus is considered a non-correlated state.

This talk will addresse the question: can light in a coherent state, such as a multi-longitudinal-mode continuous-wave (CW) laser beam, produce nontrivial intensity correlations like that of light in a thermal state? In other words, if a CW laser beam is used as the light source of an HBT intensity interferometer, do we expect similar result as that of light from a star?

Interestingly, we have experimentally observed an HBT-type intensity correlation from a coherent multi-longitudinal-cavity-mode CW laser beam. The multi-mode laser is a standard fiber ring laser consisting of an 8 m Erbium-doped single-mode optical fiber coupled into a 10 km single-mode fiber ring cavity. This laser generates approximately 450,000 longitudinal cavity modes all in the TEM_{00} transverse mode and, through stimulated emission, each individual cavity mode reaches coherent state, representing a group of identical photons. This observed nontrivial HBT-type intensity correlation is the result of two-photon interference.

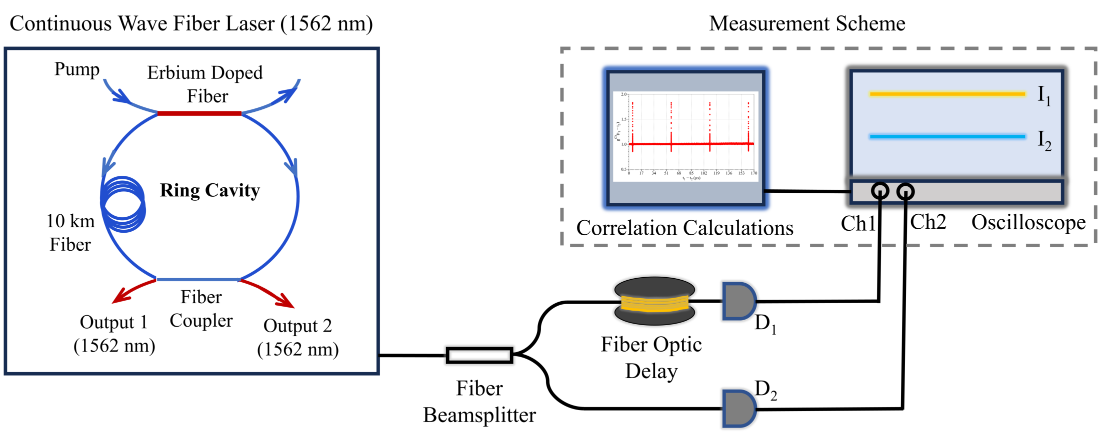

Figure 1: Schematic setup for intensity correlation measurement of a multi-mode fiber laser.

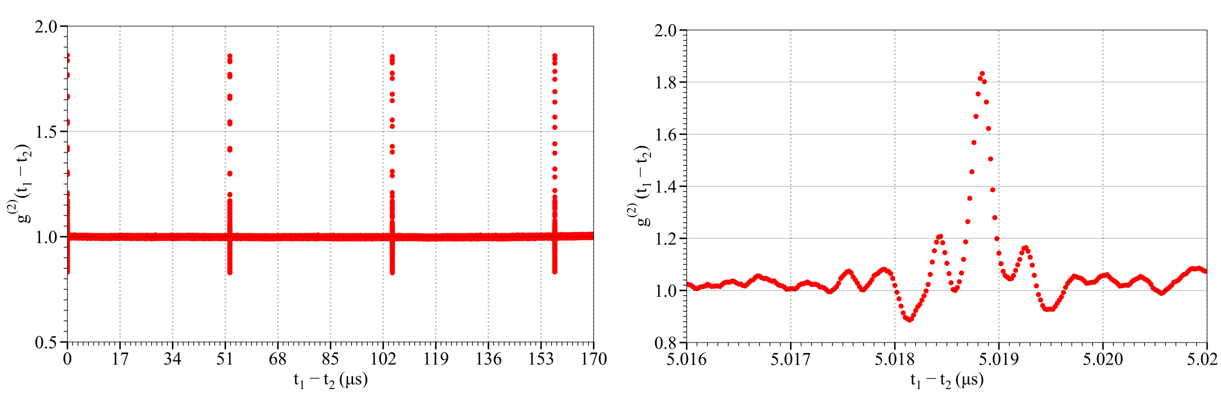

Figure 2: Typical observed temporal intensity correlation.

Novel Nonlinear Optics Enabled by Quantum Coherence

Alexei V. Sokolov*

Institute for Quantum Science and Engineering; Departments of:
Physics and Astronomy, Electrical and Computer Engineering,
Texas A&M University, College Station, TX 77843-4242, USA

Quantum coherence is the central feature of multiple techniques and corresponds to a situation where atoms or molecules of a sample are prepared in a coherent superposition state. High degree of coherence can lead to amazing results. Atomic coherence has earlier been used in electromagnetically induced transparency, ultraslow light propagation, and lasing without inversion. Molecular coherence enables a variety of applications, including, for example, a technique termed molecular modulation, which produces a coherent optical bandwidth spanning infrared, visible, and ultraviolet spectral regions [Fig. 1(a)], allowing arbitrary ultrafast space- and time-tailored sub-cycle optical field synthesis. Building upon these ideas, we have shown that an increased and cleverly manipulated molecular coherence enables improvements in optical detection and sensing, including remote sensing scenarios. Another remarkable example is the use of molecular coherence for the purpose of combining high-power laser beams through stimulated Raman scattering [Fig. 1(b)] - a technique adopted by the laser-fusion community, particularly in the inertial-confinement approach where excimer lasers are used as drivers.

* A large number of people have contributed to this work; I will give proper acknowledgements during my presentation. I want to give special thanks to Aleksei Zheltikov, Marlan Scully and Zhenhuan Yi.

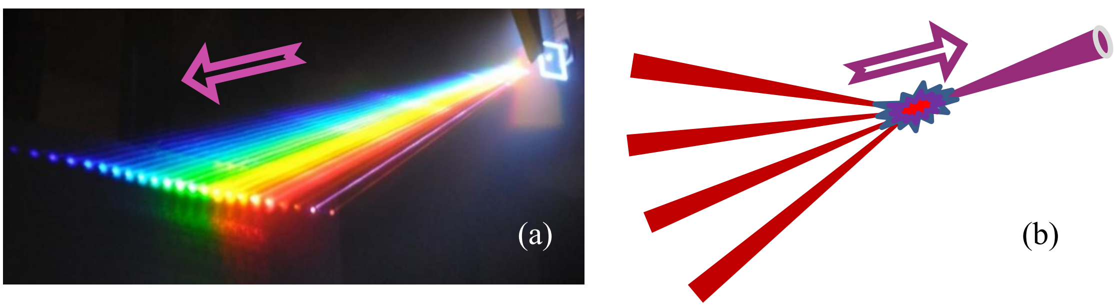

Fig. 1: Applications of quantum molecular coherence to (a) coherent multi-sideband generation, and (b) high-power laser beam combining in the excimer laser approach to inertial fusion energy.

QUANTUM AVALANCHES

P.C.E. Stamp **Univ. of British Columbia (Vancouver, BC, Canada)**

Avalanche processes pervade Nature. Examples range from earthquakes, electrical discharges, Geiger counters, chemical and nuclear explosions, and of course snow avalanches, to many processes occurring in chemical and biological systems, and in populations. However all of these are classical – an obvious question is whether one can have quantum avalanches, in which the system remains in the quantum regime throughout the process.

In this talk I will discuss first a toy model for quantum avalanches (which nevertheless contains much of what happens in real systems). I then describe in detail how the theory works for magnetic quantum Ising systems, where avalanches of domain wall motion at low T occur via the quantum nucleation of "plaquettes" of displaced wall (see figure), and the system remains in the quantum regime throughout the avalanche process. The theory **[1,2]** has been verified experimentally **[2]** in the well-known quantum Ising magnet $LiHo_xY_{1-x}F_4$.

I will then discuss how quantum avalanches can occur in other systems, notably in superfluids; and I discuss the relevance to the theory of quantum measurements **[1].**

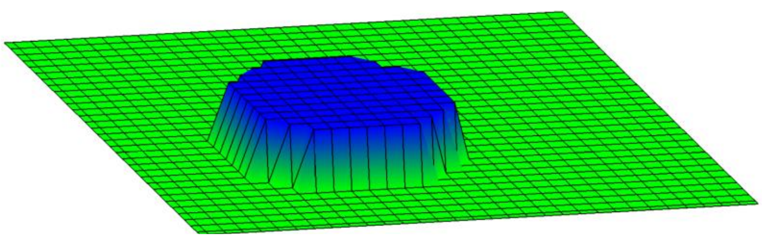

<u>Figure caption</u>: A plaquete of displaced magnetic domain wall – it nucleates via quantum tunneling, and then initiates further plaquette nucleation on nearby domain walls, leading to a quantum avalanche process.

[1] P.C.E. Stamp (to be published)

[2] "Quantum Barkhausen noise induced by domain wall cotunneling", C. Simon, D.M. Silevitch, P.C.E. Stamp, T.F. Rosenbaum, PNAS **121** (13) e2315598121 (2024) https://doi.org/10.1073/pnas.2315598121 **(see particularly the supplementary information)**

The nature of dark energy and electromagnetic origin of electron mass

Anatoly Svidzinsky

IQSE, Texas A&M University, College station, TX 77843, USA

General relativity (GR) is incomparable with the standard model of elementary particles. Namely GR is incompatible with quantum mechanics, and it predicts mass of elementary particles many orders of magnitude greater than the experimental values. I calculated mass of the electron m_e in the framework of vector theory of gravity (VG) [1,2] making expansion in powers of $\ln(\gamma)$, where $\gamma = \sqrt{\frac{4\pi}{G\mu_0}\frac{\mu_B}{e^2}} \gg 1$ and μ_B is the Bohr magneton. In the leading order I find

$$m_e \approx \frac{e^3}{2^{1/4}8\pi\varepsilon_0 c\mu_B}\left[\frac{1}{3}\ln^{3/2}\gamma + \left(\frac{3}{2}\ln 2 + 2 + \frac{1}{\sqrt{2}}\right)\ln^{1/2}\gamma\right] = 8.84 \times 10^{-31}\, kg,$$

which deviates from the experimental value by 2%. Such striking agreement indicates that electron mass has electromagnetic origin, and the Higgs mechanism gives a negligible contribution, if any. VG yields small m_e on the Planck scale because gravitational field induced by particle's angular momentum can have negative energy density which screens the large positive contribution from EM field. Spin is what makes particles light. I also find that for fermions with no electric charge, gravitational field produced by particle's spin doesn't contribute to the mass. That is VG predicts almost zero mass of neutrino.

VG passes all available gravitational tests and quantum vector gravity is equivalent to QED [1]. For cosmology VG predicts the same evolution of the Universe as GR with cosmological constant and zero spatial curvature. However, VG provides explanation of dark energy (Fig. 1) as energy of longitudinal gravitational field induced by Universe expansion and yields, with no free parameters, the value of $\Omega_\Lambda = 2/3 \approx 0.67$ which agrees with results of Planck collaboration and Dark Energy Survey $\Omega_\Lambda = 0.686 \pm 0.02$ [1,2]. In addition, polarization of gravitational waves measured by LIGO and Virgo is compatible with the vector polarization prediction of VG and is inconsistent with the tensor polarization of GR [3].

Arguments mentioned above rule out Einstein's general theory of relativity in favor of vector gravity.

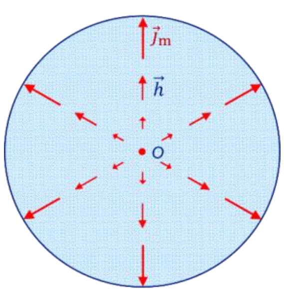

Figure 1: Explanation of dark energy in VG: Expansion of the Universe generates matter current $\vec{J}_m$ directed away from an observer O. Such current induces gravitational field pointing along $\vec{J}_m$ which has negative energy density and accelerates expansion of the Universe. Dark energy does not affect universe evolution in the co-evolving reference frame. Thus, in reality, universe is expanding at a continually decelerating rate, with expansion asymptotically approaching zero.

[1] A.A. Svidzinsky, *Vector theory of gravity: universe without black holes and solution of dark energy problem,* Phys. Scr. **92**, 125001 (2017).

[2] A.A. Svidzinsky, *Simplified equations for gravitational field in the vector theory of gravity and new insights into dark energy*, Phys. Dark Universe **25**, 100321 (2019).

[3] A.A. Svidzinsky, R.C. Hilborn, *GW170817 event rules out general relativity in favor of vector gravity*, Eur. Phys. J. Spec. Top. **230**, 1149 (2021).

Attosecond Physics: From High Harmonic Generation to Measuring the Electric Field of Light and Attosecond Quantum Eraser

A.J. Verhoef[1], A. Fernández[1], A.M. Zheltikov[1], and A. Baltuska[2]

[1]Texas A&M University, College Station, TX 77843, USA

[2]Technische Universität Wien, 1040 Vienna, Austria

Last year's Nobel prize announcement "for experimental methods that generate attosecond pulses of light for the study of electron dynamics in matter," to Prof. Agostini, Prof. Krausz, and Prof. L'Huillier, was of especial interest to us, as we worked with Prof. Krausz on this topic. In this presentation, we will discuss the fundamental processes and developments that lead to this scientific breakthrough. This includes the generation of ultrashort pulses, the control of the electric field waveform of such pulses and high-harmonic generation. We will also discuss first attosecond experiments and breakthroughs, such as the attosecond streaking experiment [1] and highlight a few current applications. Finally, we will review the possibility to observe double slit interference [2] and quantum erasure with attosecond precision.

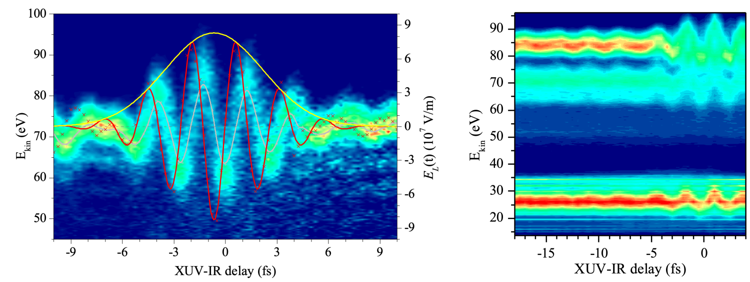

Fig. 1. Attosecond streaking of electrons ionized from neon reveals the electric field of light (left). A streaking experiment with xenon indicates how long it takes different electrons to leave atoms upon ionization (right).

The attosecond quantum eraser scheme is as follows: A broadband soft x-ray pulse excites or ionizes a core-shell electron (3d) from a krypton atom [3]. Following this pulse, the highly excited krypton atom or ion will emit an Auger electron from the 4p shell when another 4p electron fills the 3d hole. Under normal conditions, even when the emitted 4p (resonant) Auger electrons can have overlapping energy spectra, no interference of these electrons can be observed, as there is the option for detection of the charge state of the resulting Kr ion, as well as the presence or absence of a low-energy electron, to allow determination of the excitation-decay path. Thus, to erase the path information, two factors need to be addressed: First of all, the Rydberg electron needs to be removed from the resonantly excited krypton; and second, this electron needs to be made indistinguishable from the low-energy electron that is emitted when the 3d electron is ionized. We achieved this with a strong infrared field slightly delayed to the soft x-ray pulse. At this point, the Auger decay is well underway, and the infrared field can efficiently address the possibly present Rydberg electron, ionize it and mix it with the possibly present ionized (from the 3d shell) electron. Thus, we erase which-path information from a 3-particle "entangled" state. An intriguing part in this experiment is that while in essence a single photon process, infrared ionization from the Rydberg state is very weak, and its probability is strongly modulated by the Auger decay: Therefore, we observe that the interference pattern shifts with delay between the soft x-ray pump and infrared probe pulse.

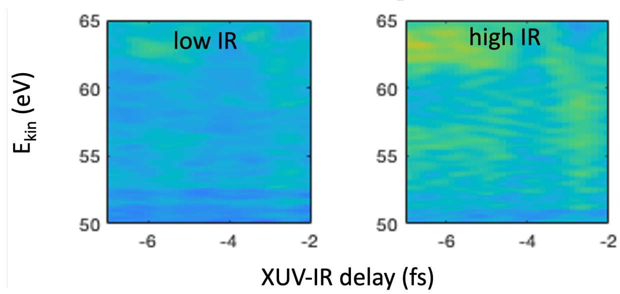

Fig. 2. Erasure of 'which-path' information (causing spectral interference, left image) by the infrared streaking field observed for Auger electrons in Krypton.

References

[1] E. Goulielmakis et al., Direct measurement of light waves. Science 305, 1267–1269 (2004).

[2] F. Lindner et al., Attosecond Double Slit Experiment. Phys. Rev. Lett. 95, 040401 (2005)

[3] A.J. Verhoef et al., Time-and-energy-resolved measurement of Auger cascades following Kr 3d excitation by attosecond pulses. New. J. Phys. 13, 113003 (2011).

Raman Bronchoalveolar Lavage

Dmitri Voronine

Department of Physics, University of South Florida, Tampa, FL 33612, USA

ABSTRACT

Bronchoalveolar lavage (BAL) is a medical diagnostic procedure for lung diseases based on minimally invasive sample collection from the lungs using a bronchoscope. Raman spectroscopy is a convenient chemical analytical method that may be used to rapidly analyze the chemical composition of BAL fluid samples. Raman BAL of human samples revealed the presence of various types of microplastics that could potentially have detrimental effects on health. The spatial resolution of BAL was improved using tip-enhanced Raman scattering (TERS), leading to the detection of nanoplastics. These techniques provide quantitative analysis of plastic pollution once the procedural controls are properly implemented. Knowledge of plastic pollution levels in humans and the environment is important for sustainability and better health.

From Loop Quantum Cosmology to Loop Quantum Black Holes: A Rough Road

Anzhong Wang
GCAP-CASPER, Department of Physics, Baylor University, Waco, TX, 76798-7316, USA
(Dated: June 10, 2024)

General relativity (GR) has achieved great success since its incarnation in 1915, ranging from cosmology to black holes. However, it also faces severe challenges in front of the big bang and black hole (BH) singularities, due to the divergence of curvatures at these points. At these points, quantum gravitational effects are expected to be strong. In fact, it is the general belief that such corrections are so strong that they will dominate physics, whereby the singularities are smoothed out and physics becomes predictable. However, a century after the first claim by Einstein that GR needs to be quantized, the unification of quantum mechanics and GR still remains an open question, despite enormous efforts. So far, various theories have been proposed, among which string/M-Theory and loop quantum gravity (LQG) have been extensively investigated.

String/M-Theory unifies all interactions and could therefore provide a framework from which we may hope to derive all physical laws. In this respect, it goes far beyond the simple quantization of GR, although from a methodological point of view, it is still a natural extension of perturbative quantum gravity and uses methods of constrained quantization.

On the other hand, LQG is based on a canonical approach to quantum gravity (QG) introduced earlier by Dirac, Bergmann, Wheeler, and DeWitt, but formulated in terms of holonomy and described by the SU(2)-valued Ashtekar's connection. Then, one can construct the full kinematical Hilbert space in a rigorous and well-defined manner. An open question of LQG is its semiclassical limit, i.e., are there solutions of LQG that closely approximate those of GR in the semiclassical limit? Although the above question still remains open, concrete examples can be found in the context of loop quantum cosmology (LQC) [1]. In LQC, the resolution of the big bang singularity is crucially related to the fact that in LQG, the area operator has a minimal and non-zero area gap after the quantization of the spatial geometry. Due to these quantum geometric corrections, the Big Bang singularity is generically replaced by a quantum bounce. The resultant LQC is consistent with all cosmological observations and could also explain some anomalies in recent cosmic microwave background (CMB) observations [2, 3].

When applying the techniques of LQC to BHs, several issues raise [4–11], and so far, studies of loop quantum BHs have not been as successful as those in LQC. In this talk, I shall first give a brief review of LQC and then clearly state the obstacles that we have been facing when applying LQC to BHs, and then discuss some possibilities to overcome these problems.

[1] A. Ashtekar and P. Singh, *Loop Quantum Cosmology: A Status Report*, Class. Quant. Grav. **28**, 213001 (2011) [arXiv:1108.0893].
[2] B.-F. Li, P. Singh, A. Wang, *Phenomenological implications of modified loop cosmologies: an overview*, Front. Astron. Space Sci. **8** (2021) 701417 [arXiv:2105.14067].
[3] I. Agullo, A. Wang, E. Wilson-Ewing, *Loop quantum cosmology: relation between theory and observations*, in the "Handbook of Quantum Gravity", C. Bambi, L. Modesto, I. Shapiro (editors), Springer (2023).
[4] G. Ongole, P. Singh, . Wang, *Revisiting quantum black holes from effective loop quantum gravity*, Phys. Rev. D**109**, 026015 (2024) [arXiv:2311.10166].
[5] H. Zhang, W.-C. Gan, Y. Gong, A. Wang, *On the improved dynamics approach in loop quantum black holes*, Commun. Theor. Phys. **76** (2024) 035401 [arXiv:2308.15574].
[6] W.-C. Gan, X.-M. Kuang, Z.-H. Yang, Y. Gong, A. Wang, B. Wang, *Nonexistence of quantum black and white hole horizons in an improved dynamic approach*, SCIENCE CHINA Physics, Mechanics & Astronomy (in press) (2024) [arXiv:2212.14535].
[7] G. Ongole, H. Zhang, T. Zhu, A. Wang, B. Wang, *Dirac observables in the 4-dimensional phase space of Ashtekar's variables and spherically symmetric loop quantum black holes*, Universe **8** (2022) 543 [arXiv:2208.10562].
[8] W.C, Gan, G. Ongole, E. Alesci, Y. An, F.W. Shu, A. Wang, *Understanding quantum black holes from quantum reduced loop gravity*, Phys. Rev. D**106**, 126013 (2022) [arXiv:2206.07127].
[9] J.-M. Yan, Q. Wu, C. Liu, T. Zhu, A. Wang, *Constraints on self-dual black hole in loop quantum gravity with S0-2 star in the Galactic Center*, JCAP **09** (2022) 008 [arXiv:2203.03203].
[10] Y.-C. Liu, J.-X. Feng, F.-W. Shu, A. Wang, *Extended geometry of Gambini-Olmedo-Pullin polymer black hole and its quasinormal spectrum*, Phys. Rev. D**104** (2021) 106001 [arXiv:2109.02861].
[11] W.-C. Gan, N.O. Santos, F.-W. Shu, A. Wang, *Properties of the spherically symmetric polymer black holes*, Phys. Rev. D**102**, 124030 (2020) [arXiv:2008.09664].

Quantum simulation in superradiance lattices

Dawei Wang

School of Physics, Zhejiang University

Abstract: In order to investigate quantum many-body problems beyond classical computational capability, artificial quantum systems are used to synthesize and simulate the target Hamiltonian. As a widely used platform, ultracold optical lattices have realized various exotic quantum phases of matter. However, quantum control inevitably results in heating effect that destroys the simulated quantum matter. In order to address this issue, a room-temperature quantum simulation platform is developed based on momentum-space superradiance lattices. In this talk I will report on the recent progress on superradiance lattices, including the observation of chiral edge currents, flat-band localization, and dynamical localization-delocalization. Based on superradiance lattices, a spectroscopic method is presented to measure the geometric phases of topological matter, and various optical devices such as the optical diode can be designed. Superradiance lattices provide new techniques and methods for quantum metrology and quantum computing.

Wide-Field *In Vivo* Label-free Imaging with kHz frame rate

Jizhou Wang[1], Nathan Marshall[1], Zehua Han[1], Kai Wang[2], Richard Sprague[1], Wenxuan Yu[3], Zhenhuan Yi[1], Xingqi Xu[3], Dawei Wang[3], Marlan O. Scully[1,4], Alexei V. Sokolov[1,4]

[1]Institute for Quantum Science and Engineering, Texas A&M University, College Station, TX 77840, USA

[2]School of Physics and Astronomy, Sun Yat-sen University, Zhuhai, 519082, China

[3]Interdisciplinary Center for Quantum Information, Zhejiang Province Key Laboratory of Quantum Technology and Device, and School of Physics, Zhejiang University, Hangzhou, China

[4]Baylor Research Innovative Center, Baylor University, Waco, TX 76798, USA

Infrared (IR) spectromicroscopy can provide label-free imaging based on intrinsic molecular vibrations. However, conventional IR microscopy encounters challenges in achieving high spatial resolution and measuring samples that contain water such as biological specimens. These difficulties arise from the long wavelength of IR light and the strong absorption by water in this spectral region. Additionally, the long acquisition time significantly limits its applications in fast imaging. To overcome the above issues, we developed a wide-field spectromicroscopy based on infrared-resonant third-order sum-frequency (ITS) generation [1]. The energy diagram is shown in Fig 1(a). In this experiment, a femtosecond pulse train is used to resonantly excite C-H vibrational modes (2900 cm^{-1}) while another pulse train centered at 1.55 µm probes the coherence at a certain time delay. The signal is emitted by sum-frequency generation at around 633 nm and used for imaging. The schematic diagram of the ITS imaging setup is illustrated in Figure 1(b).

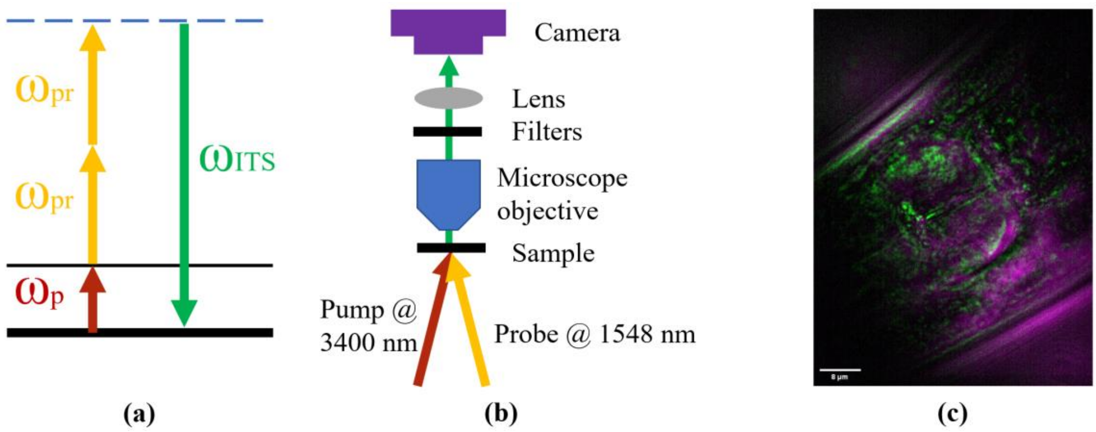

Fig. 1. (a) Energy diagram of ITS spectroscopy. (b) Schematic drawing of the wide-field ITS microscope. (c) Single-shot ITS image of the grinder area of a *C. elegans* worm.

In Figure 1(c), a single-shot overlay ITS image of a live *Caenorhabditis elegans* worm is displayed. The spatial resolution is around 400 nm. The green color is the four-wave-mixing background, while the purple color corresponds to the resonant C-H vibration signal.

In this experiment, single-shot imaging means the actual exposure time for one frame is around 1 ps during which the ultrafast pulses overlap temporally and the sum-frequency signal is generated. This not only reduces motion artifacts when imaging dynamic samples, but also increases the video frame rate to the level of laser's repetition rate.

[1] Wang, Jizhou, et al. "Femtosecond Time-Resolved Infrared-Resonant Third-Order Sum-Frequency Spectroscopy." *ACS Photonics* 8.4 (2021): 1137-1142.

Exploring Universality in Scattering Theory through General Dispersion Relations

Yidan Wang
Harvard University
yidanwang@fas.harvard.edu

Universality in physics generally refers to situations when systems very different at short distances share identical long-distance behavior. In scattering systems, many physical properties become universal in the low-energy limit, determined primarily by the scattering length and independent of the microscopic details of the interaction. The discussion of universality in scattering theory has traditionally been limited to quadratic dispersions. In this talk, we introduce a novel perspective of universality by examining scattering models with general dispersions [1], as depicted in the figures. We establish that when the density of states diverges at $E = 0$, the S-matrix approaches a universal limit solely dependent on the divergence rate and a few parameters characterizing the low-energy behavior of the interactions. Our investigation into general dispersions aligns perfectly with the experimental progress in synthetic quantum systems, which allows for broad control of dispersion relations through tunable periodic structures such as atomic arrays or photonic crystal waveguides.

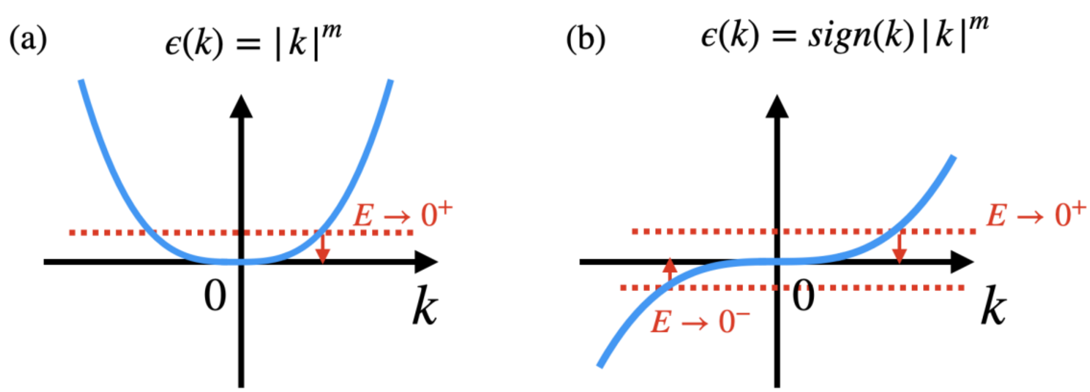

Fig 1. An illustration of the two types of dispersions being considered, where the density of states diverges at $E = 0$ for $m > 1$. The S-matrix approaches a m-dependent universal limit when $E \to 0$.

[1] Wang, Y., Gullans, M.J., Na, X., Whitsitt, S. and Gorshkov, A.V., 2022. Universal scattering with general dispersion relations. *Physical Review Research*, *4*(2), p.023014.

Excimer Driver Technology for Laser Driven Inertial Confinement Fusion Energy

Dr. Matthew F. Wolford (Code 6733)

U.S. Naval Research Laboratory, Washington D.C.

Abstract: The challenge is immense to find a viable inertial confinement energy configuration that will be economical with our present energy options. Laser drivers show promise due to their precise control and significant stand-off from the fusion fuel. Investigation of 'alternative' laser drivers are explored including the excimer lasers of krypton fluoride (KrF, which has amplified stimulated emission centered near 248 nm) and argon fluoride (ArF, which has amplified stimulated emission centered near 193 nm). The experimental accomplishments, and theoretical developments for repetitively pulsed electron beam pumped excimer lasers for laser fusion energy will be reviewed. In addition, discussion of ongoing challenges for excimer laser systems and more importantly opportunities for you to make significant scientific and technical contributions for achieving large scale excimer laser drivers available for low cost fusion energy expeditiously. The future directions of the Electra facility including development of ultrashort ArF laser and solid state pulsed power system for the Electra will also be mentioned.

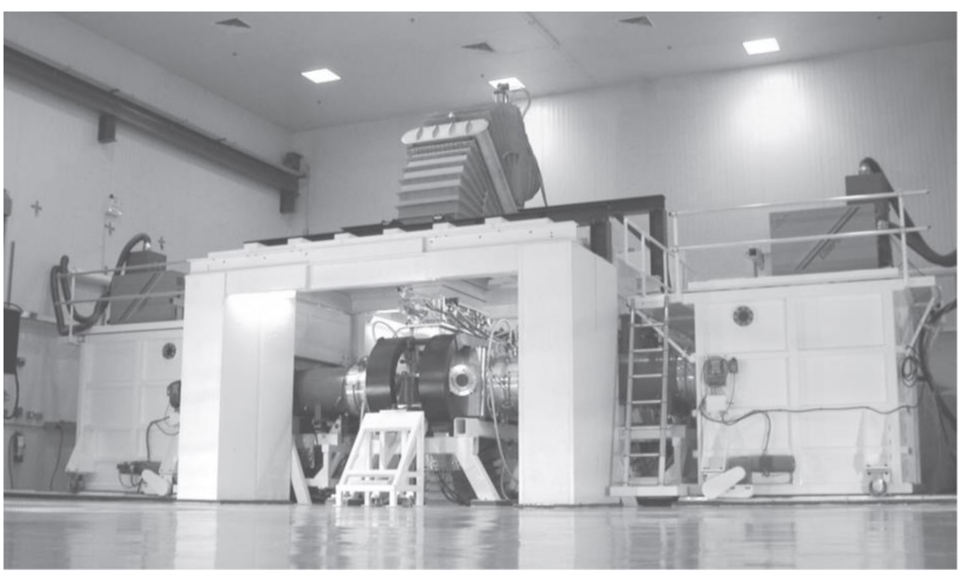

Figure Caption. The repetitively pulsed electron beam pumped excimer laser amplifier Electra at the U.S. Naval Research Laboratory, which has been under development and in operation from 1999 to present.

Distribution Statement A. Approved for Public Release. Distribution Unlimited.

Programmable Simulations of Molecules and Materials with Reconfigurable Quantum Processors

Nishad Maskara, Stefan Ostermann, James Shee, Marcin Kalinowski, Abigail McClain Gomez, Rodrigo Araiza Bravo, Derek S. Wang, Anna I. Krylov, Norman Y. Yao, Martin Head-Gordon, Mikhail D. Lukin, Susanne F. Yelin

Simulations of quantum chemistry and quantum materials are believed to be among the most important potential applications of quantum information processors, but realizing practical quantum advantage for such problems is challenging. Here, we introduce a simulation framework for strongly correlated quantum systems that can be represented by model spin Hamiltonians. Our approach leverages reconfigurable qubit architectures to programmably simulate real-time dynamics and introduces an algorithm for extracting chemically relevant spectral properties via classical co-processing of quantum measurement results. We develop a digital-analog simulation toolbox for efficient Hamiltonian time evolution utilizing digital Floquet engineering and hardware-optimized multi-qubit operations to accurately realize complex spin-spin interactions, and as an example present an implementation proposal based on Rydberg atom arrays. Then, we show how detailed spectral information can be extracted from these dynamics through snapshot measurements and single-ancilla control, enabling the evaluation of excitation energies and finite-temperature susceptibilities from a single-dataset. To illustrate the approach, we show how this method can be used to compute key properties of a polynuclear transition-metal catalyst and 2D magnetic materials.

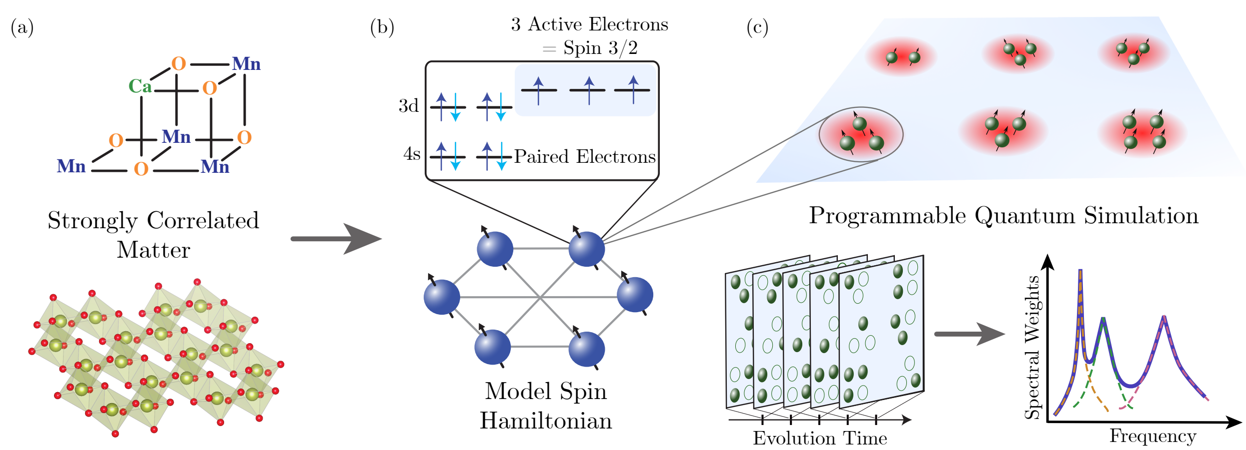

Figure 1: Model Hamiltonian approach to quantum simulation of strongly-correlated matter.

Cooperative Emissions in Atomic and Molecular systems

Zhenhuan Yi[1], M. O. Scully[1,2,3]

[1]Texas A&M University, [2]Baylor University, [3] Princeton University

ABSTRACT

Quantum coherence has been an import resouce for many facinating effects, e.g, Electromagnetically Induce Transparency (EIT), Laser Without Inversion (LWI), Stopped light, etc. In extended sytems, atoms act coherently and produce cooperative emissions such as superfluorescence and superradiance. Atomic coherence and cooperative emissoin are also the bases of induced Rabi oscillation effect and quantum beat spectroscopy [1]. On the other hand, the core of coherent Raman techniques is molecular coherence. While traditional visible-light-pumped CARS techniques use transitoin dipoles between the electronic ground state and excited states, as shown in Fig. b), infrared (IR) light can also help achieve comparable Raman coherence in a fundamentally different way, e.g., Mid-infrared Assisted Coherent Anti-Stokes Raman Scattering (MIRA CARS) [2].

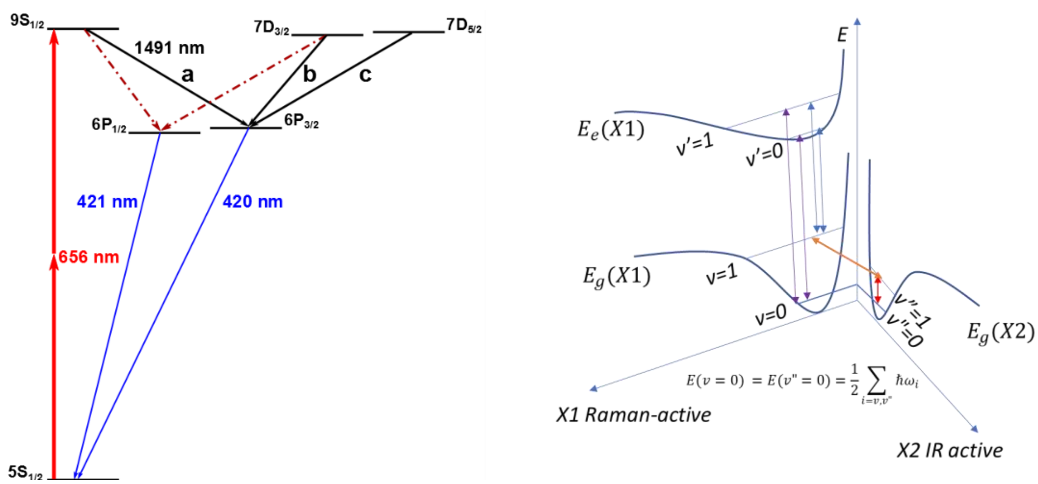

Figure: a) Excitation of atomic coherence in ^{87}Rb. b) Typical coherent Raman schemes use transition dipoles between electronic ground state (E_g) and excited states (E_e) to excite Raman coherence. This can also be done within the electronic ground state, as shown in MIRA CARS.

[1] Yi Z., Begzjav T.K., Ariunbold G.O., Zheltikov A.M., Sokolov A.V. and Scully M.O., Multiple pathway quantum beat spectroscopy. Front. Phys. **10**, 921499 (2022).

[2] [2] A. J. Traverso et al., Phys. Rev. Lett. 120, 063602 (2018).

Quantum evolution of mixed states and efficiency of quantum heat engines

Anatoly Svidzinsky, and Wenzhuo Zhang

Texas A&M University, College station, TX 77843, USA

Quantum evolution of a system can be qualitatively different from the classical counterpart. E.g., the increase of electric current along a normal metal ring yields heating. However, if the metal ring is in a quantum superconducting state, then adiabatic increase of the electric current can result in a cooling effect [1]. We investigate quantum evolution of mixed states using a formalism similar to the Heisenberg representation of quantum mechanics in which operators incorporate a dependency on time. We find the exact solution for the evolution of two and three coupled harmonic oscillators initially prepared in thermal states at different temperatures. We show that such systems exhibit interesting quantum dynamics in which oscillators swap temperatures due to entanglement induced in the process of heat exchange (Fig. 1a) and yield noise induced coherence. A photonic quantum heat engine (QHE) composed of two optical cavities can be modeled as coupled harmonic oscillators with time-dependent frequencies (Fig. 1b). Photons in the cavities become entangled during the engine operation. We show that work done by such an engine is maximum if at the end of the cycle the oscillators swap number of excitations which can be achieved when the engine operates under the condition of parametric resonance. We also show that Carnot formula yields limiting efficiency for QHEs under general assumptions. Although quantum engines do not beat the second law of thermodynamics, there is a host of quantum resources that can be exploited to outperform classical technologies.

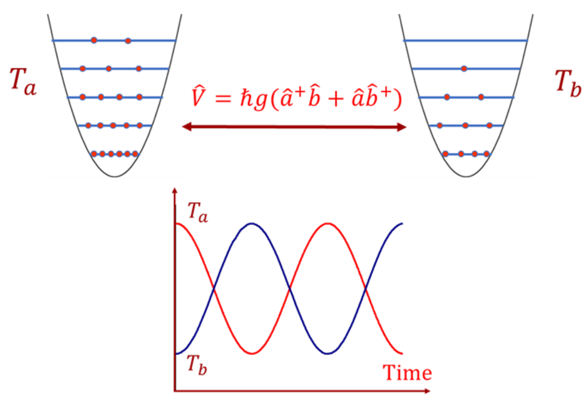

(a)

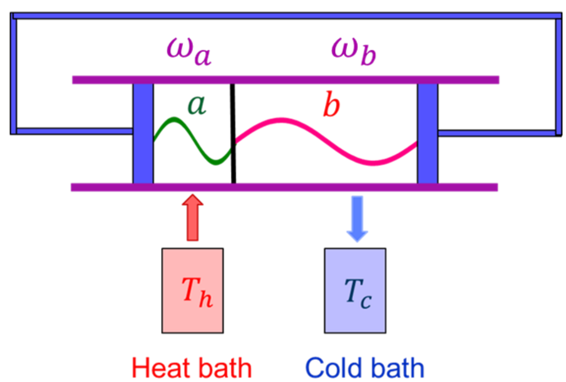

(b)

Figure 1: (a) Heat flow in quantum evolution. Identical harmonic oscillators at different temperatures are brought into contact with each other. During evolution, the state of each oscillator is thermal, but oscillators become entangled which yields Rabi oscillations of the oscillator's temperatures. (b) Photonic QHE composed of two optical cavities with different frequencies coupled via a partially transmitting common mirror. Outside mirrors can move and act as a piston of the engine. The working fluid of the engine is photon gas in the cavities which exerts radiation pressure on the mirrors and can do mechanical work on the surroundings.

[1] A.A. Svidzinsky, *Possible cooling effect in high temperature superconductors*, Phys. Rev. B **65**, 144504 (2002).

Facile control of hard X-ray quantum memory

Xiwen Zhang[1], and Olga Kocharovskaya[1]
[1]*Department of Physics and Astronomy and Institute for Quantum Science and Engineering, Texas A&M University, College Station, Texas 77843, USA*

Email: xiwen@tamu.edu

The exploration and exploitation of quantum optics have flourished in the past several decades across the spectrum, from microwaves to soft X-rays. Hard X/γ-ray quantum optics holds the potential for a groundbreaking leap in future quantum optical technologies. However, its progress has been impeded, in part due to the absence of bright coherent sources and effective control methods for these energetic photons.

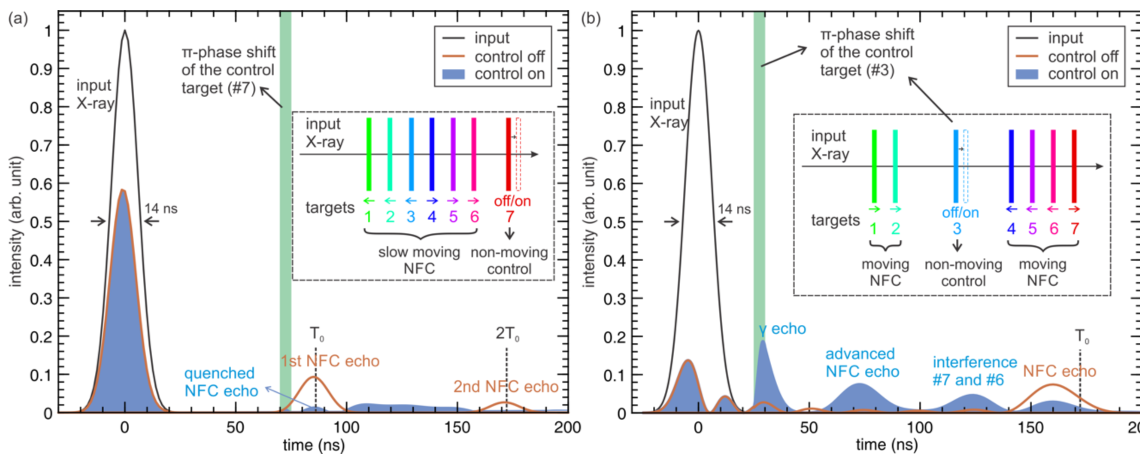

Fig. 1. Illustration of the scheme for controlling X-ray quantum memory, shown in insets, comprising a nuclear frequency comb (NFC) implemented by 6 slowly moving (~ 1 mm/s) nuclear Mössbauer absorbers and a non-moving (stationary) control nuclear absorber that can be fast displaced by half wavelength. (a) Quenching and (b) advancing of a hard X-ray echo by fast displacing the control target by half wavelength.

A diverse range of functionalities for hard X-ray photon control can be accomplished through synchronized motion of Mössbauer resonant nuclear absorbers with different velocities producing a frequency comb in the absorption spectrum via the Doppler effect [1]. Quantum memory based on such nuclear frequency comb (NFC) has been recently experimentally demonstrated [2]. Here we suggest a simple method to control a quantum memory echoes by a fast half-wavelength displacement of a stationary absorber. The scheme is shown in insets of Fig. 1. It allows a quench [Fig. 1(a)] or an advancement [Fig. 1(b)] of an NFC echo.

[1] Xiwen Zhang *et. al.*, Nuclear quantum memory and time sequencing of a single γ photon, Phys. Rev. Lett. **123**, 250504 (2019).
[2] Sven Velten *et. al.*, Nuclear Quantum Memory for Hard X-Ray Photon Wave Packets, Sci. Adv. **10**, eadn9825 (2024).

Phase Transition and Melting of Oxide via Plasmonic Heating

Zhenrong Zhang
Department of Physics, Baylor University, Waco, Texas, 76798

Understanding the reactivity of various crystal faces in different polymorphs of TiO_2 in photoreaction is important for many photocatalytic applications. Here, we studied the anatase-rutile phase transition (ART) processes of individual micro-sized TiO_2 crystals and nanocrystals via thermal annealing and plasmonic heating. Micro-Raman spectroscopy mapping and scanning electron microscope (SEM) images were obtained at different ART stages to correlate the crystal structure transformation with the morphology change. The crystal orientation after phase transition is obtained via polarization-dependent Raman spectroscopy (Figure 1a and 1b).

Plasmonic heating has been utilized in many applications including photocatalysis, photothermal therapy, and photocuring. However, how high the temperature can be reached for the surrounding media due to the collective heating of the plasmonic nanoparticles (NPs) and the impact of the heat dissipation on the surrounding media is not clear. In the second part of my talk, I will present the impact of plasmonic heat generated by resonantly excited gold (Au) NPs on P25 TiO_2 nanoparticle film. Under 532 nm continuous laser irradiation at the surface of the Au-TiO_2, the surface evaporation of Au nanoparticles and phase transition of TiO_2 were observed at moderate laser power (Figure 1c). More importantly, as high as the melting point of TiO_2 of 1830 °C is confirmed from the molten TiO_2 rutile phase. The temperature calculation shows that the heating generated by Au nanoparticles is not localized. The collective heating from an ensemble of Au nanoparticles in the irradiated area produces a global temperature rise that melts TiO_2. Our results suggest that the photothermal effect could be a major mechanism in the plasmon-assisted photocatalytic reactions. The experimental observation of the high temperature of the supporting media suggests new applications for utilizing plasmonic heating.

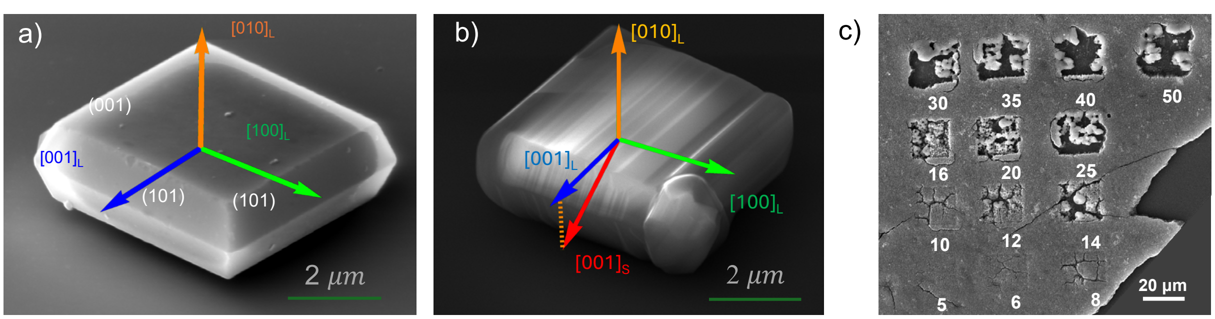

Figure 1. Micro-sized TiO_2 anatase crystal (a) before and (b) after phase transition. c) Phase transition and melting of P25 TiO_2 due to plasmonic heating.

Rogue waves, black swans, and laser beam instabilities

Aleksei Zheltikov

Institute of Quantum Science and Engineering, Department of Physics and Astronomy, Texas A&M University, College Station TX

In this talk, we will review manifestations of *extreme events in optical physics*. A bigger-picture perspective on such events and their inner workings will be shown to encompass a remarkable variety of phenomena, spanning across various disciplines and areas of science, ranging from *rogue waves* in the ocean to *black swans* in the stock market.

Unlike deterministic optics, which describes nonlinear processes in terms of well-defined field intensities, as well as well-resolved thresholds and gain spectra, its stochastic counterpart is concerned with a question as to how probable these processes are. Remarkably, despite an enormous variety of output statistics found in optics, all these statistics converge, in their extreme-value limit, to one of only three *universal extreme-value distributions*. Specifically, in the class of polynomial nonlinearities, such as those found in self-focusing, self-phase modulation, weak-field harmonic generation, and multiphoton ionization, the statistics of the nonlinear-optical output converges, in the extreme-value limit, to the *exponentially tailed*, Gumbel distribution. Exponentially growing nonlinear signals, on the other hand, such as those induced by parametric instabilities and stimulated scattering, are shown to reach their extreme-value limits in the class of the Fréchet statistics, giving rise to extreme-value distributions with heavy, manifestly *nonexponential tails*, thus favoring *extreme-event outcomes* and *rogue-wave buildup*.

We will discuss *deterministic* and *stochastic* aspects in wave instabilities in optics and will search for a fine line between *avoidable* and *unavoidable* in *laser beam instabilities*. As one important finding, stochastic laser beams that nominally meet the deterministic beam-stability criterion may emerge as *unstable on large pulse samples*.

In a rapidly changing scenery of modern optical science and laser technologies, nonlinearity-induced instabilities keep posing new challenges, exhibiting unexpected features, sometimes showing up in an unrecognizable form, as completely new actors in a complex spatiotemporal dynamics of high-power optical field waveforms. Clear understanding of these complex scenarios and the pertinent *beam-stability parameter space* is critical for adequate *laser-beamline design* in many areas of optical science and laser technologies, including *laser-fusion research* and *laser-fusion plants* moving forward. These pressing questions are the focus of research that the *IQSE* team at Texas A&M University conducts as a part of the multi-institution *RISE Hub* effort[1] aiming to *advance laser-driven fusion energy*.

[1] supported by the DOE Office of Science through the DOE Inertial Fusion Energy Science and Technology Accelerator Research (IFE-STAR) program (grant # DE-SC0024882).

Poster Abstracts

(Listed Alphabetically by Presenter's Last Name)

Understanding Plasmonic-TiO_2 Interactions: Au Nanoparticles on Single Bulk Crystal TiO_2 Surfaces for Redox Photocatalysis

Olawale Ayoade, Weigang Lu, Hao Zhu, and Zhenrong Zhang

Department of Physics, Baylor University, Waco, TX 76798

The Au/TiO_2-based systems are promising photocatalysts that promote light-induced chemical conversions from the ultraviolet (UV) to the visible region of the spectrum due to the surface plasmon resonance effect, with plasmonic metal nanostructures being investigated to enhance reaction efficiency and sustainability. The photocatalytic activities of Au nanoparticles (NPs) on several nano- and micro-sized TiO_2 morphologies, including P25, have been extensively studied; however, Au NPs adsorbed on well-defined TiO_2 crystal facets in a liquid environment are lacking for widespread practical applications. To advance the development of effective Au/TiO_2-based photoreduction materials, we propose combining Au NPs with well-defined bulk single-crystal anatase (001), anatase (101), rutile (001), and rutile (110) facets. We propose Au NPs on these TiO_2 facets as the characteristics of the noble metal influence the simultaneous separation of the photogenerated charge carriers (electron-hole pairs) at the surface and in the bulk.

To better understand the effects of Au NPs on the reactivity of the TiO_2 facets, we investigated the modulation of hot electron generation and the enhancement of electric fields. For this purpose, we used an on-resonance 532 nm laser to excite the 40 nm-sized nanoparticles, utilizing their localized surface plasmon resonance (LSPR) properties. These metallic nanoparticles were drop-cast onto TiO_2 and subsequently annealed at 100 ºC for one hour, a process that did not affect the crystal structure of the samples (Figure 1a). We studied the photocatalytic reduction activity of resazurin (RZ). A liquid cell containing Au/TiO_2 crystal and RZ solution was used in the experiment. The photoluminescence (PL) spectra of RZ were monitored using a lab-built fluorescence microscope. When the solution on the Au/TiO_2 crystal facets was illuminated by the 532 nm laser and 365 nm UV source, we observed an increase in peak intensity at 583 nm and a decrease at 630 nm in the PL spectra, indicating a conversion from RZ to its product, resorufin (RS) (Figure 1b). We estimated the concentrations of RZ and RS using their peak ratios (Figure 1c) because both have distinct peaks. This allowed us to evaluate the crystals' conversion and reaction rates. To better improve the reactivity of the Au/TiO_2-based photocatalyst, we further explore the precision study of the Au nanoparticles by using Au bowtie structures on the reactivity of the same TiO_2 facets.

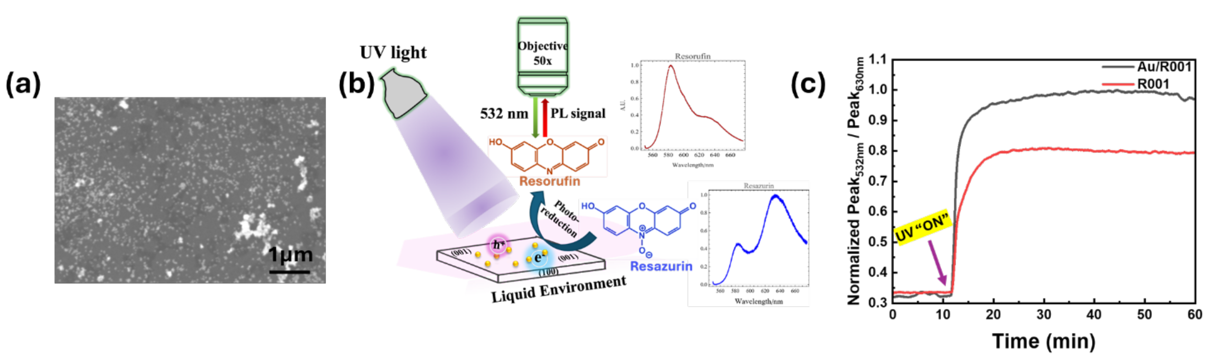

Figure 1. (a) SEM image of 40 nm Au NPs deposited on TiO_2 (b) schematic of the experimental setup for exciting and monitoring the Au/TiO2 light-induced selective reduction of resazurin ($C_{12}H_7NO_4$) to resorufin ($C_{12}H_7NO_3$) in liquid (c) peak ratio plot of pure rutile 001 and Au/rutile 001 crystal, comparing reactivity based on the peak ratio at 583 nm and 630 nm.

Power-optimized amplitude modulation for robust trapped-ion entangling gates

Luke Ellert-Beck and Wenchao Ge

Department of Physics, University of Rhode Island, Kingston, RI 02881

ABSTRACT

Trapped-ion systems are a promising route toward the realization of both near-term and universal quantum computers. The electronic state of an individual ion is incredibly stable and can be controlled very precisely, but errors are easily introduced when preparing an entangled state between two such ions. The standard method of performing entangling operations is the Mølmer-Sørensen protocol, where off-resonant lasers excite the two ions via intermediate vibrations within the trap. We suggest an improvement of this protocol, whereby the sensitivity of the protocol to errors in laser pulse duration is reduced by modulating the amplitude of the laser pulse via a Fourier series treatment. By generating and imposing linear constraints on the Fourier coefficients, our protocol effectively finds all possible pulses with a given sensitivity and allows us to select the one which uses the least laser power to implement.

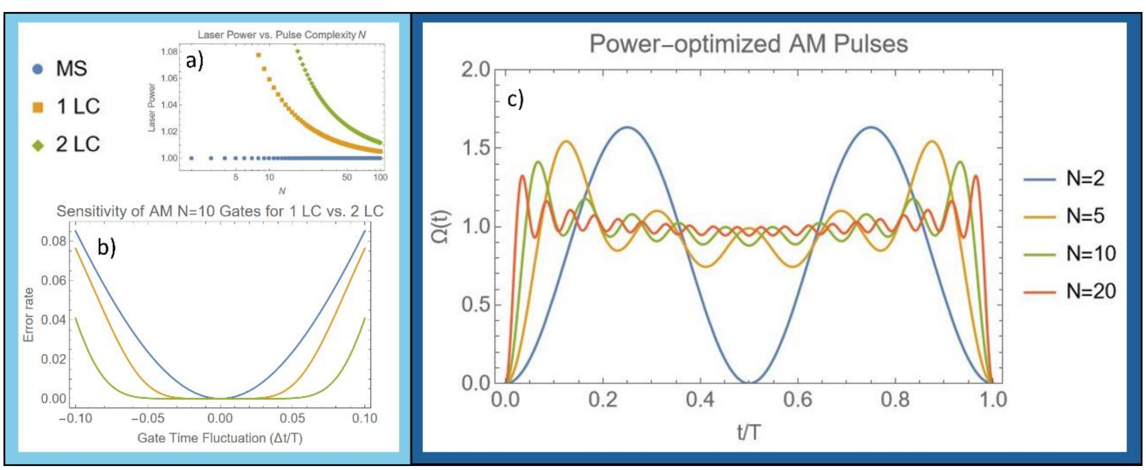

Figure: The amplitude modulated (AM) pulses take minimal additional laser power (a) when compared to the traditional Mølmer-Sørensen (MS) pulse yet reduce the sensitivity (b) by four asymptotic orders for each linear constraint (LC) added. The pulse envelopes take the shapes (c) for different numbers of Fourier coefficients N.

From Classical Mechanics to Symplectic Manifolds in Mathematics

Kevin Chauwinoir

Abstract

Symplectic manifolds have originated from the Hamiltonian formulation of classical mechanics. The Hamiltonian $H\colon M \to \mathbb{R}$, where M is a differentiable $2n$-dimensional manifold, $n \in \mathbb{N}$, can induce a symplectic structure on M in the following way: For any point $x = (p, q) \in M$, let the local coordinates $p_1 \dots p_n$ and $q_1 \dots q_n$ represent momentum and position. Then

$$\omega := \sum_{i=1}^{n} dp_i \wedge dq_i$$

is a symplectic form on M, where $\wedge$ is the wedge product.

A Symplectic manifold is a smooth manifold equipped with a 2-form that satisfies an analytical condition (closedness) and an algebraic condition (nondegeneracy). More precisely, a symplectic manifold is a pair (M, ω) where M is a differentiable manifold and ω is a 2-form such that $d\omega = 0$ (this is the closedness condition where the operator d is the exterior differentiation) and for every $p \in M$, $\omega_p : T_pM \times T_pM \to \mathbb{R}$ is a non-degenerate skew-symmetric bilinear form. The 2-form ω is called a symplectic form. The nondegeneracy condition implies that symplectic manifolds are even-dimensional.

The word *symplectic* was coined by Hermann Weyl who substituted the Latin root in *complex* by the Greek root in order to label the symplectic group.

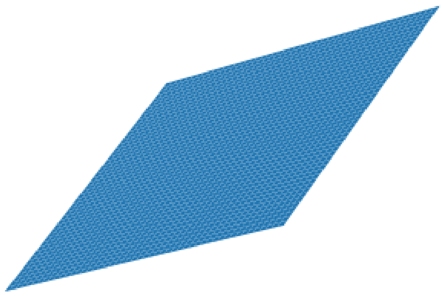

The Euclidean plane is the simplest nontrivial symplectic manifold.

References

[1] Dusa McDuff and Dietmar Salamon. *Introduction to symplectic topology*, volume 27. Oxford University Press, 2017.

[2] *Ana Cannas Da Silva. Lectures on symplectic geometry*, volume 3575. Springer, 2008.

[3] Kevin Chauwinoir. *Symplectic fibrations and connections*, 2022.

Hanbury Brown and Twiss Demonstration: Intensity Autocorrelation Function of a Thermal Light

Sheila Chauwinoir[1] Alexei V. Sokolov[1,2]

[1]Department of Physics & Astronomy, Texas A&M University, TAMU 4242, College Station, TX 77843, USA
[2]Institute for Quantum Science & Engineering, Texas A&M University, TAMU 4242, College Station, TX 77843, USA

Abstract

Hanbury Brown and Twiss (HBT) is a classical experiment demonstrating how second order correlations can be used to study thermal sources of light[1,2]. In our experiment we model thermal light by using a moving laser speckle pattern. Here, the speckle patterns emerge due to random interference phenomenon when coherent light passes through a rough surface.

The speckle pattern, which continuously varies, is incident on two photodiodes (by using a beamsplitter). We calculate the unnormalized second order correlation function by making incremental changes in the distance between the photodiodes. We show that the width of this autocorrelation function provides a reasonable measure of the average width of a speckle[4]. We also demonstrate that this method allows us to calculate the width of the laser beam that illuminates the rough surface.

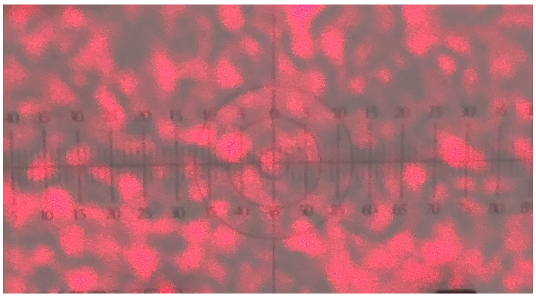

A photograph of a speckle pattern formed when a laser beam was trasnsmitted trough a ground glass diffuser onto a paper.

References

[1] Hanbury Brown, R., Twiss, R. Q., Correlation between photons in two coherent beams of light. Nature, **177**, 27 (1956).

[2] R. Hanbury Brown, R. Q. Twiss, A Test of a New Type of Stellar Interferometer on Sirius. Nature (London), **178**, 1046 (1956).

[3] Goodman, Joseph W., Laser speckle and related phenomena. Statistical Properties of Laser Speckle Patterns. Springer-Verlag Berlin Heidelberg GmbH (1975).

Unveiling Molecular Mysteries: Integrating AFM-TERS for Enhanced Raman Spectroscopy and Surface Analysis

Ming-Hsun Chou, Zhenhuan Yi, Alexei V. Sokolov and Marlan O. Scully

Institute for Quantum Science & Engineering, Texas A&M University

Abstract:

Traditional Raman spectroscopy, lauded for its molecular fingerprinting capabilities, encounters limitations such as low scattering efficiency, prolonged acquisition times, and limited lateral resolution. It provides substantial chemical composition and molecular binding data, yet it lacks comprehensive molecular insight when it comes to large molecules, e.g., proteins. This research targets these shortcomings by leveraging tip-enhanced Raman analysis to improve molecular studies.

At the core of our approach is the use of Atomic Force Microscopy-based Tip-Enhanced Raman Spectroscopy (AFM-TERS). This technique harnesses the plasmonic effects around the AFM tip to significantly amplify the electromagnetic field, thereby enhancing Raman scattering signals. The integration of AFM-TERS serves a dual purpose: it not only strengthens molecular signal detection but also facilitates high-resolution surface tomography. This combination allows for an unprecedented level of detail in both molecular structure construction and surface shape analysis of sample molecules.

Our TERS preparation includes coating the AFM tip with noble metals to intensify local plasmonic effects. We select a range of proteins as sample molecules to showcase the technique's versatility. The research aims to gather diverse data, encompassing Stoke/anti-Stoke spectroscopy, ultra-low frequency insights, and detailed molecular surface topography.

The integration of ultra-low frequency information with enhanced Raman signals and surface tomography obtained via AFM-TERS enables a more holistic construction of molecular structures. This includes intricate molecular binding details and precise surface shape characterizations of the sample molecules. Furthermore, the anti-Stoke/Stoke intensity ratio, analyzed through Boltzmann distribution concepts, together with plasmon response profile, can be used to estimate the sample temperature under the tip. This innovative technique facilitates time series analysis, as well as making TERS spectra much more comparable from tip to tip.

Photonic Biosensor in Young Interferometer Configuration

Sahar Delfan

Department of Physics and Astronomy, Texas A&M University,
Institute of Quantum Science and Engineering, Texas A&M University

In this research, we present the development and characterization of a highly sensitive photonic biosensor based on the Young interferometer configuration. The sensor leverages the principles of photonic waveguides and interference to achieve precise measurements of biomolecular interactions.

The core of our biosensor consists of a 54 nm thick Si_3N_4waveguide, optimized for single-mode operation in air. This waveguide exhibits excellent sensitivity due to its enhanced interaction with the surrounding medium. We demonstrated bulk sensing measurements using glucose solutions of varying concentrations, with the sensor producing high-quality interference fringes in the output. The visibility of these fringes, defined as (I_{max}-I_{min})/ (I_{max}+I_{min}) exceeded 0.75 in all experiments, indicating high signal clarity and low noise.

Our photonic chip's ability to produce clear and consistent fringes allows for accurate phase estimation from the fitted interference patterns. The low error in phase estimation is attributed to the superior fringe visibility and reduced interference noise. This research highlights the potential of photonic waveguide-based biosensors in achieving high sensitivity and specificity for various biochemical sensing applications.

The results demonstrate that our photonic biosensor can serve as a powerful tool for real-time monitoring of biomolecular interactions, offering significant advantages in fields such as medical diagnostics, environmental monitoring, and industrial process control.

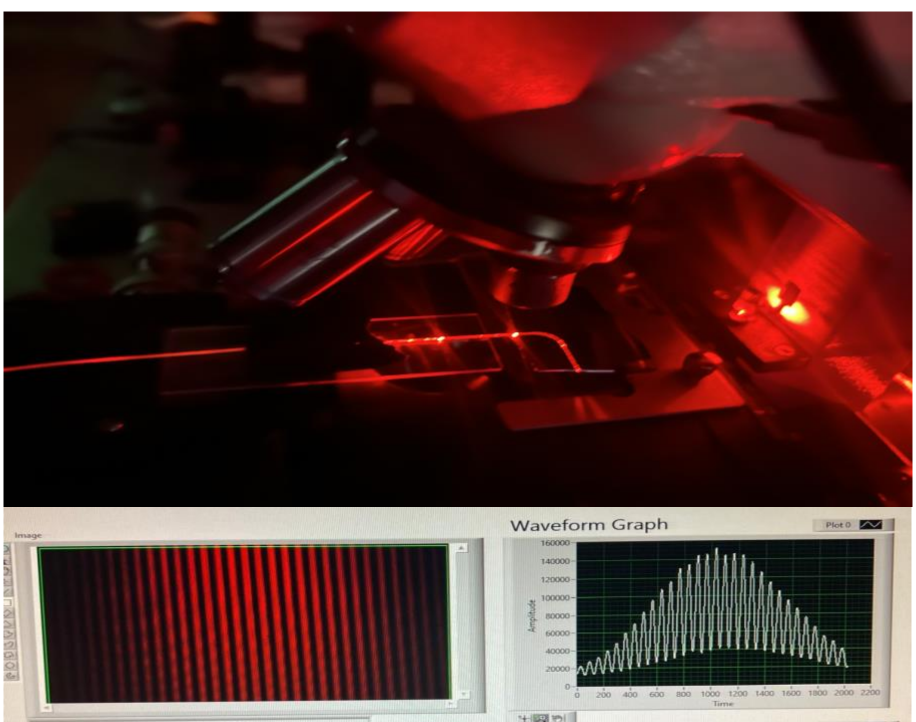

Impacts of Static Magnetic Fields and Roles of Photoreceptors in slime mold *Physarum polycephalum*

Kyra Frank[1,2], Suyash Bajpai[1], Philip Kurian[1], Suzannah Beeler[2], Kevin Cash[2]
[1]Quantum Biology Laboratory, Howard University, Washington, DC, 20060
https://quantumbiolab.com
[2]Department of Chemical and Biological Engineering, Colorado School of Mines, Golden, CO, 80401
https://cashlab.org/

Plasmodial slime molds are unicellular, multinucleated organisms that exhibit remarkable sensory behavior that helps them navigate their environments, locate food sources, and reproduce. Previous research has established that *Physarum polycephalum* displays magnetotaxis. This research project aims to investigate the impact of static magnetic fields on the foraging behavior of *Physarum polycephalum*, specifically examining whether the presence of a static magnetic field deters the organism from accessing food sources (Fig. 1). The experimental setup involves cultivating slime molds in controlled environments with food sources placed in the presence or absence of a static magnetic field (Fig. 2). The behavior of slime molds towards these food sources was observed and analyzed using time-lapse imaging. Preliminary results show that *Physarum polycephalum* displays preferential growth to food sources positioned away from strong static magnets (Fig. 3). In some other magnetotactic organisms, notably birds, the photoreceptor cryptochrome participates in a radical pair mechanism to create a magnetic compass. Genome analysis of *Physarum polycephalum* has confirmed the presence of cryptochrome-encoding genes in the organism, but the physiological role of these proteins has not been determined, indicating a possible involvement in the organism's magnetotaxis. Additionally, phytochrome photoreceptors have been identified to have roles in life-cycle regulation in *Physarum polycephalum*. We aim to explore the roles of these proteins and examine how light exposure, including radiation across various wavelengths such as visible and UV, impacts the organism.

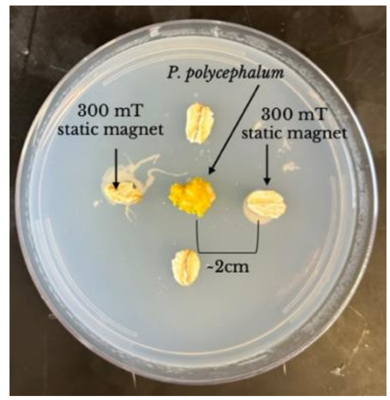

Figure 1: Experimental setup with four oat food sources, two opposing oats atop static magnets with a strength of 300 mT

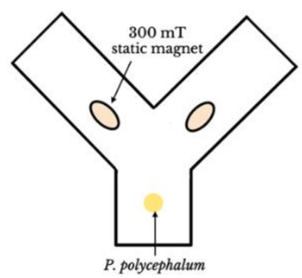

Figure 2: Experimental setup with two oat food sources, one oat atop a static magnet with a strength of 300 mT

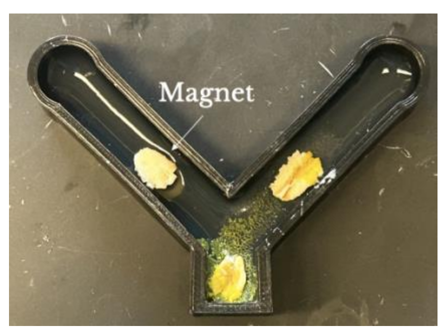

Figure 3: *P. polycephalum* exhibiting growth towards food source away from static magnet

Development of Photonic Biosensor based on Whispering-gallery Modes

Ayla Hazrathosseini, Mohit Khurana, Lanyin Luo, Zhenhuan Yi, Alexei Sokolov, Philip Hemmer, Marlan Scully
Texas A&M University, IQSE, College Station, TX 77840, USA

Whispering-gallery modes represent a class of waves capable of circumnavigating a concave structure. Initially observed in sound waves within the whispering gallery of St Paul's Cathedral, these modes are also observed in light and various other wave phenomena, holding significance across multiple fields including non-destructive testing, laser technology, thermal management, sensing, and astronomy. Given that the efficacy of a whispering-gallery mode micro-laser can be gauged by the quality factor (Q-factor) of its optical resonator, our project commenced with the design, simulation, and fabrication of high-quality resonators (HQR). Subsequently, these resonators will be employed as biosensors in bio-photonic applications, constituting the next phase of our endeavor. In this project, we employed the Finite-Difference Time-Domain (FDTD) method as a valuable resource for nano/micro-scale optical device modeling, directly solving Maxwell's equations (Fig. 1). The fabrication starts with a Si wafer with 2 μm thermal silicon wet oxide and 200 nm LPCVD Si_3N_4. The process involves sonication, dehumidification, spin-coating with PMMA, patterning with TESCAN EBL, electron beam evaporation of Cr as an etching mask, and vertical etching of Si_3N_4 using the Oxford ICP system, ending with a lift-off step (refer to Fig. 2).

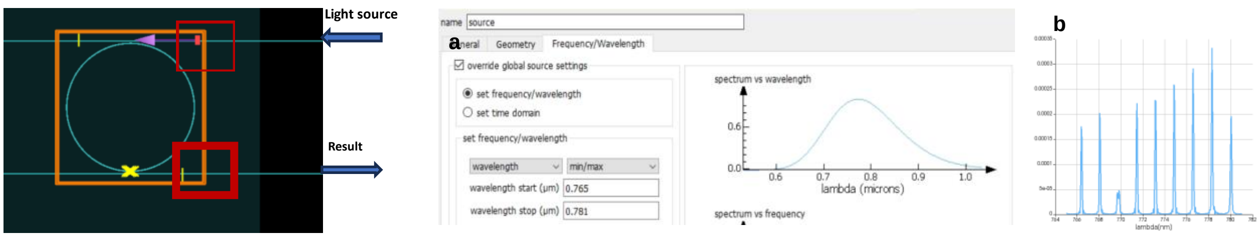

Fig. 1 Lumerical FDTD software. a) Expected spectrum for laser source around 760 nm, b) Simulated transmission spectrum of ring/elliptical cavity.

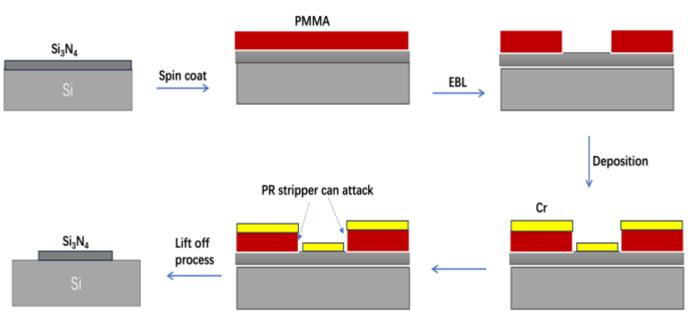

Fig. 2 Fabrication process.

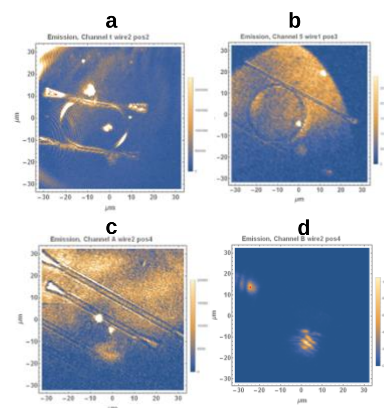

Fig.3 Confocal images of optical experiment a) ellipse resonator b) ring resonator c) shining laser on waveguide in channel A d) observable coupling in channel B.

We utilize confocal microscopy to adjust the wavelength of the laser in Channel A, while simultaneously recording the respective counts per second (Kc/s) from Channel B. The resulting curve is expected to resemble a Lorentzian function or exhibit a bell-shaped profile. By fitting this curve, we extract the Q-factor, representing the resonance mode of the resonator. Recently, we have successfully achieved coupling and out coupling in grating structures in confocal microscopy optical setup. We further continue working on measurement of the Q-factor of resonators (Fig. 3).

Quantum Entanglement in the Ground State in Ultrastrong Coupling Regime

Qingtian Miao

Institute for Quantum Science and Engineering and Department of Physics and Astronomy, Texas A&M University, College Station, TX, USA 77843.

Abstract: The ultrastrong coupling between the elementary excitations of matter and microcavity modes is studied in a fully analytical quantum-mechanical theoretical framework. The elementary excitation could be phonons, excitons, plasmons, etc. From the diagonalization of the Hamiltonian, we obtain the ground state of the polariton Hamiltonian. The ground state belongs to the Gaussian class. Using the Gaussian property, we calculate the quantum entanglement in the ground state. We use two different measures for quantum entanglement— entanglement entropy and the logarithmic negativity parameter—and obtain rather simple analytical expressions for the entanglement measures. Our findings show that the amount of quantum entanglement in the ground state is quite significant in the ultrastrong-coupling regime. It can be obtained from the measurement of the polariton frequencies.

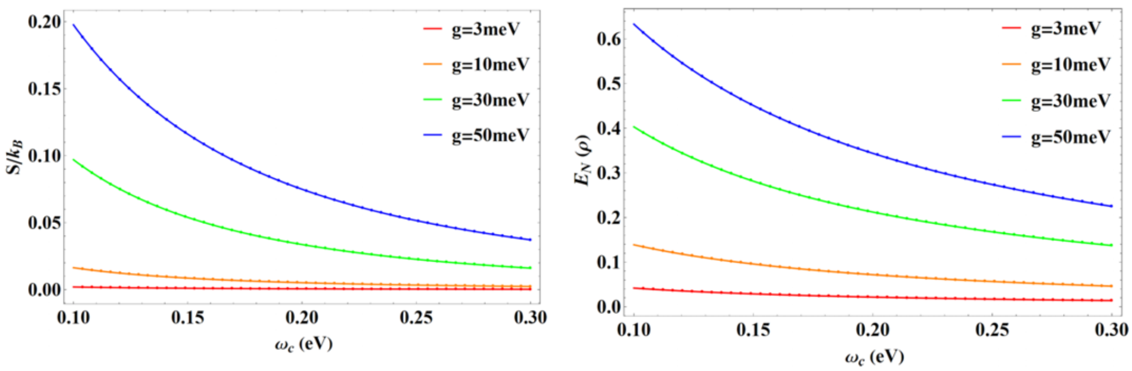

(a) **(b)**

Figure (a) Entanglement entropy plotted against the bare cavity energy with transverse-optical (TO) phonon energy 169.1 meV and different values of coupling strength g. (b) Logarithmic negativity plotted against the bare cavity energy with TO phonon energy 169.1 meV and different values of g.

Quantum Fourier Transform for Medical Resonance Imaging Data Reconstruction

Srila Palanikumar[1,2], Suyash Bajpai[1], Philip Kurian[1]
[1]Quantum Biology Laboratory, Howard University, Washington, DC, 20060
[2]The University of Texas at Austin, Austin, TX, 78712

The Fourier transform decomposes a complex waveform into the frequencies that it comprises. The quantum Fourier transform (QFT) performs the same operation but provides a significant computational advantage by leveraging quantum parallelism. This enables an exponential speedup over the classical algorithm; whereas the time complexity of the classical Fourier transform is $O(N \log N)$, the quantum Fourier transform has a time complexity of $O(\log^2 N)$.[1] For a given quantum state $|a\rangle$ prepared in a complete superposition, the quantum Fourier transform of $|a\rangle$ is given by:

$$|a\rangle \rightarrow \frac{1}{\sqrt{q}} \sum_{c=0}^{q-1} e^{2\pi i \frac{ac}{q}} \; |c\rangle$$

where q is the dimensionality of the Hilbert space of $|a\rangle$, c is the index running over each possible state in the Hilbert space, and a is the integer representing the input state.[2]

Current magnetic resonance imaging (MRI) reconstruction techniques are computationally intensive, resulting in lengthy processing times. For instance, Fig. 1(a) shows noisy and non-normalized 3D MRI models of five different pancreases, classically reconstructed from multiple 2D slices using vtk in Python. Fig. 1(b) depicts the same data, cleaned using the iterative closest point (ICP) algorithm by registering four of the noisy models to an arbitrarily chosen ground truth model (in chartreuse), with a time complexity of $O(N^2)$.[3] The models are color-coded to keep track of their ICP transformations. Future work will explore quantum speedups over this classical data processing, with a larger set of pancreases.

Figure 1(a): Noisy 3D MRI models of five pancreases.

Figure 1(b): Same data as in (a), cleaned using the ICP algorithm.

An inverse quantum Fourier transform can improve image reconstruction from raw MRI data. By converting MRI data from the frequency domain, in which it is collected, to the spatial domain, it allows for the accurate reconstruction of high-resolution images[4], aiding in diagnostics and treatment planning. The reduction in complexity makes the QFT a promising avenue for accelerating image reconstruction, potentially enabling more efficient medical imaging workflows.

1. Musk, D. R. (2020). A Comparison of Quantum and Traditional Fourier Transform Computations. Computing in Science & Engineering, 22(6), 103–110. https://doi.org/10.1109/mcse.2020.3023979
2. Muhammad Suhail Zubairy. (2020). Quantum Mechanics for Beginners: With Applications to Quantum Communication and Quantum Computing (p. 248). Oxford University Press.
3. Mora, H., Mora-Pascual, J. M., García-García, A., & Martínez-González, P. (2016). Computational Analysis of Distance Operators for the Iterative Closest Point Algorithm. PLOS ONE, 11(10), e0164694. https://doi.org/10.1371/journal.pone.0164694
4. Kiani, B., Villanyi, A., & Lloyd, S. (2020). Quantum Medical Imaging Algorithms. https://arxiv.org/pdf/2004.02036

Detection and Classification of Aerosol Particles using Digital Inline Holography

Punyasloka Sahoo [1,2], Alma Fernandez Gonzalez [1,2,3], Cameron Garman[4], Mark Harlow[4], Bikas Vaidya[4], Aart Verhoef[1,3], Alexei V. Sokolov[1,2]

[1]Institute of Quantum Science and Engineering (IQSE), Texas A & M University, College Station, TX-77840

[2]Department of Physics and Astronomy, Texas A & M University, College Station, TX-77840

[3]Department of Soil & Crop Sciences, Texas A & M University, College Station, TX-77843

[4]Lynntech Inc., College Station, TX- 77845

Aerosols are suspensions of particles or droplets in air. By detecting and understanding the morphological characteristics of these particles, we can assess the air quality of our atmosphere and detect any chemical or biological threats. This information is also valuable for understanding the impact of aerosols on the atmosphere including their contribution to radiative energy transfer. Digital Holography is an excellent contact-free way for examining the morphological characteristics of aerosol particles [1]. A significant amount of research has been done in this area, particularly in the field of digital inline holography, where the reference beam and the object beam are incident on the sensor in a coaxial manner. For example, Kemppinen et al. were able to image particles as small as 10 um using a portable device attached to an unmanned aerial vehicle [2], and McLeod et al. were able to image particles as small as 100 nm by trapping them on a polyethylene glycol film on a cover slip [3]. In this research work we are striving to understand the morphological features of the aerosol particles and will analyse the holograms to classify these particles into biological and non-biological categories based on the morphological information. This classification will enable us to detect chemical or biological agents in both rural and urban settings. We are confident that with modifications and improvements our setup can achieve real-time measurement and classification of biological and non-biological aerosol particles.

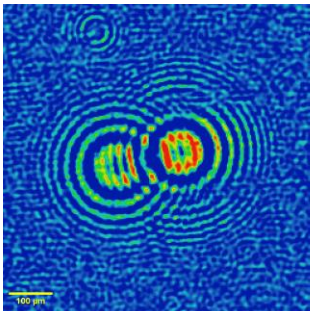

1(a)

1(b)

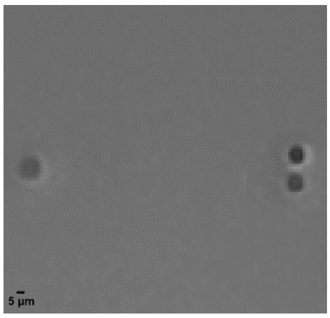

1(c)

Figure 1 (a) Diffraction pattern (holograms) of 15 um glass microspheres (b) Silhouette of the microspheres as obtained from the diffraction patterns computationally using Fresnel transformation (c) Image of the microspheres as seen under an optical microscope with 20x objective

References

1. Berg M.J. Journal of Aerosol Sciences, **2022, 165, 106023-47.**
2. Kemppinen O et al., Sci. Rep. **2020,10, 16085-96.**
3. McLeod E et al, ACS Appl. Nano Mater., **2023, 6, 13, 11166-74.**

This material is based upon work supported by the Department of Defense Small Business Innovation Research (SBIR) Program, Office of the Secretary of Defense-Basic Research Office (OSD-BRO) and the Army Research Office under Contract No.W911NF-24-C-0050. Any opinions, findings and conclusions or recommendations expressed in this material are those of the author(s) and do not necessarily reflect the views of the Department of Defense Small Business Innovation Research (SBIR) Program, OSD-BRO, or the Army Research Office. Distribution A

High Resolution Imaging of Soil Aggregate Pore Space and Microbial Activity using Optical Coherence and Multiphoton Microscopy

Riva Salzman[1], Alma Fernandez[1], Peyton Smith[1], Aart Verhoef[1]
[1]: Texas A&M University, College Station TX 77843, USA

One major asset in soil science is the ability to obtain a detailed understanding of soil structure from any sample. The soil pore space is perhaps the most physically relevant feature of soil structure because it determines how a soil behaves under physical stresses, permits gas and water transport, and makes up the major surfaces and pathways upon which biological and chemical processes take place[2]. We present a method of using optical coherence tomography (OCT) as a means of gathering 3D structural information of the interior of a soil aggregate so it can be analyzed for porosity and pore size distribution (PSD) characteristics. Potential benefits of OCT include faster imaging times and better spatial resolution for more accurate pore characterization (as compared with X-ray CT, the current standard method for imaging porosity[3]). Our current Fourier Domain Optical Coherence Microscopy (FD OCM) setup[1] can achieve a lateral resolution of down to 2.5 um. This ability to extract pore features of soil samples can help us understand and predict how soils will respond to environmental or agricultural stress.

A central process in soils related to pore space is the activity of microbes upon organic matter in soil. More information is needed on the precise spatial distribution of microbial enzyme activity in aggregates. Having this knowledge will assist in the development of mechanistic models that explain several soil processes in which microbial metabolism plays a key role, including aggregate formation and breakdown, and carbon storage and release in soils[4]. In this study we use multiphoton fluorescence imaging to generate high resolution images of hotspots of microbial activity. One such image is at right (below).

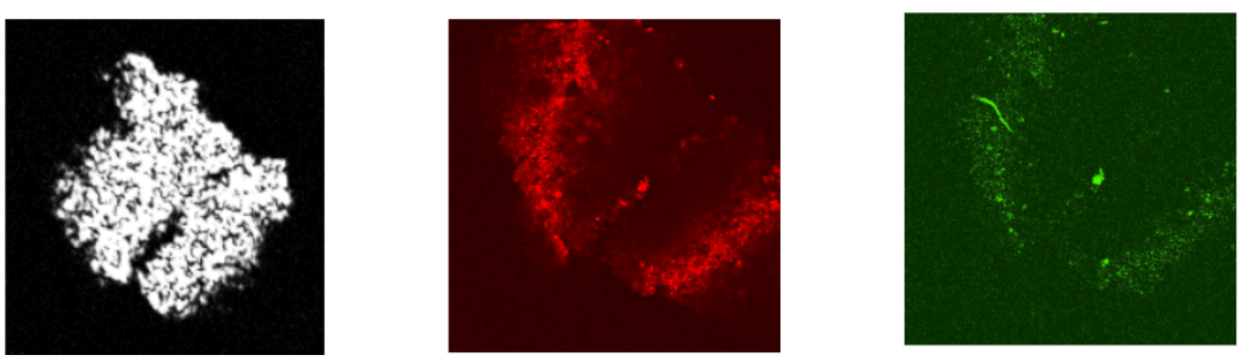

Cross sectional images of soil aggregate; OCT (left), red fluorescence of organic matter(center), blue fluorescence from bacterial metabolism (right).

References:
[1] D. Sen et al, Extended focal depth Fourier domain optical coherence microscopy with Bessel-beam – LP02 mode – from a higher order mode fiber. (2021).
[2] Pagliai, Marcello, Vignozzi, Nadia, The Soil Pore System as an Indicator of Soil Quality.
[3] Houston, A.N. et al, Quantification of the pore size distribution of soils: Assessment of existing software using tomographic and synthetic 3D images. (2017).
[4] Blanco-Canqui, Humberto, La, Rattan, Mechanisms of Carbon Sequestration in Soil Aggregates. (2010).

On demand Zeeman Frequency Comb Quantum Memory via reversing the B direction

Yanli Shi, Xiwen Zhang and Olga Kocharovskaya

Institute for Quantum Science &Engineering, Department of Physics & Astronomy, Texas A&M University

Various protocols of quantum memory have been realized for optical photons in atomic ensembles [1]. Some of them (such as Raman or EIT memory) are based on coherently driven ensemble of three-level systems. Others (such as atomic frequency comb (AFC) or gradient echo memory) can be implemented in an ensemble of the long lived resonant two-level systems by introducing a controllable inhomogeneous broadening. Absence of the proper coherent sources in X-ray range currently prevents realization of the Raman/EIT memories in the X-ray range, while AFC for storage of the X-ray photons has been experimentally realized very recently using a set of movable resonant absorbers which absorption frequencies produce a comb via the Doppler effect [2] in accordance with our earlier theoretical proposal [3]. However, the moment of the photon wave packet retrieval in this protocol was predetermined by the frequency comb interval.

In this work we suggest a new protocol for on demand hard X-ray photon nuclear memory. It uses the Zeeman frequency comb produced by splitting the initially degenerate high nuclear spin ground state in the external magnetic field (Fig.1). Numerical calculations have been performed for the 6.214 keV nuclear transition in Ta-181 [4]. We show that the stored X-ray photon wave packet can be retrieved on demand by reversing the direction of the magnetic field (Fig. 2). It is worth noting that time reversing of quantum beats in the synchrotron experiments with Fe-57 has been demonstrated previously [5] and inspired a proposed protocol. It is shown also that a new B switching protocol allows to achieve about the same efficiency and fidelity as in the pre-determined Zeeman comb quantum memory without B switch and/or a Doppler Frequency Comb quantum memory in ensemble of the Ta-181 absorbers with the degenerate ground and excited states in the absence of B, but with an on-demand retrieval. The storage time is limited by the resonant transition coherence time, 8.73μs.

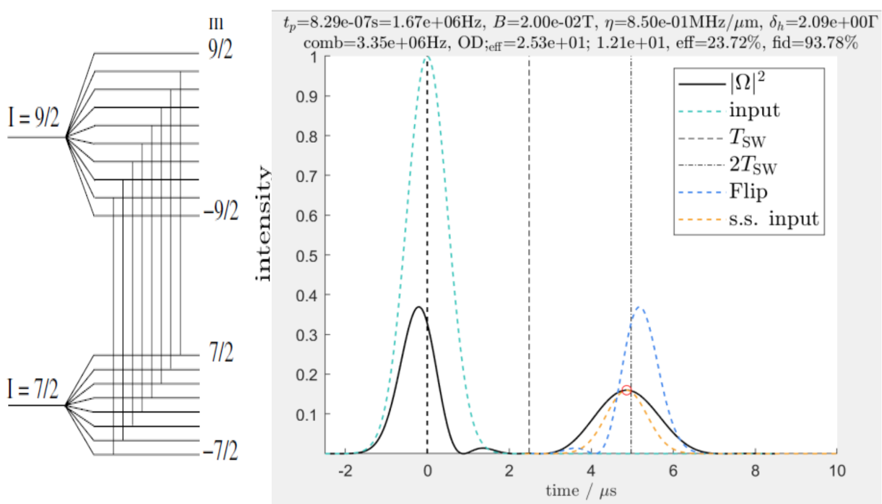

[1] Y. Lei, F. K. Asadi, T. Zhong, A. Kuzmich, C. Simon, M. Hosseini, Quantum optical memory for entanglement distribution. *Optica, OPTICA* **10**, 1511–1528 (2023).
[2] S. Velten, L. Bocklage, X. Zhang, K. Schlage, A. Panchwanee, I. Sergeev, O. Leupold, A.I. Chumakov, O. Kocharovskaya, R. Röhlsberger, Nuclear quantum memory for hard X-ray photons, Science Advances, accepted.
[3] X. Zhang, W.-T. Liao, A.A. Kalachev, R.N. Shakhmuratov, M.O. Scully, O. Kocharovskaya, Nuclear quantum memory and time sequencing of a single γ photon, Phys. Rev. Lett. **123**, 250504 (2019).
[4] Yu.V. Shvydko *et. al.*, “Reversed time in Mossbauer time spectra”, Phys. Rev. B, **R711**, 52 (1995).
[5] O. Leopold, A.I. Chumakov b, E.E. Alpc, W. Sturhahnc and A.Q.R. Baron, Noniron isotopes, Hyperfine Interactions **123/124**, 611 (1999).

Single – photon scattering in a cavity with giant atomic mirrors, coupled to a 1D waveguide

Amal Vijayalekshmi Sivakumar[1], Jiru Liu[1], M. Suhail Zubairy[1]

[1]*Institute of Quantum Science and Engineering (IQSE) and Department of Physics and Astronomy, Texas A&M University, College Station, TX 77843-4242, USA*

Abstract

Atoms in the ground state typically are of the size of order r ≈ 10^{-10} m. Hence, for interactions with optical wavelengths ($\lambda \approx 10^{-7}$ to 10^{-6}m), the atoms can be considered to be point-like. Recently, artificial two-level atoms have been developed using superconducting circuits, quantum dots etc. These are called 'giant atoms' considering the comparable size of the artificial atom (*e.g.* size of the circuit) with that of the interacting radiation. The multiple coupling points of the atom to the waveguide gives rise to effects such as Lamb shift in the atomic level and frequency dependent coupling strength. Here, we examine single-photon scattering in a cavity formed by giant atom mirrors coupled to the waveguide and compare it to the point-atom case. The interaction between the photon and the collective modes of the atomic arrays in the cavity gives rise to superradiance, Fano-type interference and photonic band gaps. The phase delays between the different coupling points can be used to modify these interference effects. The reflectance, spectra of the emitted fields and the field decay in the cavity are analyzed and compared with the point-atom case.

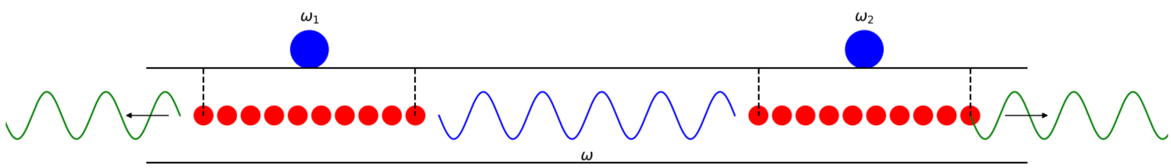

Fig 1: A cavity with two giant atom mirrors. The two-level atoms (blue circles) have transition frequencies ω_1 and ω_2. The initial plane wave inside the cavity (blue wave) has a frequency of ω. The red circles represent the multiple coupling points of each atom to the waveguide. The green waves represent the reflected and transmitted waves.

Nanoscale Chemical Sensing Using Optical Fiber-based Near Field Scanning Microscopy (NSOM)

Nusrat Zahan Tanwee, Rohil Kayastha, Blake Birmingham, and Zhenrong Zhang
Baylor University, Department of Physics, Waco, TX 76798

Tip-Enhanced Raman Spectroscopy (TERS) offers sub-nanometer resolution in chemical imaging but is constrained by low signal collection efficiency, substantial background noise, and complex optical alignment. Conventional TERS systems have low collection efficiency of Raman signals, limiting their effectiveness in dynamic or fluid environments. Near-field Scanning Optical Microscopy (NSOM), while capable of imaging below the diffraction limit of light, typically achieves lower resolution due to inadequate light confinement using traditional aperture probes and lacks chemical sensing capabilities.

This study advances the setup by integrating TERS with the NSOM, utilizing an optical fiber-based metallic probe to guide and nano-focus the light at the tip apex, which aids in improving the overall focusing precision at the probe tip and substantially boosts signal coupling efficiency. The innovation centers on using Surface Plasmon Polaritons (SPPs) to achieve nano-focusing and light confinement directly at the probe apex, leveraging the specialized design of the probe, which incorporates metallic elements to enhance the plasmonic effects. This approach markedly reduces background noise and boosts the excitation and collection efficiency of Raman signals with an alignment-free optical setup. Our goal is to achieve high-resolution nanoscale chemical imaging and spectroscopy across various environments, including liquids, using our FTERS setup.

In this study, we utilized a lab-built AFM (Atomic Force Microscopy) -based TERS setup (**Figure I**) with a fiber-based metallic probe to perform the experiment in air, focusing on improving Raman signal detection and resolution through advanced optical and plasmonic techniques. Our setup utilizes an integrated NSOM and AFM system onto a sample using a metallic fiber probe attached to a tuning fork, allowing for precise scanning and high-resolution spectroscopic imaging with Raman signals. Preliminary results show substantial improvements in image and spectroscopy quality, with ongoing enhancements aimed at refining probe quality and temporal resolution to further improve spatial resolution. Currently, the system correlates AFM data with AFM transmission and Raman spectroscopy results, providing comprehensive topographical and chemical sample information in the air. This integration allows for the simultaneous mapping of surface structures and identification of molecular constituents, delivering a comprehensive sample analysis. A 150 nm resolution AFM image (**Figure II**), as well as a transmission Raman image, has been observed using this setup. Future work will focus on optimizing the system to consistently produce high-quality transmission Raman images and detailed spectra, significantly expanding our capabilities to explore and understand material properties at the molecular level in a liquid environment. This research not only makes TERS more accessible for various scientific and industrial applications but also significantly advances the field of nanoscale optical characterization in different environments, paving the way for new insights in materials science, biotechnology, and nanotechnology.

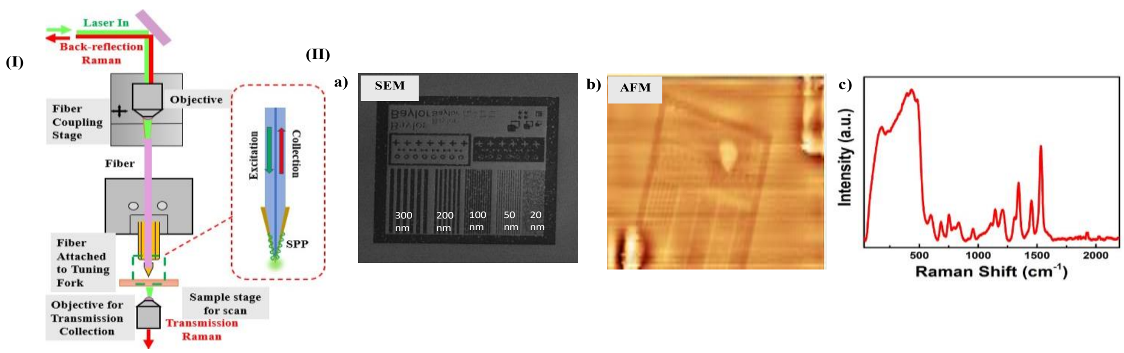

Figure: **(I)** Schematic of fiber-based TERS experimental setup. **(II)** Experimental results: (a) SEM of calibration nano-pattern, (b) AFM image, (c) Raman spectra of R6G molecules

Enhancing Optical Fiber Sensitivity with Diatoms and Nanoparticles

Sanjib Thapa[1], Rohil Kayastha[1], Subhavna Juneja[2], Alan X. Wang[2], and Zhenrong Zhang[1]

[1]Department of Physics, Baylor University, Waco, TX 76798
[2]Department of Engineering and Computer Science, Baylor University, Waco, TX 76798

Diatoms, microalgae characterized by their periodic nanoporous silica shells, exhibit photonic crystal cavities with optical properties akin to those found in fabricated photonic crystals. Diatoms functionalized with plasmonic metallic nanoparticles on glass substrates have been used as effective sensors. However, these glass substrate-based sensors face significant challenges, including difficulties in achieving remote sensing, signal loss, and lack of flexibility. In this work, we propose the development of an advanced probe sensor that integrates plasmonic nanoparticles on photonic crystal cavities of diatoms on optical fiber. The plasmonic resonance of nanoparticles coupled with the resonance mode of diatoms significantly enhances the localized electric field, thereby enhancing the signal. Moreover, Optical fibers, known for their low signal loss and ability to transmit signals over long distances, are ideal for long-range and remote sensing in hazardous or unreachable environments. Their flexibility and ease of integration further enhance their practical sensing applications.

To optimize signal performance, we vary the density and uniformity of nanoparticles on diatom frustules to determine the optimal configuration to maximize signal. Additionally, we study the orientation and density of diatom frustules on the fiber facet, selecting suitable species to achieve optimal resonance properties and maximize coupling with the plasmonic resonance of the nanoparticles, thereby enhancing the signal. Using Rhodamine 6G (R6G) molecules as analytes, we test these modified fibers and aim to detect concentrations as low as 10^{-15} M by enhancing the very weak Raman spectra demonstrating extreme sensitivity. This method improves sensitivity and provides specific benefits that solve the problems posed by glass substrates.

This innovative approach opens new possibilities for developing highly sensitive optical fiber sensors. Our proposed sensor has wide-ranging applications, from environmental monitoring to biomedical diagnostics and chemical detection. Combining the unique properties of diatom frustules with optical fibers and plasmonic nanoparticles achieves a level of sensitivity and specificity unattainable with traditional glass substrate-based sensors.

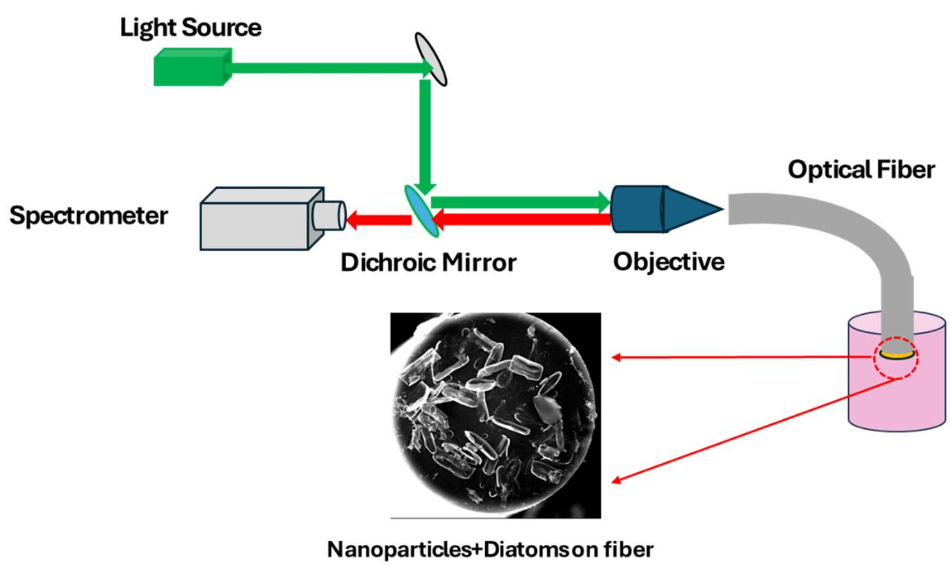

Figure: Experimental setup for measuring the Raman spectra of R6G molecules.

The electronic structure calculations of Fe doped monolayer MoS2 using density functional theory

AmirAli VanakiFarahani, Adeleh Mokhles Gerami, Hasan Jamnezhad

Affiliation (respectively): TAMU – CERN – KNTU

Abstract: Recently, the single-layer two-dimensional (2D) of MoS2 which is an important transition metal dichalcogenides (TMDs) compound has been investigated. Similar to the graphene, the monolayer of MoS2 is used in a wide range of application including field-effect transistors, photodetectors, solar cells, chemical sensors and supercapacitors electrodes. In order to understand its application in nano-electronics, the investigation of the electronic structure and magnetism of MoS2 is crucial.

Several attempts have been made to improve electronic structures, magnetic property of MoS2 nanolayers. For example, Kou et al. have demonstrated that the electronic and magnetic properties of zigzag MoS2 nanoribbons exhibit sensitive response to the change of strain and electric field. Introducing transition metal (TM) in 2D system of MoS2 is another effective route to modify its electronic and magnetic properties. Conley et al. have revealed that TM doping not only profoundly influences the electronic structure of 2D materials, but also promotes magnetic properties of the system.

In this work, the magnetic and electronic properties of monolayer MoS2 doped with Fe atoms have been investigated by first-principal calculations in the framework of density functional theory (DFT) based on the full-potential linear augmented plane wave (FP-LAPW) method as implemented in the wien2k code. The various configurations of Fe doped MoS2 (I. Substitutional Fe doped Mo site, II. Interstitial Fe on the surface of monolayer MoS2) have been simulated. The charge state of Fe and the density of states of each configuration are discussed. The results of this work provide information about the change of the electronic structure in the monolayer MoS2 with different implanted Fe site.

Suppression of Wigner Weisskopf Decay by the Acceleration of Entangled Atoms

Charles Wallace

The vacuum in quantum field theory is an interesting object that can act in an unintuitive manner–contrary to what is expected of the vacuum in the classical theory. Many theoretical studies have been written and practical applications have been implemented which involve the effects of the vacuum on quantum systems. Two interesting and important effects arising from the interaction of two-level systems and the vacuum are decay of a two-level atom from the excited state to the ground state (here referred to as Wigner Weisskopf decay) and the Unruh effect wherein a uniformly accelerated atom moving along a Rindler trajectory experiences a thermal bath of photons at a temperature proportional to the acceleration. The thought experiment for demonstrating the Unruh effect is that of a uniformly accelerated two level system (referred to from here as an atom) through a vacuum while interacting with the vacuum modes. Here, we vary this thought experiment such that there are two atoms with transition frequencies ω_1 and ω_2 accelerating through the vacuum with uniform accelerations of a_1 and a_2. If the atoms are prepared in an entangled state, it is demonstrated that, for interaction with a single mode of the vacuum, the Wigner Weisskopf decay due to the interaction with the vacuum can be suppressed entirely given the correct confluence of conditions. Thus, the entanglement of the atoms can be almost entirely preserved throughout their motion due to the uniform acceleration. Moreover, it is demonstrated that the entanglement of the initial state can be entirely preserved for identical atoms. The interaction of the pair of atoms with multiple modes of the vacuum is also examined.

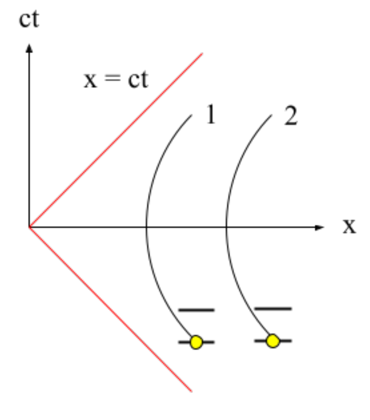

Figure 1: Two atoms that are uniformly accelerated moving along Rindler trajectories

Quantum Simulator in Room Temperature

Jiefei Wang, Ruosong Mao, Xingqi Xu, Han Cai, Da-Wei Wang

School of Physics, Zhejiang University, Hangzhou,310027, China

Quantum simulation offers an analog approach for exploring exotic quantum phenomena using controllable platforms, typically necessitating ultracold temperatures to maintain the quantum coherence. Superradiance lattices (SLs) have been harnessed to simulate coherent topological physics at room temperature, but the thermal motion of atoms remains a notable challenge in accurately measuring the physical quantities. To overcome this obstacle, we invented and validate a velocity scanning tomography technique to discern the responses of atoms with different velocities, allowing cold-atom spectroscopic resolution within room-temperature SLs. By comparing absorption spectra with and without atoms moving at specific velocities, we can derive the Wannier-Stark ladders of the SL across various effective static electric fields, their strengths being proportional to the atomic velocities. We extract the Zak phase of the SL by monitoring the ladder frequency shift as a function of the atomic velocity, effectively demonstrating the topological winding of the energy bands. Our research signifies the feasibility of room-temperature quantum simulation and facilitates their applications in quantum information processing.

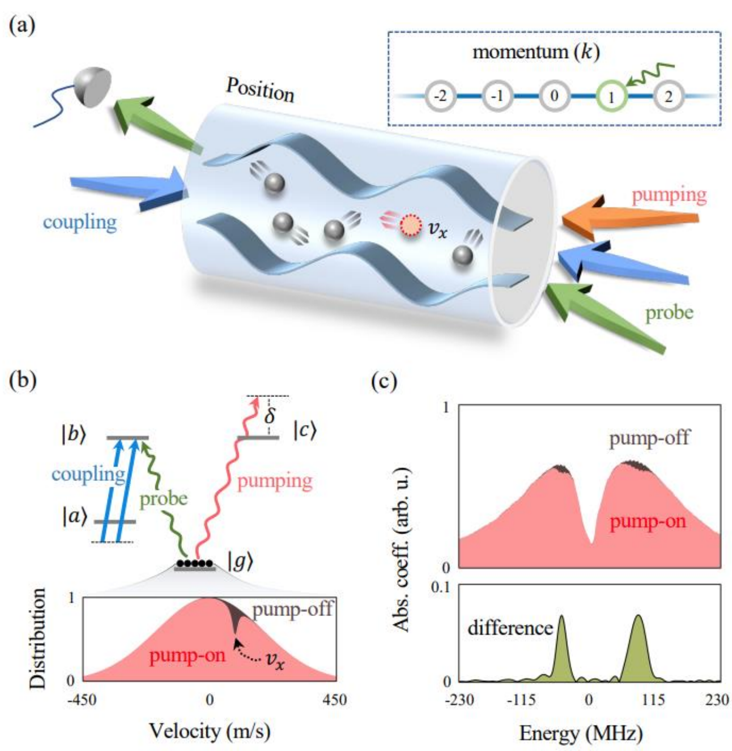

Schematics of the experimental set-up.

Dynamics of Unruh effect and manifestation of Minkowski vacuum entanglement

Fan Yang[1], Wenzhuo Zhang[1], Anatoly Svidzinsky[1], Marlan Scully[1,2,3], and William Unruh[4]

[1]Texas A&M University, [2]Baylor University, [3]Princeton University, [4]University of British Columbia

The particle content of the vacuum depends on the mode functions we adopt to describe photons. For a plane-wave basis set, the Minkowski vacuum is a state with no photons. However, if we choose Rindler modes, then in such a description, Minkowski vacuum is filled with Rindler photons whose number in different space regions is correlated. This property of the Minkowski vacuum yields observable effects. For example, two ground-state oscillators of frequency ω accelerated in causally disconnected regions (Fig. 1) become excited in a correlated fashion by absorbing Rindler photons, so that state vector of the system in the resonant mode approximation evolves as

$$|\psi(\tau)\rangle = \sqrt{1-\gamma^2}\, e^{\gamma\left(\cos(g\tau)\hat{b}_1^{+} - i\sin(g\tau)\hat{\sigma}_1^{+}\right)\left(\cos(g\tau)\hat{b}_2^{+} - i\sin(g\tau)\hat{\sigma}_2^{+}\right)}|0_R\rangle\ |0\rangle,$$

where $\hat{b}_{1,2}^{+}$ are Rindler photon creation operators, $\hat{\sigma}_{1,2}^{+}$ are oscillator's raising operators, g is the oscillator-photon coupling constant, and τ is the oscillator's proper time. The average number of the oscillator excitations is

$$\bar{n}_1 = \bar{n}_2 = \frac{1}{exp\left(\frac{\hbar\omega}{k_B T_U}\right) - 1} sin^2(g\tau),$$

where $T_U = \frac{\hbar a}{2\pi c k_B}$ is Unruh temperature. One can see the entanglement is transferred between the field and the oscillators periodically.

The Rabi oscillation dynamics is a feature attributed to the single-mode approximation. We also study dynamics of the Unruh effect including all field modes. This yields evolution similar to that of a damped harmonic oscillator. In particular, we find that the average number of oscillator excitations approaches the steady state.

We also consider generation of entanglement between two oscillators accelerated in causally disconnected regions taking into account all modes of the field. Our findings suggest a novel mechanism for the entanglement generation between space-like separated oscillators.

$$\bar{n}_1 = \bar{n}_2 = \frac{1 - e^{-g^2\tau/\omega}}{exp\left(\frac{\hbar\omega}{k_B T_U}\right) - 1}$$

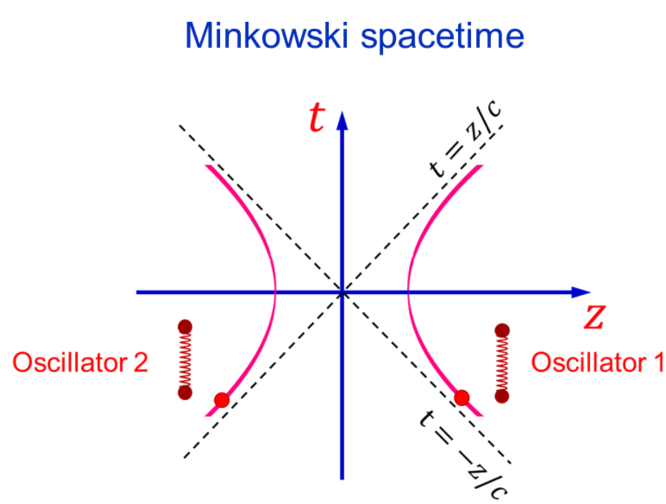

Figure 1: Oscillators are uniformly accelerated in causally disconnected regions with proper acceleration a and become excited in correlated fashion.